THE EFFECT OF STRUCTURE SLOPE AND PACKING ARRANGEMENT ON THE HYDRAULIC STABILITY OF GEOTEXTILE SAND CONTAINER REVETMENTS

by

Christophe Marc Eric Baret

Thesis presented in fulfilment of the requirements for the degree of Master of Science in the Faculty of Civil Engineering at Stellenbosch University

Supervisor: Mr Geoff Toms

March 2013

Declaration

By submitting this thesis electronically, I declare that the entirety of the work contained therein is my own, original work, that I am the sole author thereof (save to the extent explicitly otherwise stated), that reproduction and publication thereof by Stellenbosch University will not infringe any third party rights and that I have not previously in its entirety or in part submitted it for obtaining any qualification.

Date: ………………………………………..

i

Abstract

Innovative and versatile coastal protection structures made of Geotextile Sand Containers (GSCs) are increasingly being incorporated into coastal management solutions because of their cost effective and environmentally friendly characteristics. This is as opposed to conventional 'hard' coastal protection solutions that utilise rocks and or concrete units to protect the coastline.

With GSC structures being a relatively new coastal protection solution, few design and construction guidelines are available. Research into the behaviour of GSC structures under wave attack is on-going with particular emphasis on the hydraulic processes that affect GSC structures and cause them to fail.

The use of GSC revetments as coastal protection solutions has become more popular in South Africa during recent times, particularly along the coastline of KwaZulu-Natal. However, the chosen design of these GSC revetments falls outside the range of applicability of the available design charts and stability equations. Therefore the hydraulic stability of these structures is largely unknown.

The primary objective of this study is to investigate the effect of structure slopes and packing arrangements on the hydraulic stability of GSC revetments. The application of available design charts and stability equations was also evaluated. Two-dimensional physical modelling was undertaken and a total of 12 GSC revetment permutations were tested during the physical modelling test series. The results of the physical modelling showed that the structure slope had the most significant effect on the hydraulic stability. Steeper structure slopes were more hydraulically stable than gentler structure slopes. The packing arrangements of the GSCs had less of an effect on the hydraulic stability of the GSC revetments. Single layer GSC armour revetments matched or out-performed the equivalent double layer GSC revetments; while GSC revetments with GSCs orientated with the long axis perpendicular to the wave attack performed marginally better than the equivalent GSC revetments with GSCs orientated with the long axis parallel to the wave attack.

The available design charts and stability equations were assessed against the results of the physical modelling and showed varying degrees of correlation. The stability equation proposed by Recio (2007) proved to be particularly accurate.

Samevatting

Innoverende en veelsydige kusbeskermingstrukture wat van geotekstielsandhouers (GSH's) gemaak is, word al hoe meer by kusbestuursoplossings ingesluit weens die kostedoeltreffendheid en omgewingsvriendelike aard daarvan. Dít is in teenstelling met konvensionele 'harde' kusbeskermingsoplossings, wat van rotse en/of betoneenhede gebruik maak om die kuslyn te beskerm.

Aangesien GSH-strukture 'n betreklik nuwe kusbeskermingsoplossing is, is weinig ontwerp- en konstruksieriglyne beskikbaar. Navorsing oor die werkverrigting van GSH-strukture onder golfaanslag duur voort, met bepaalde klem op die hidrouliese prosesse wat GSH-strukture beïnvloed en die werking daarvan benadeel.

Die gebruik van GSH-bedekte hellings as kusbeskermingsoplossings het in die laaste tyd al hoe gewilder geword in Suid-Afrika, veral langs die kus van KwaZulu-Natal. Tog val die gekose ontwerp van hierdie GSH-bedekte hellings buite die toepaslikheidsbestek van die beskikbare ontwerpriglyne en stabiliteitsvergelykings. Die hidrouliese stabiliteit van hierdie strukture is dus grotendeels onbekend.

Die hoofoogmerk van hierdie studie was om ondersoek in te stel na die effek van struktuurhellings en pakformasies op die hidrouliese stabiliteit van GSH-bedekte hellings. Die toepaslikheid van beskikbare ontwerpriglyne en stabiliteitsvergelykings is ook geëvalueer. Tweedimensionele fisiese modellering is onderneem en altesaam 12 GSH-bedekte hellings is gedurende die fisiese-modelleringstoetsreeks getoets. Die resultate van die fisiese modellering toon dat die struktuurhelling die beduidendste effek op hidrouliese stabiliteit het. Steiler struktuurhellings was hidroulies meer stabiel as platter hellings. Die pakformasies van die GSH's blyk 'n kleiner effek op die hidrouliese stabiliteit van die GSH-bedekte hellings te hê. GSH-bedekte hellings wat met 'n enkele laag GSH's versterk is, het ewe goed of beter presteer as die keermure met 'n dubbele laag GSH's, terwyl GSH-bedekte hellings met die lang-as van die GSH's loodreg op die rigting van die golfaanslag effens beter presteer het as dié met die lang-as parallel met die golfaanslag.

Die beskikbare ontwerpriglyne en stabiliteitsvergelykings is geëvalueer aan die hand van die resultate van die fisiese modellering, en het 'n wisselende mate van korrelasie getoon. Veral die stabiliteitsvergelyking van Recio (2007) blyk besonder akkuraat te wees.

Acknowledgements

I would like to express my gratitude and heart-felt thanks to a number of people who contributed to the successful completion of this thesis:

I would like to first thank Mr Geoff Toms, my study supervisor, who guided me through my thesis. He was always on hand to offer support and motivation with patience and genuine interest. I consider Mr Toms to be a great mentor and role model and will continue to seek out his advice as I begin an exciting career in the field of Coastal Engineering.

Advice and suggestions from Mr A. Theron, Mr D. Phelp and Mr K. Tulsi from the CSIR proved to be invaluable. Their support and guidance allowed me to undertake the physical modelling with confidence.

Professor B. Brinkman (Leuphana University Lüneburg) and Ms K Werth (NAUE) involvement in the research project proved helpful, especially in the initial phases of this thesis. MS Werth also facilitated the sponsoring, through *NAUE GmbH & Co. KG. / Bauberatung Geokunststoffe GmbH & Co. KG,* of the geotextile material used in the physical modelling.

Without the help of the Hydraulic Laboratory personnel: Mr C. Visser, Mr N. Combrinck, Mr A. Lindoor and Mr E. Wanza, this study would not have been possible.

Moreover, I would like to thank my friends with whom I studied with at Stellenbosch University: Herman Kriel, Pierre Hugo, George Roux, Padhraic O'Connor and Felipe Guerrero. Together we have had some fantastic times and I look forward to many more.

Lastly, but certainly not least, I would like to thank my parents Ann and Christian, my sister Natasha as well as my grandparents, aunts and uncles for their unwavering love and support.

Christophe Baret

Contents

List of Figures

List of Tables

1   Introduction

The interaction between human development and the coastal zone has not always been a harmonious one. Erosion of sandy beaches along certain stretches of the South African coastline has become a critical concern to municipalities and private land owners alike. Many buildings and municipal facilities are under threat from wave attack after erosion has taken place. These buildings and facilities have been placed too close to the dynamic sea-shore interface and as a consequence may be damaged or lost completely and could ultimately even endanger human lives. This situation will only be exacerbated in the future with predicted climate change and anticipated sea-level rise. This interaction thus has to be carefully managed with coastal engineering solutions that protect infrastructure as well as taking care not to compromise sensitive and valuable coastal ecosystems.

Innovative and versatile structures made of Geotextile Sand Containers (GSCs) are increasingly being incorporated into coastal management solutions because of their cost effective and environmentally friendly characteristics. This is as opposed to conventional 'hard' coastal protection solutions that utilise rocks and or concrete to protect the coastline

The use of GSC structures had initially been quite limited in South Africa with some applications in the form of groynes and revetments. The use of GSC structures became more popular, especially along the KwaZulu-Natal coastline after a particularly severe series of storm events eroded up to 40 meters (horizontal) of coastline in some areas (Phelp et al, 2009). Municipal infrastructure and private properties were damaged and immediate protection solutions were necessary. Geotextile sand container revetments were used as a coastal protection solution in many instances.

There are many advantages for using geotextile sand containers as coastal protection solutions. As mentioned previously, the 'soft' coastal protection solution is both more environmentally and economically beneficial than alternative 'hard' coastal protection solutions. Construction requirements are relatively simple and can be done with standard earth moving equipment and non-skilled labour. This is ideal in developing countries where labour and sand is abundant and in close proximity to most sites. GSC structures are flexible and conform readily to site conditions and the use of GSC structures allows for a more flexible and adaptive approach that can more easily be modified if the desired outcome is not satisfactory or if the design conditions change. GSC structures can even be easily removed in the event that the GSC structure does not perform. Fauna and flora indigenous to the area can be encouraged to grow on these GSC structures which result in a visually low impact solution.

With GSC structures being a relatively new coastal protection solution, few design guides and stability equations are available. Research into the behaviour of GSC structures under wave attack is on-going with particular emphasis on the hydraulic processes that affect GSC structures and cause them to fail.

1.1 General Overview of Geotextiles Used in Coastal Engineering Structures

This section provides brief look into how geotextiles have been used in different applications.

1.1.1 GSC Sea Wall: Kingscliff, Australia

A surf club situated at Kingscliff was at increased risk of damage due to continuing beach erosion problems. In 2011 a single layer GSC armour sea wall was constructed with 2.5m³ GSCs after 0.75m³ GSCs proved to be unstable under wave attack during the initial construction phase.

Figure 1-1: Kingscliff Seawall (Geofabrics Australasia Kingscliff Seawall Case Study, 2011)

1.1.2 GSC Revetment: Jumeirah Open Beach, Dubai

An amenities block which was prone to wave attack on the Jumeira Open beach was in need of protection. A GSC revetment was installed in 2003 with two sizes of GSCs. Containers of 0.75m³ and 2.5m³ were used. This was a temporary measure prior to beach nourishment.

Figure 1-2: Jumeirah Open Beach (Geofabrics Australasia Jumeirah Beach Seawall Case Study, 2003)

1.1.3   Geotextile Wrap-around Revetment: Kliffende Haus, Germany:

Arguably one of the more famous applications of geotextile applications is that of Kliifende Haus. A fast eroding cliff face put the classic farm house in danger of falling into the sea. A geotextile wrap-around revetment was constructed in 1990 to halt the cliff erosion. This proved effective, as can be seen in the photograph below.

Figure 1-3: GSC Wrap-around Revetment in Sylt, Germany (Pianc, 2011)

3

1.1.4 GSC Artificial Reef: Narrowneck Reef, Australia

In order to protect the beach capacity along a critical section as well as improve surfing conditions, an artificial reef was constructed with 400 sand filled geotextile tubes placed on the seabed. The reef was constructed in the year 2000 and has proved effective in maintaining beach capacity. The tubes are 20m long and 4m in diameter.

Figure 1-4: Artificial reef constructed of geotextile tubes. (Geofabrics Australasia Narrowneck Reef Case Study, 2000)

1.1.5 GSC Groyne: Langebaan, South Africa

GSC groynes were constructed to prevent further erosion of a popular beach in Langebaan. Various municipal facilities and residential houses were at risk from wave attack and flooding. The GSC groynes were constructed with 3.5 to 4.0 ton containers.

Figure 1-5: Photograph of GSC Groyne in Langebaan, South Africa (Author, 2011)

1.1.6 Temporary Geotextile Structures

Geotextiles can also be utilised in temporary coastal structures either as emergency coastal protection or for temporary construction works. The adaptable and easily removed nature of geotextile structures makes them ideal for temporary applications. Theron et al (1994) and Theron et al (1999) investigated, with the use of prototype testing, the effectiveness of several types of temporary geotextile structures. Geotextiles in the form of sand bag revetments, sand sausage revetments, sand-envelopes, sand bars and sand bag groynes are examples of some of the structures investigated. Theron et al (1994) and Theron et al (1999) reported that sand bag revetments and sand-envelopes proved the most effective.

These temporary structures differ from permanent geotextile structures predominantly in how they are constructed. Temporary geotextile structures are placed directly on the sand so they can sink into the sand during wave action. This occurs quickly after deployment and forms a stable toe on which to support the rest of the structure (Theron et al, 1999). This is as opposed to permanent structures in which time is taken to construct a formal toe through more conventional means, such as embedding the toe of the structure well beneath the sand.

A particularly novel use of temporary geotextile structures, as reported by Schoonees et al (1999), was used along the False Bay coastline of South Africa. Two temporary groynes constructed of large sand bags were constructed to trap sediment. In this way the longshore sediment transport rates could be measured and used in the design of coastal structure within False Bay.

1.2 Geotextile Structures in South Africa

The use of geotextile structures as a means of coastal protection is gaining in popularity in South Africa due the advantages they offer over traditional rock and concrete structures, as previously mentioned. The most common geotextile structures found in South Africa today are revetments constructed with geotextile sand containers (GSCs). In this report, a 'revetment' is daefined as a slope reinforcement at the interface between the upper beach and the raised hinterland, simply referred to as: the back of the beach. The revetment would typically be placed in front of an existing primary dune. This allows the structure to accommodate seasonal variations in the beach profile as shown in Figure 1-6 through to Figure 1-9.
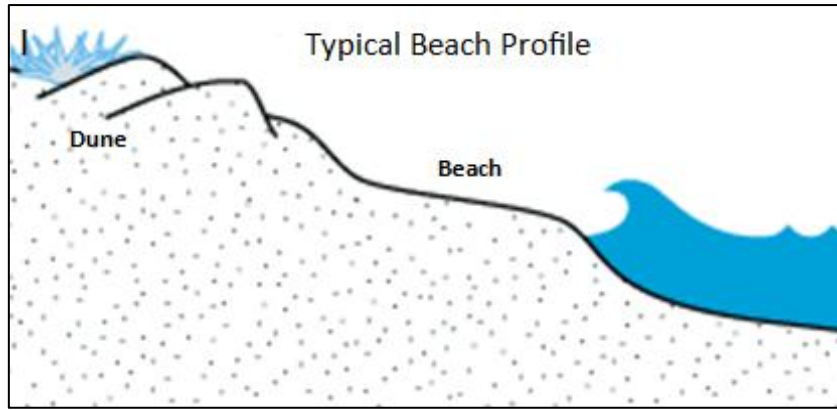
Figure 1-6: Typical Beach Profile
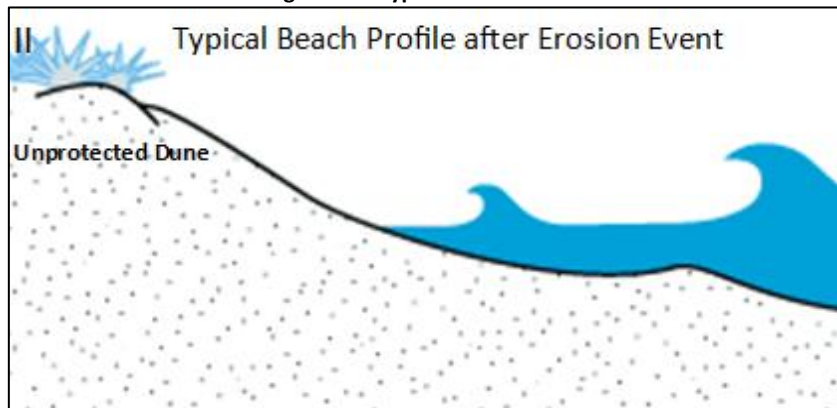
Figure 1-7: Beach Profile after Erosion Event
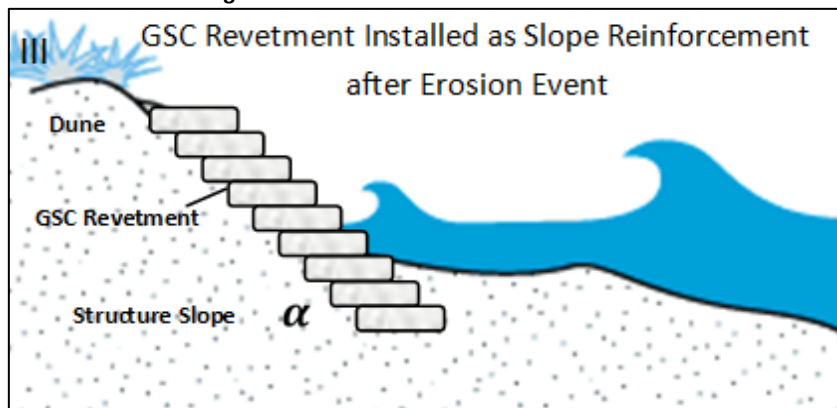
Figure 1-8: GSC Revetment as Slope Reinforcement
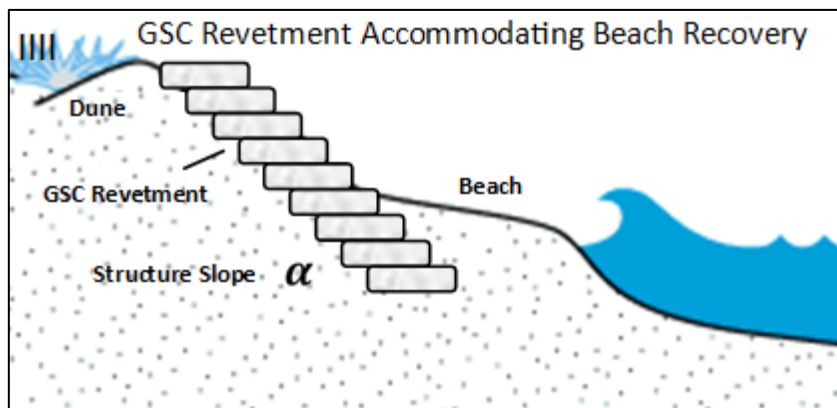
Figure 1-9: GSC Revetment as Slope Reinforcement Accommodating Beach Recovery

The Figures above illustrate the seasonal variations of a typical beach profile as well as its interaction with the GSC revetment. This seasonal variation is site specific but most beaches in South Africa recede during the stormy winter months accrete during the calmer summer months. In some cases the GSC revetment is completely buried in the primary dune and is then referred to as a sleeping defence. As with most coastal structures the toe of the GSC revetment is critical to the stability of the structure as a whole. Typically the toe is buried deep enough that when an erosion event occurs it will remain buried, as illustrated in Figure 1-8. This usually results in the toe being buried to more or less the high water mark (HWM). These GSC revetments are usually associated with temporary works, but as is often the case these structures become a more permanent solution and are increasingly built as such. Certain GSC structures have been in place for over 20 years and are still performing well (see Chapter 1.1.3) and thus showing great potential. Equally there have been many GSC structures that have performed very poorly due a number of factors including under-design and poor construction techniques.

GSC revetments in South Africa are predominantly found along the KwaZulu-Natal coastline. The eThekwini Municipality (Durban) has constructed numerous GSC revetments to protect private properties and municipal facilities against wave attack. The need for such protection came about after an extreme wave event, which coincided with the highest tide of the year (HTOY), caused widespread erosion of the beaches and damage to various structures along large stretches of the coastline (Phelp *et al*, 2009). As part of this thesis an inspection of this coastline was conducted by the author, which revealed that Umhlanga and Umdloti were particularly badly affected. Single layer GSC revetments were constructed along these beaches with GSCs of 2.4mx2mx0.5m or 3.5-4.0 tonnes each, usually nine bags high at a slope of around 1V:1.5H. Figure 1-10 to 1-11 show the completed installation of GSC revetments as seen along Umhlanga and Umdloti beaches.

Figure 1-10: Photographs of GSC Revetment at Umdloti (Author, 2011)

Figure 1-11: Photographs of GSC revetments at Umhlanga (Author, 2011)

The erosion of the beaches in certain areas lasted longer than the storm event. This was particularly evident where rocky headlands prevented nourishing of down-drift beaches (Phelp *et al*, 2009.)The construction of these revetments was done as a priority to avoid further loss and there was little time to thoroughly validate the design used before construction commenced. Similar GSC revetments constructed before the storm had proved successful against localised erosion (Phelp *et al*, 2009). However, no detailed investigation was undertaken in the design of these structures and the hydraulic stability is somewhat unknown.

1.3   Motivation

The hydraulic stability of the GSC revetments constructed in KwaZulu-Natal, South Africa, is largely unknown. The GSC revetment design falls outside the limitations of available design charts and stability equations. This is due to the unique structure slope and packing arrangements of this particular revetment design. This thesis addresses back of beach GSC revetments as described in Section 1.2. The motivation of this study is thus to broaden the current understanding of the effects that different structure slopes and packing arrangements have on the hydraulic stability of GSC revetments.

1.4   Study Objective

The primary objective of this study is to investigate the effect of structure slopes and packing arrangements on the hydraulic stability of GSC revetments. The application of available design charts and stability equations will also be evaluated.

1.5   Methodology

In order to meet the objectives of this study the following methodology is undertaken:

I.   Undertake a detailed literature review so as to identify and understand the most relevant aspects to the hydraulic stability of GSC revetments.

II.   Perform two-dimensional physical model tests to investigate the effect that various structure slopes and packing arrangements have on the hydraulic stability of GSC Revetments.

III. Analyse the results of the two-dimensional physical model test and compare the results with available design charts and stability equations for evaluation purposes.

IV.   Comment on the effect of that various structure slopes and packing arrangements have on the hydraulic stability of GSC Revetments as well as the applicability of design charts and stability equations.

```
┌─────────────────────────────────────────────┐
│              Literature Review               │
└─────────────────────────────────────────────┘
                      ↓
┌─────────────────────────────────────────────┐
│              Physical Modelling              │
└─────────────────────────────────────────────┘
                      ↓
┌─────────────────────────────────────────────┐
│ Results Analysis as well as Evaluate Design  │
│        Chart and Stability Equation          │
└─────────────────────────────────────────────┘
                      ↓
┌─────────────────────────────────────────────┐
│         Recomendations and Conclusions       │
└─────────────────────────────────────────────┘
```
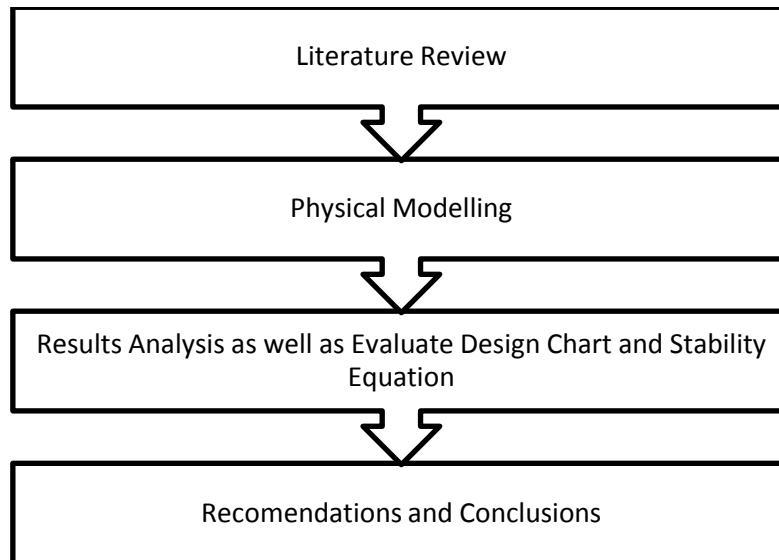
Figure 1-12: Methodology of this Study

In addition to the methodology outlined above, the author was fortunate enough to conduct site visits in South Africa as well as in Germany as part of the research project: "Development of Sustainable as well as Environmental-friendly, Adaptive and Cost-effective Technical Protection Measures for Sandy Beaches", funded by the BMBF and the NRF and undertaken in co-operation with the CSIR (Stellenbosch). Valuable insight into the application of geotextiles to the various prototype coastal structures was gained. It is evident from the site inspections that the range of applications of geotextile structures is wide and that they are relevant as a current coastal protection solution.

1.6 Report Layout

This report comprises of six main chapters which strives to guide the reader through the steps taken in order to meet the objectives of this study. The first Chapter introduces the reader to the application of geotextiles in coastal structures and provides the background context on which this study is based. Chapter Two, presenting a detailed literature review on the topic, follows. Chapter Three covers details related to the two-dimensional physical modelling design and construction. Details on the tests and test results from the physical modelling are presented in Chapter Four. Chapter Five covers the analysis of the physical model test results and evaluation of the available design charts and hydraulic stability equations. This report ends with Chapter Six containing final remarks on the effect of structure slope and packing arrangements on the hydraulic stability of GSC revetments based on the findings of the before mentioned chapters as well as recommendations of avenues of further research.

2   Literature Review

A literature review is undertaken to identify the important aspects relating to the hydraulic stability of GSC revetments. This chapter covers six main sections:

1. Mechanical Properties of GSCs and GSC Revetments
2. Hydraulic Permeability of GSC Revetments
3. Processes relevant to the Hydraulic Stability of GSC Revetments
4. Failure Modes of GSC Revetments
5. Available Design Charts and Stability Equations.

2.1   Mechanical Properties of GSCs and GSC Revetments

The mechanical properties of GSCs are important to the overall hydraulic stability of GSC revetments. The nature of these mechanical properties is that many of them are interrelated as shown in Figure 2.1.
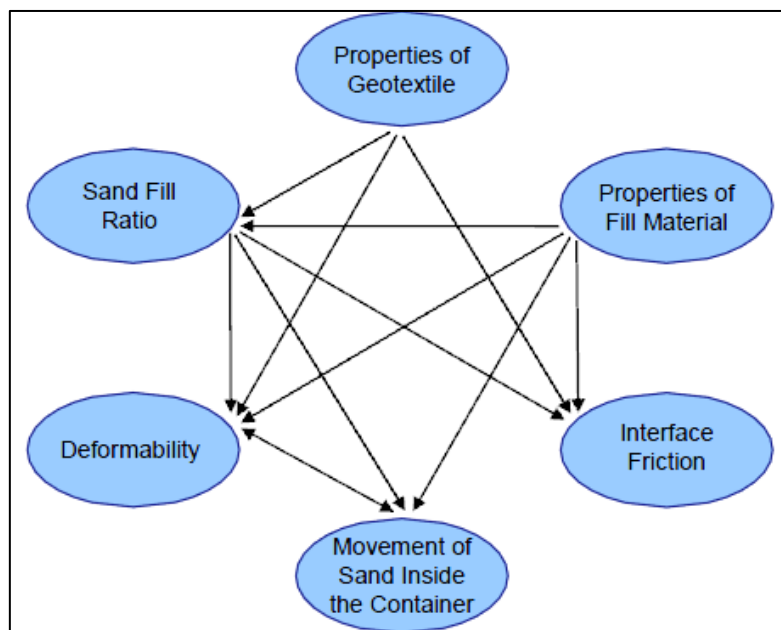
Figure 2-1: Interrelationship of mechanical properties of GSCs (Dassanayake *et al*, 2012a)

This interrelated nature of the GSC mechanical properties is what makes the assessment of the hydraulic stability of GSC revetments complex. In order to proceed with this assessment the mechanical properties of GSCs are first defined and discussed.

2.1.1   Properties of Geotextile Material

The geotextile material used to fabricate GSCs largely dictates the performance of a GSC and subsequently that of a GSC revetment. Geotextile materials can be subdivided into three main types (PIANC ,2011):

- Woven geotextiles: produced by interlacing two or more filaments, usually at right angles
- Non-woven geotextiles: produced by randomly orientated fibres, which are bonded mechanically, thermally or chemically or a combination thereof
- Knitted geotextiles: produced by interloping one or more filaments
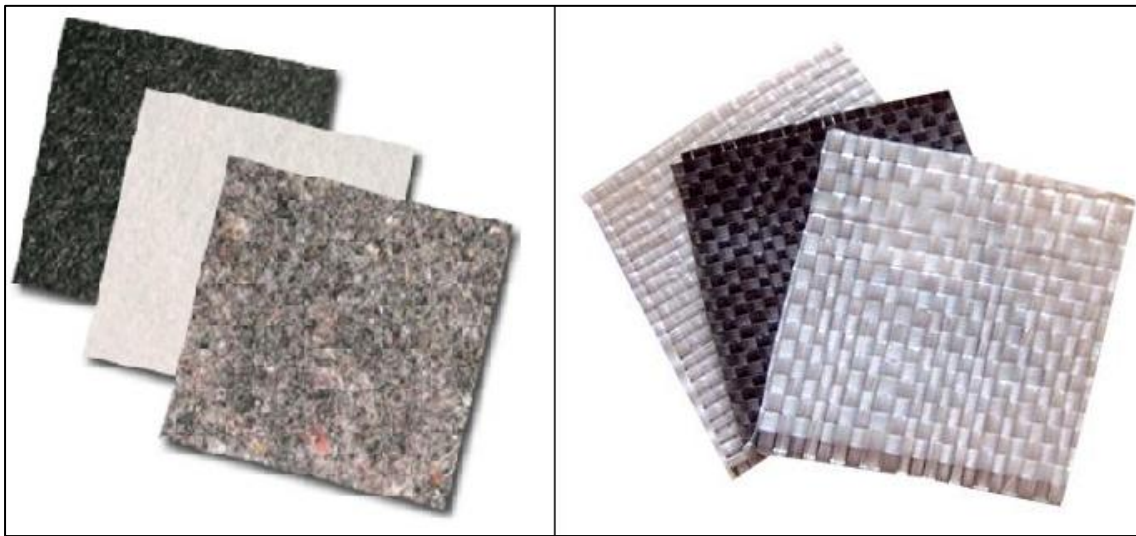
Figure 2-2: Non-woven Geotextile (Left) and Woven Geotextile (Right), (Photo: Geosintex, 2012)

The majority of geotextiles are made from polypropylene polymers (PP) of which the physical properties are shown in Table 2.1 below. Woven and knitted geotextiles are used when high tensile strength is required and non-woven geotextiles are used when deformation capabilities, robustness and porosity for filtration efficiency is required (PIANC, 2011). The characteristics of non-woven geotextile make it ideal for use in sand container applications such as GSCs.

Property	(PP)	Units
Density	900	kg/m³
Tensile Strength	400-600	N/mm²
Elasticity	2000-5000	N/mm²
Strain at Failure	10-40	%
Melting Point	160	˚C

Table 2-1: Physical properties of polypropylene polymers (PP), (PIANC, 2011)

As is evident from Table 2-1, the elongation (strain) that a geotextile can withstand before failure is quite high. This elongation property influences the deformability of GSCs which in turn causes the lowering of the sand fill ratio. The significance of the sand fill ratio is discussed in 2.1.4.

The effective strength of a geotextile depends, to a large extent, on the connection strength of the seam. The seam strength depends on the type of geotextile sewing joint (PIANC, 2011). In the case of GSCs, which are usually filled and sealed on site, the strength of the sewing joint can vary from 30-70% of the strength of the geotextile. An overview of the types of seams and their efficiencies are shown in Table 2.2.

Seam type	Description	Strength of a seam, sewn in the selvage side
	Prayer seam	30-50 % of the strength of the fabric
	Butterfly seam	40-70 % of the strength of the fabric
	J-seam	30-60 % of the strength of the fabric
	Double J-seam	50-70 % of the strength of the fabric
	Z-seam	> 70 % of the strength of the fabric This type of seam can only be made in the factory

Table 2-2: Strengths of various types of seams (adapted from PIANC, 2011)

The friction factors and friction angles of the geotextile materials used for GSCs have a significant effect on GSC revetments when one considers the influence these have on the interface friction between neighbouring GSCs, and thus on the overall hydraulic stability of the GSC revetment. Initially, direct shear stress tests were used to determine the friction angles and friction factors of geotextile materials (as those in Table 2.3 have been). More recent studies however (Krahn *et al*, 2007), have shown that the estimations of interface friction determined by direct shear tests are not accurate enough. Krahn *et al* (2007) conducted large scale interface shear testing of sandbags and found that the shear strength between sand filled bags is greater than that of geotextile material by itself. However, this is difficult to quantify as the shear strength between sand filled bags is dependent on many other variables (such as the sand fill ratio) than just the friction characteristics of the geotextile material. It is nonetheless worth keeping in mind when considering GSC revetment

design. Friction angles and friction factors for geotextile materials derived from direct shear tests are presented below.

	Interface Materials	Friction Angle ϕ	Friction Factor $\tan \phi$
Nonwoven Geotextile	Terrafix 1200R (mechanical nonwoven) vs. Sand	30.11	0.57
	Terrafix 1200R (mechanical nonwoven) vs. Terrafix 1200RP	25.97	0.48
	Terrafix 1200RP (mechanical nonwoven) vs. Terrafix 1200RP	22.53	0.41
Woven Geotextile	Geolon PP120S (woven) vs. Geolon PP120S	20.38	0.37
	Mirafi GT1000 (woven) vs. Mirafi GT1000	14.80	0.26
	Mirafi GT500 (woven) vs. Mirafi GT500	11.91	0.21

Table 2-3: Friction Angles and Friction Factors as determined from direct shear tests (after Naue (2004) as cited by Recio, 2007)

2.1.2   Properties of Fill Material

The properties of the fill material of GSCs can affect many aspects of a GSCs overall behaviour and as such, also affect the hydraulic stability of a GSC revetment. The properties of the fill material have the potential to affect the movement of fill, or transport of fill, within the GSC through migration caused by hydraulic processes. In doing so the fill material can influence important hydraulic stability aspects of a GSC, such as: sand fill ratio, deformability of the GSC and the interface friction of GSCs.

GSCs are usually filled with sand, local to the area in which they are being installed, so as to keep the cost of transporting materials to a minimum. Sand properties vary widely around the world and as such it is important to understand the effect that different types of fill material (sand) will have on the hydraulic stability of GSC revetments. Unfortunately, this effect has not been widely investigated and influence of the fill material properties on GSC revetment hydraulic stability remains unclear.

2.1.3   Interface Friction

The interface friction between geotextile-geotextile and geotextile-sand interfaces is of great importance to the hydraulic stability of GSC structures. Interface friction depends on the type of geotextile material, the sand fill ratio and the overlapping length of the GSC (Dassanayake and Oumeraci, 2012a). Recio (2007) developed equations for the hydraulic stability of GSCs that take the interface friction of the geotextiles into account. Although progress is being made, there is still more research to be done in order to fully understand and quantify the interface friction between GSCs.

2.1.4   Sand Fill Ratio

The sand fill ratio of GSCs is an important parameter when considering the hydraulic stability of GSC structures (Recio, 2007). As is evident in Figure 2-1, which illustrates the interrelationship properties, the sand fill ratio affects the interface friction between GSCs, the movement of sand within the GSC as well as the deformability of the GSC. Despite its importance there are no existing stability formulae that account for this variable. In addition, the definition of the sand fill ratio itself is not accurate or consistent enough. The problem with accurately defining the sand fill ratio is encountered when considering what the maximum fillable volume is, as geotextile materials tend to elongate during the filling process.

Dassanayake and Oumeraci (2012a) proposed that the maximum volume of a GSC be calculated in terms of a theoretical maximum as developed by Robin (2004). This theoretical maximum is relevant for a flat rectangular bag that can neither stretch nor shear and yields the maximum volume when fully inflated. The concept is described in Figure 2.3
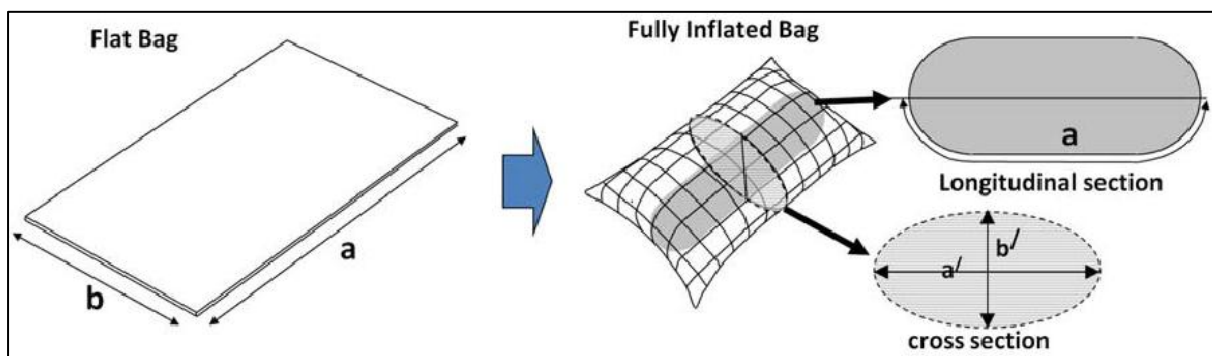
Figure 2-3: Theoretical Volume of a GSC (Dassanayake and Oumeraci, 2012)

The equation for the theoretical maximum theoretical volume of a GSC as proposed by Dassanayake and Oumeraci (2012a) and developed by Robin (2004) is as follows:

$$V_{theory} = a^3 \left[\frac{b}{\Pi a} - 0.142 \left(1 - 10^{-\frac{b}{a}} \right) \right]$$

Where:

- a = the length of a GSC (m)
- b = the width of a GSC (m)

The actual volume (V_{actual}) of a particular GSC is then calculated based on its mass and the bulk density of the fill material. The sand fill ratio can thus be expressed as:

$$Sand\ Fill\ Ratio = \frac{V_{actual}}{V_{theory}} \times 100$$

Where:

- $V_{actual} = \frac{Mass_{GSC}}{\rho_s}$
- $Mass_{GSC}$ = the measured mass (kg)
- ρ_s = the bulk density of the fill material (kg/m³)

Dassanayake and Oumeraci (2012b) performed physical model tests to establish which sand fill ratio was optimal for the hydraulic stability of a GSC revetment. The model tests were designed to test the hydraulic stability of GSCs at different fill ratios. Through these model tests they found that the optimum sand fill ratio is between 90%-100%. This goes against previous studies which recommend that the fill ratio should not exceed 80% as the GSC would become too stiff and would therefore not to be able to adjust to the sand bed or surrounding GSCs (PIANC, 2011). Dassanayake and Oumeraci (2012b) explained that the reason behind greater hydraulic stability of GSCs with greater sand fill ratios (100%) than those with moderate sand fill ratio (80%) is that the advantages of increased weight and possibly increased permeability are more important than the disadvantages of lesser overlapping length and contact areas.

2.1.5   Deformability and Movement of Fill Material

The deformability of a GSC, depends on the elongation characteristics of the geotextile material, the sand fill ratio of the GSC, the properties of the fill material as well as the movement of sand within the GSC. The deformability of a GSC is one of the most important aspects of the stability of a GSC revetment. The process of deformation is unique to GSCs and GSC structures and as such, it is the focus of many of the investigations on hydraulic stability of GSC revetments focus on it.

The deformation of a GSC occurs when fill material (sand) migrates under hydraulic process such as wave attack. The extent of this deformation is governed by the elongation characteristic of the geotextile material as well as the fill ratio of the GSC. The fill material properties influence the magnitude of the hydraulic process required to begin the migration of fill material (sand).

2.2   Hydraulic Permeability of GSC Revetment

In general the permeability of a revetment is directly associated with its stability. The higher the permeability; the higher the stability of a revetment. This is due to a higher permeability reducing the seepage forces and pressures in the structure (Recio, 2007). Little Information was available on the permeability of GSC structures until Recio (2007) completed hydraulic model test. Recio, determined the permeability of GSC structures with various packing arrangements and different sizes of GSCs, and then went further and tested the stability of these permutations under wave attack.

From the process based physical model tests, Recio (2007) concluded the following:

I.   The flow through and therefore the permeability of the GSC structure is governed by the size of gaps between the individual GSCs

II.   GSC structures with smaller GSCs will have smaller permeability coefficients. This is due to a GSC structure with smaller GSCs having more but smaller gaps and as such the friction losses of the gap flow will be higher.

III. Longitudinal and transverse GSC arrangements yield similar total flows through the structure. However, the hydraulic stability of a transversely placed GSC under wave attack is lower than of a longitudinally placed GSC.

IV.   The permeability of a GSC structure is considerably reduced if there is a second layer of overlapped containers that obstructs the flow from the gaps in the first layer.

V.   If no reliable data is available, a permeability coefficient of $k = 10^{-2}$ m/s is suitable for GSC revetments.

VI.   The mode of placement of the GSCs considerably affects the permeability of the structure

2.3   Processes Relevant to the Hydraulic Stability of GSC Revetments

The hydraulic processes affecting the hydraulic stability of GSC revetments are now considered. The main processes identified (Recio, 2007) are as follows:

- Wave Reflection
- Wave Overtopping
- Wave Runup
- Wave Uprush and Downrush
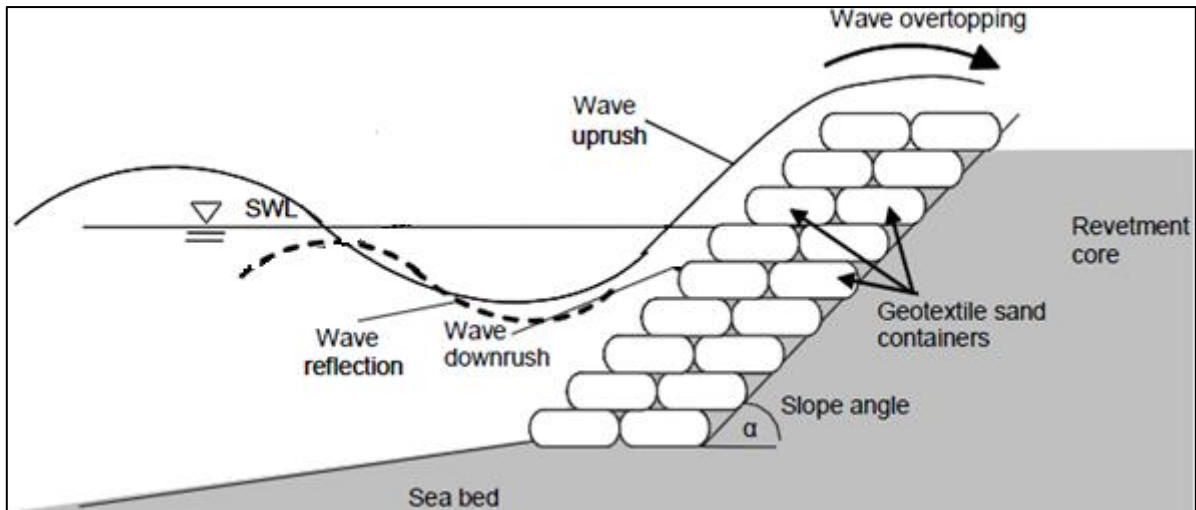
Figure 2-4: Main Hydraulic Processes acting on a GSC Revetment (adapted from Recio, 2007)

The interaction of these hydraulic processes and the characteristics of GSC structures were thoroughly investigated by Recio and Oumeraci (2009). Based on this interaction the following processes were considered important to the hydraulic stability of GSC revetments and investigated with a series of physical model tests:

I.   Wave-induced loads on the GSCs

II. Wave induced flows on the GSCs

III. Internal movement of sand in the GSCs

IV. Variation of contact areas among neighbouring GSCs during wave attack

V.   Types of displacements of GSCs within a GSC revetment

VI. The effect of deformation of GSCs on the stability of GSC revetments

The physical model tests were performed at the Leichtweiss Institute wave flume. A scale model structure made with GSCs was placed at one end and subjected to varying heights of regular and irregular waves. Various types of equipment are used to record data from the tests, including: a particle image velocimetry (PIV) system to record wave-induced flows, a permeable transparent container filled with coloured sand to investigate sand movements inside the container, an instrumented container was used to record pressure data from which wave induced forces and moments could be calculated and common resistance type wave gauges were used to record surface water variations. More details about the experimental setup can be found in Recio and Oumeraci (2005b). To date, these physical model tests are the only detailed investigation into the processes that affect the hydraulic stability of GSC revetments. Considering the objectives of this study, the physical model tests of Recio and Oumeraci (2005b) are important and receive significant attention in this literature review.

18

2.3.1   Wave Induced Loads on the GSCs

2.3.1.1   *Wave Induced Pressures and Forces on Instrumented Container*

The pressure data recordings are used to calculate the resultant forces and moments on the container during a wave cycle through integration. Two distinct observations were made. Firstly, the largest wave induced pressures are recorded at the container placed just below the still water level (SWL). Secondly, the largest pressures were recorded at the commencement of the downrush phase of a wave cycle.

The significance thereof is that it can thus be said that the critical area concerning the stability of GSC revetments is the area just below the SWL at the commencement of the downrush phase of a wave cycle. The reason for this is explained as a "build-up" of the hydraulic gradient inside of the structure. This "build-up" is caused by the fact that the wave uprush and wave downrush velocities differ, thus producing a hydraulic gradient. The process is summarised in Figure 2.5 below.
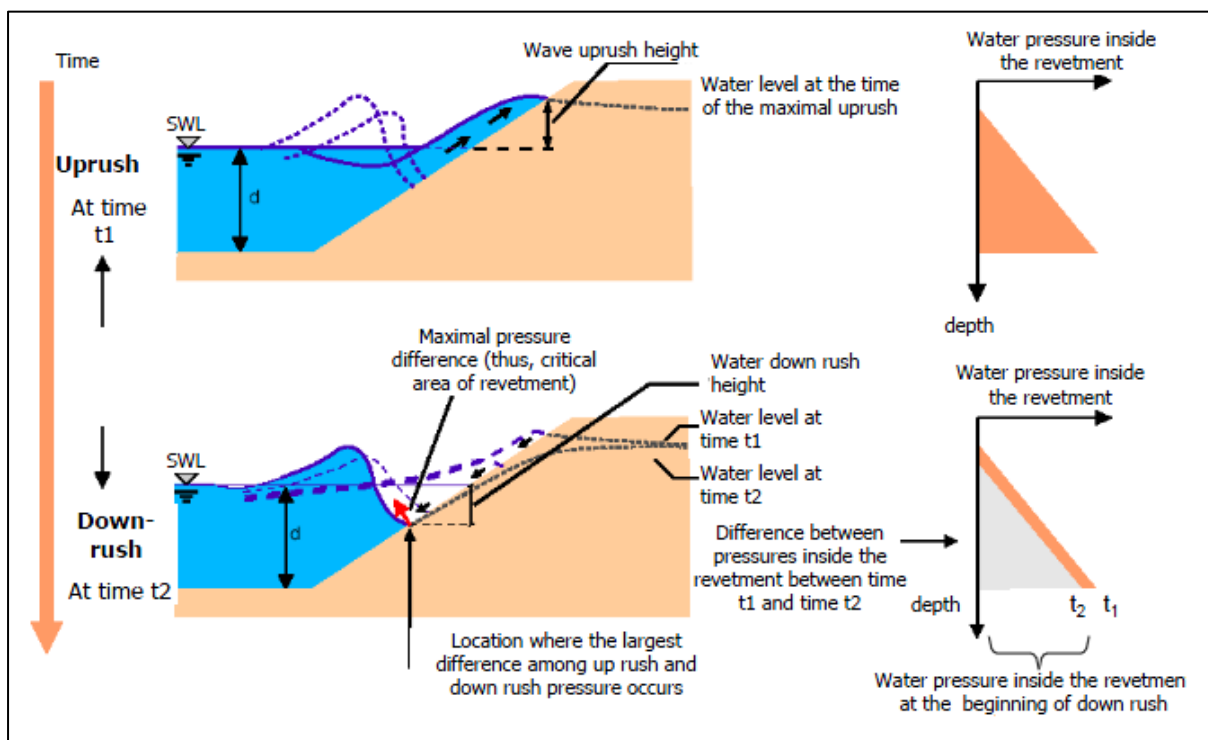
Figure 2-5: Wave-induced pressures in front and inside a GSC-Structure (as modified by Recio, 2007)

2.3.1.2   *Breaking Wave Loads on GSC Structures*

A concern with GSC revetments in terms of hydraulic stability is the presence of gaps between the GSCs. When under wave attack, the horizontal and uplift forces generated inside of the gaps may

lead to the collapse of the structure. The physical modelling tests set out to determine the pressure propagation along the gaps between GSCs.

It was found by Recio and Oumeraci (2005b) that when a breaking wave hits the area just above the SWL, the instrumented container located in the impact zone recorded the largest pressures on the front of the container. The GSC above then proceeds to lift upwards and rotate clockwise, while the GSC below proceeds to move downward and rotate anti-clockwise. Analysis of propagation inside the gap reveals that due to the flexibility and porosity of GSCs, there is decrease of pressure as it propagates along the length of the gap. This is contrary to what would be observed in a gap with rigid and impermeable boundaries as reported by Marth et al (2005)

A comparison was also made between the loads induced by breaking and non-breaking waves. The force loads were found to be similar for both types of waves. Since the duration of non-breaking waves is longer, Recio and Oumeraci (2005b) concluded that breaking waves were less critical to the stability of GSC revetments than that of non-breaking waves. The results of the comparison are shown in Table 2-4.

	Breaking Wave	Non-Breaking Wave
Maximal wave induced pressure (kPa)	3.8 (quasi static + impact = 1.8+2.0=3.8)	1.8
Duration of maximal wave-induced pressure (s)	0.1	1.2
Maximal total force (integration of pressures) (N)	33.49	55.87
Duration of maximal total force (s)	≈ 0.40	≈ 0.60

Table 2-4: Comparison between Wave-Induced Pressure by Breaking/Non-Breaking Waves (Recio, 2007)

2.3.2   Wave Induced flows on a GSC Revetment

There are two distinct wave induced flows next to a GSC structure. The main flow, relevant to the whole structure, runs up and down the revetment with velocity vectors approximately parallel to the structure slope. The second flow is localised to each step in the GSC revetment and is orbital in motion. The orbital motions are caused by vortices from the main flow and have a clockwise direction during uprush and an anti-clockwise direction during downrush. The effects are shown visually in Figure 2.6.
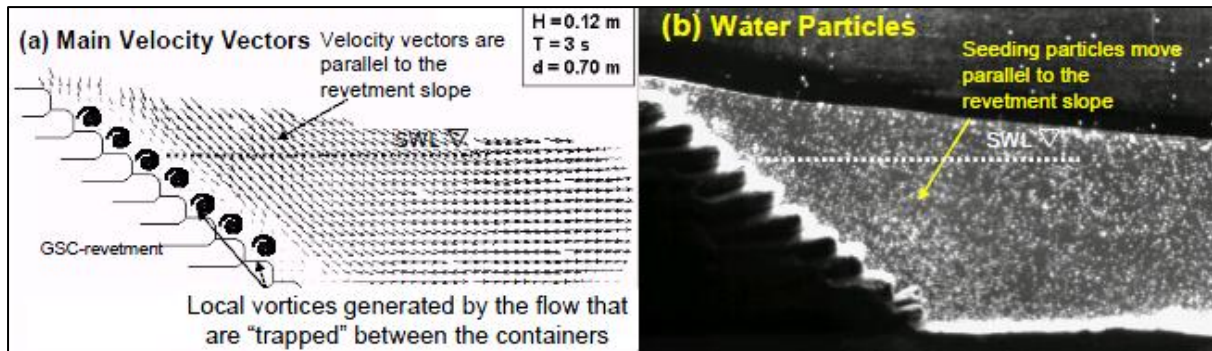
Figure 2-6: Global and Local Effects of wave induced flow on a GSC Revetment (Recio, 2007)

The main flow causes an "uplift" deformation of the GSC during the uprush phase of the wave cycle and then causes a return process of the uplifted part of the GSC to the normal position. A seaward directed force is also developed on the downrush phase of a wave cycle which is termed as the "pull-out effect". The localised orbital flow is responsible for small rotational forces on the GSCs and could also affect the hydraulic stability of a GSC revetment.

2.3.3   Internal Movement of Sand

Video analysis by Recio and Oumeraci (2005b) of the movement of coloured sand inside a transparent GSC proved useful in explaining the process caused by wave attack. Observations from video analysis concluded that:

I. A similar pattern of sand movement occurs for different wave conditions. However, noticeable movements of sand are only induced by large incident waves

II. The majority of sand movements occur within the first 30 wave cycle, after which it rapidly decreases. This is due to the sand fill re-accommodating because of the wave induced forces on the GSC

III. During the uprush phase of a wave cycle the sand movement is rotational and directed upwards

IV. During the downrush phase of a wave cycle the sand movement is directed seaward.

V. The sand accumulates at the seaward end of the GSC after a few wave cycles. This causes a deformation of the seaward end of the GSC and reduces the contact areas with the neighbouring GSCs

VI. Internal movements of sand are triggered by the incremental horizontal movement of the GSC. This is due to the contact areas of the GSC and neighbouring GSCs being reduced.

The most important conclusion drawn from these physical model tests is that the internal movement of sand in GSCs will affect the hydraulic stability of GSC revetments. Furthermore, the sand fill ratio is identified as a critical parameter to the hydraulic stability of a GSC. A GSC with a very low sand fill ratio will be much more unstable than an optimally filled GSC. Figure 2.7 below illustrates the internal movement on sand of a GSC as observed by Oumeraci et al, 2009.
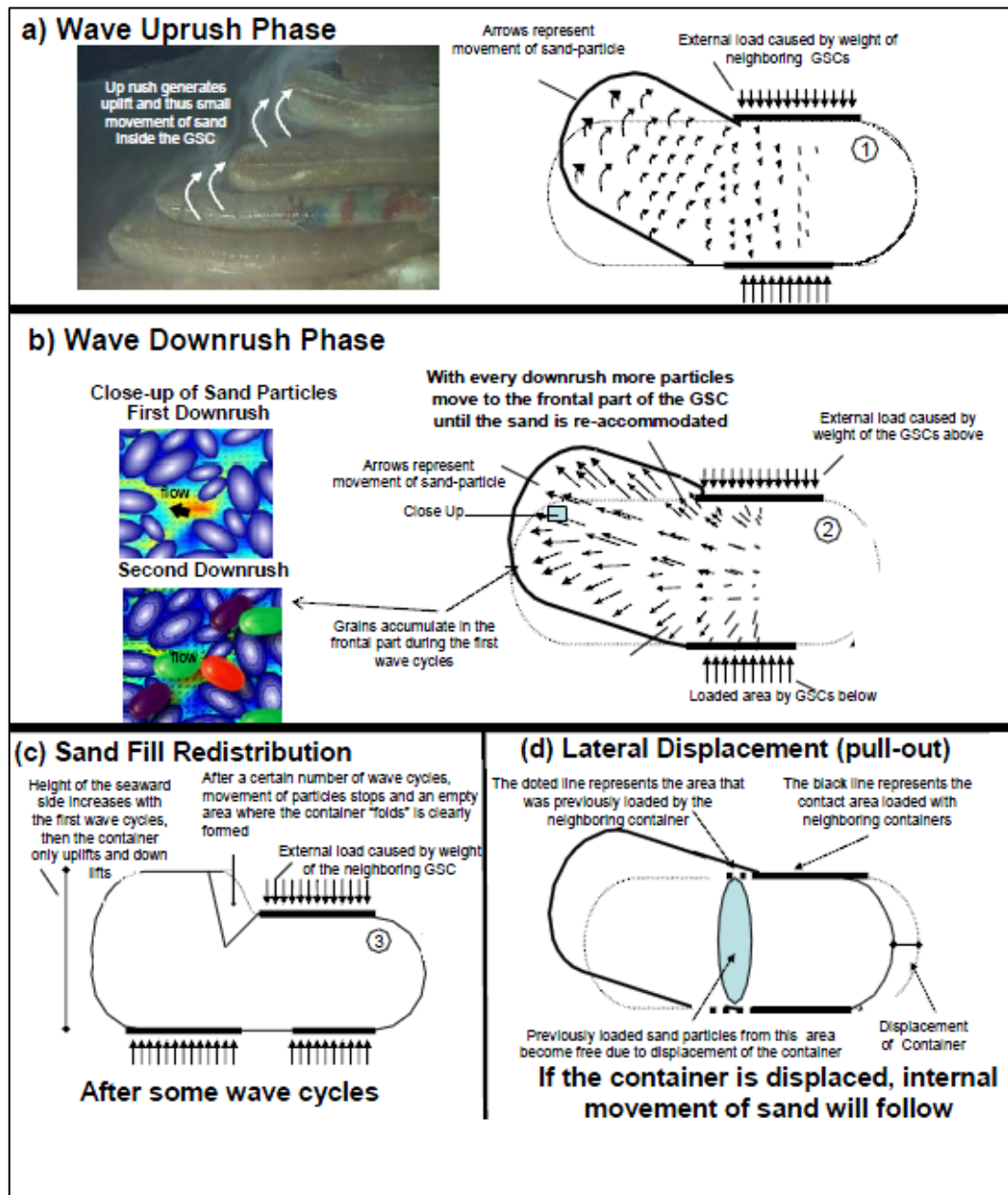
Figure 2-7: Schematisation of the internal movement of sand in a GSC (Recio, 2007)

This process of internal movement of sand can also be described as 'caterpillar mechanism' (Van Steeg and Klein Breteler, 2008) due to the incremental horizontal movement of the GSCs.

22

2.3.4 Variation of Contact Areas during Wave Action

In much a similar way that the internal movement of sand in a GSC was observed with video analysis, so too was the variation of contact areas between the GSCs observed. It was found that the contact area between the GSCs is reduced due to uplift caused by the uprush of a wave cycle. The resisting forces of a GSC are a function of its weight projected onto these contact areas. A reduction of the contact areas has a direct influence on the stability of a GSC. Furthermore the "effective" resisting contact areas are a function of the slope of the GSC revetment. The steeper the slope; the larger the contact areas and thus the greater the stability of the GSC revetment. The observed variation in contact areas in the physical model tests is shown in Figure 2.8 below.
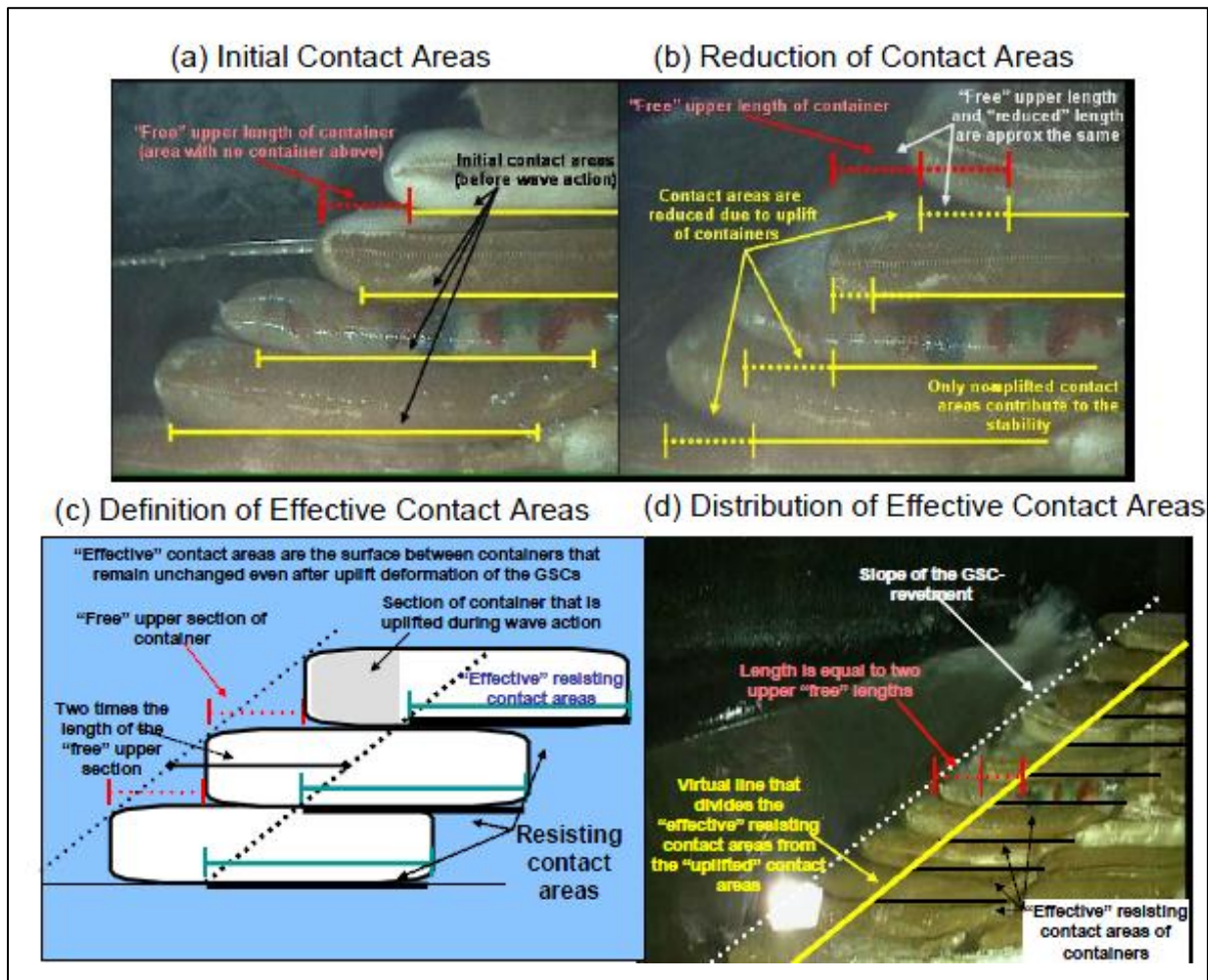
Figure 2-8: Variation of Contact Areas between GSCs when under Wave Attack (Recio, 2007)

2.3.5 Effects of GSC Deformation on the Hydraulic Stability of GSC Revetments

The physical model tests have shown that the deformation of GSCs strongly affects the hydraulic stability of GSC revetments. An analytical examination of the observations made in the physical

23

model tests explains why the deformation of GSCs has such an effect on the hydraulic stability of GSCs. In order to do so the, the GSC and the forces acting upon it during wave attack is first considered without deformations. The forces acting upon the GSC can be described as either a mobilising force (wave loads) or as a resisting force. For the GSC to be stable, these opposing forces must be in balance. There are three main mobilising forces and they are defined as (Recio, 2007):

I. Drag force: $\qquad F_D = 0.5 C_D \rho_w A_s u^2$

II. Inertia force: $\qquad F_M = C_D \rho_w V \dfrac{\delta u}{\delta t}$

III. Lift Force: $\qquad F_L = 0.5 C_L \rho_w A_T u^2$

The resisting force is defined as:

i) Resisting Force: $\qquad F_{GSC} = \rho_{GSC} g V$

Where:

- ρ_{GSC} $\;= (\rho_s - \rho_w)$ is the submerged density of the GSCs, ρ_s is the density of the fill material and ρ_w is the density of water.
- C_D, C_L, C_M are empirical force coefficients
- u and $\dfrac{\delta u}{\delta t}$ are the wave induced horizontal particle velocity and the associated horizontal acceleration respectively.
- V is the volume of the GSC, A_s is the projected are of the GSC normal to the wave direction and A_T is the projected area of the GSC in the wave direction.

The forces and geometric definitions are defined in Figure 2.9 below.
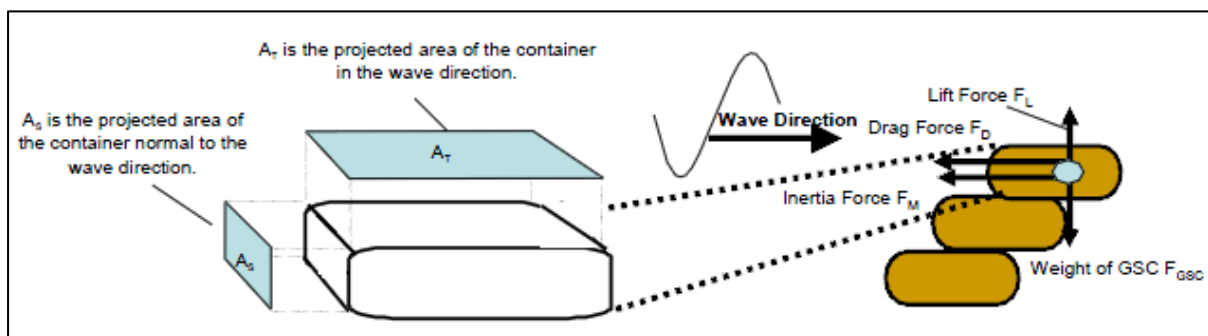
Figure 2-9: Definition Sketch of Projected Areas and Direction of Forces (Recio, 2007)

The stability of a GSC can be broken in two types: stability against sliding and stability against overturning. The stability against sliding can be described as:

$$\mu[F_{GSC} - F_L] \geq F_D + F_M$$

Where μ is the friction coefficient between the GSCs.

The stability against overturning can be described as:

$$F_{GSC} \cdot r_s \geq (F_D + F_M)m_s + F_L \cdot r_s$$

Where r_s and m_s are the horizontal and vertical projections of the distance between the centre of gravity and the rotation point of the GSC. (See Figure 2-10).

When internal movement of sand occurs, the seaward end of the GSC enlarges and the rear end reduces. The significance of this is that the contact areas reduce during uplift and the resisting forces reduce due to the forward moving of the sand mass. Ultimately the GSC stability is compromised. An illustration of the effect that deformation has on the hydraulic stability of GSC revetments is shown in Figure 2-10 and Figure 2-11.
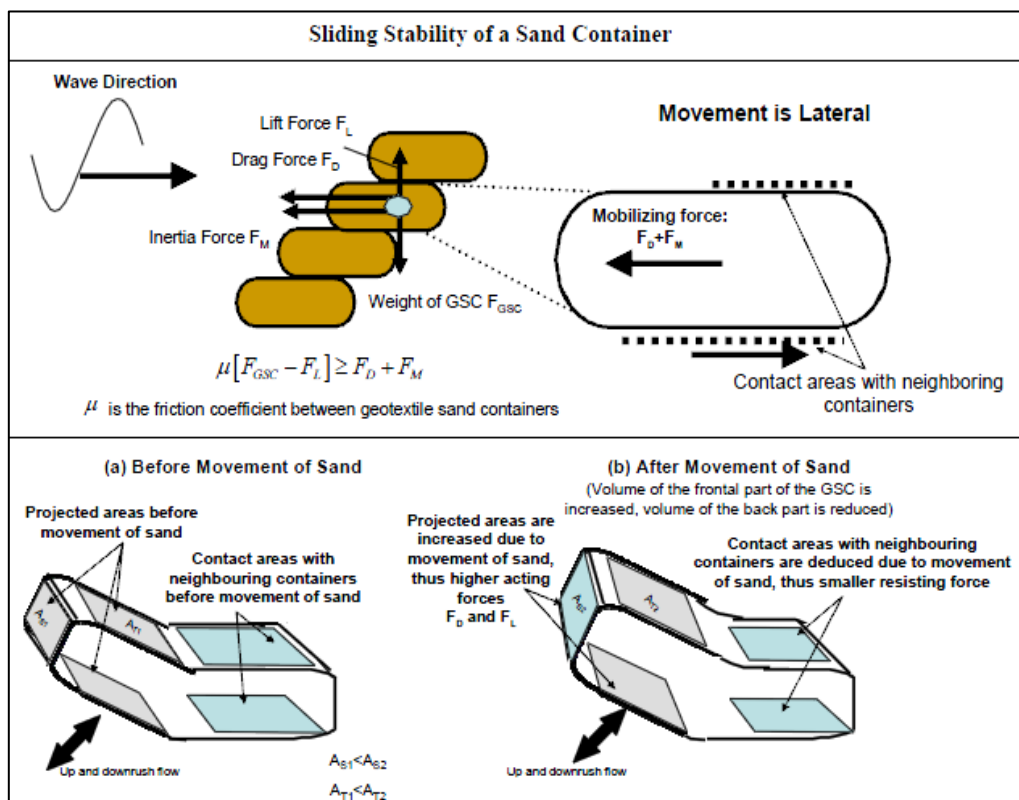
Figure 2-10: Effect of the Internal Movement of Sand on the Sliding Stability of a GSC (Recio, 2007)
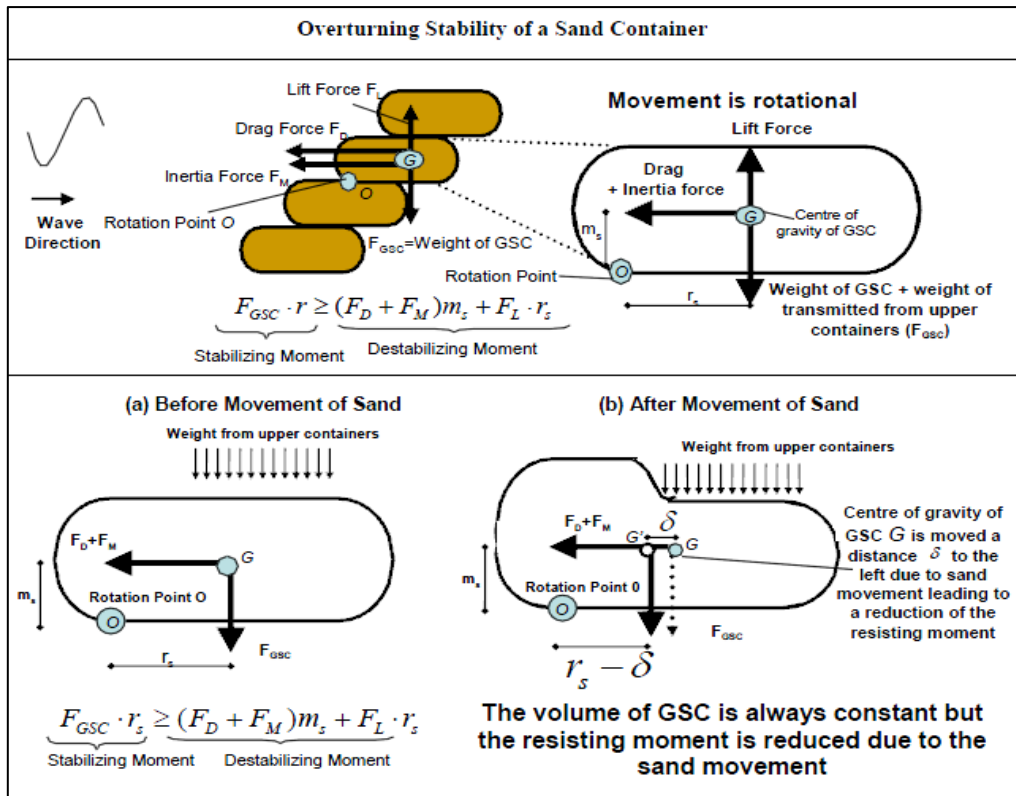
Figure 2-11: Effect of the Internal Movement of Sand on the Overturning Stability of a GSC (Recio, 2007)

2.4   Failure Modes of GSC Revetments

As with most coastal structures, GSC Revetments are prone to certain modes of failure. Undermining of the foundation though scour at the toe of the structure and instability of the slope armour through the accidental or malicious rupture of a GSC or group of GSCs are examples of such modes of failure. However, the most common modes of failure are due to groups of GSCs being displaced from the armour layer and thus compromising the structural integrity of the revetment. This displacement occurs is in the form of GSCs sliding or overturning due to a combination of "pull-out" effects and deformation of GSCs. The "pull-out" effect and deformation of GSCs is largely caused by excessive wave attack and the subsequent internal movement of sand it instigates. The processes leading to such failures are discussed in greater detail in Section 2.3.

The various failure modes applicable to GSC revetments are illustrated in Figure 2-12 below.
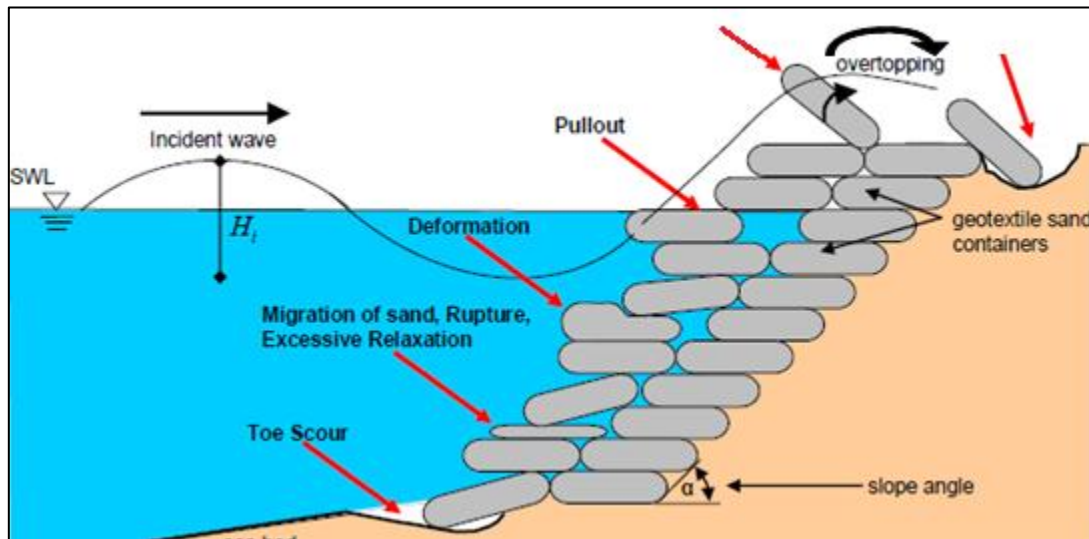
Figure 2-12: Potential Failure Modes of a GSC Revetment (Oumeraci and Recio, 2009)

2.5   Available Design Charts and Stability Equations

The use of GSC revetments is a relatively new coastal protection solution compared with that of more traditional solution constructed of rock and or concrete. The knowledge of the characteristics of GSCs and the processes that affect the hydraulic stability of GSC revetments is thus not as substantial as that of traditional solutions, making the design of such structures quite difficult. However, this knowledge is fast evolving and it is evident from the available stability equations that much progress is being made.

2.5.1   WRL Design Chart

A design chart for GSC revetments was developed by Coghlan *et al*. (2008) at the Water Research Laboratory (WRL), University of New South Wales, Australia. The design chart is a result of both field measurements of prototype GSC revetment applications as well as scale model laboratory tests.

Various GSC revetment permutations were tested with varying packing arrangements, structure slopes and foreshore slopes. Varying hydraulic conditions were used for the scale model tests:

   I.   Still Water Levels: 0.0m Australian Height Datum (AHD), +1.5m AHD and +3.0m AHD.

  II.   Peak Spectral Wave Period, (Tp): 5s, 10s, 15s

 III.   Significant Wave Height at Structure, (Hs): 0.5m to 2.0m

The scale model GSCs used in the tests are the modelled prototype units examined on site by Blacka *et al* (2006). Two size GSCs were modelled and the details of which are shown in Table 2.5 below. The units in the table have been scaled up to prototype dimensions for direct comparison purposes.

Dimension	Units	0.75 m³ Prototype	0.75 m³ Model (10 Scale)	2.5 m³ Prototype	2.5 m³ Model (13 Scale)
Length	mm	1800	1650	2600	2145
Width	mm	1500	1400	1900	1820
Depth	mm	420	430	580	559
Dry Weight in Air After Filling	kg f	1264	1250	3871	2746
Saturated Submerged Weight	kg f	609	618	1790	1358
Saturated Weight in Air	kg f	1524	1628	4527	3577
Volume	m³	0.90	1.01	2.67	2.22
Saturated Bulk Density	kgm⁻³	1708	1612	1697	1612

Table 2-5: Comparison of Scale Model and Prototype 0.75m³ and 2.5m³ GSCs (Coghlan *et al*, 2008)

The results of the scale model tests were analysed and Coughlan *et al*. (2008) made the following conclusions:

I. Single Layer GSC armour revetments failed under wave attack at lower wave heights than the equivalent double layer armour arrangement.

II. The failure mode of single layer GSC armour revetments was due to a slip/slumping mechanism which resulted in sudden failure of the structure

III. The failure mode of double layer GSC armour revetments was due to localised displacement of GSCs. The overall structure geometry was preserved up to an intermediate damage level.

IV. The design wave height to start of damage was found to decrease for longer wave periods

V. The design wave height to start of damage was found to increase for steeper revetment slopes.

From the above conclusions a double layer GSC armour revetment with a structure slope of 1V:1.5H was recommended for optimal hydraulic stability and constructability. The design chart for the 2.5m³ GSC was proposed on the up scaling of the results of the 0.75m³ GSC results and is presented in Figure 2-13.
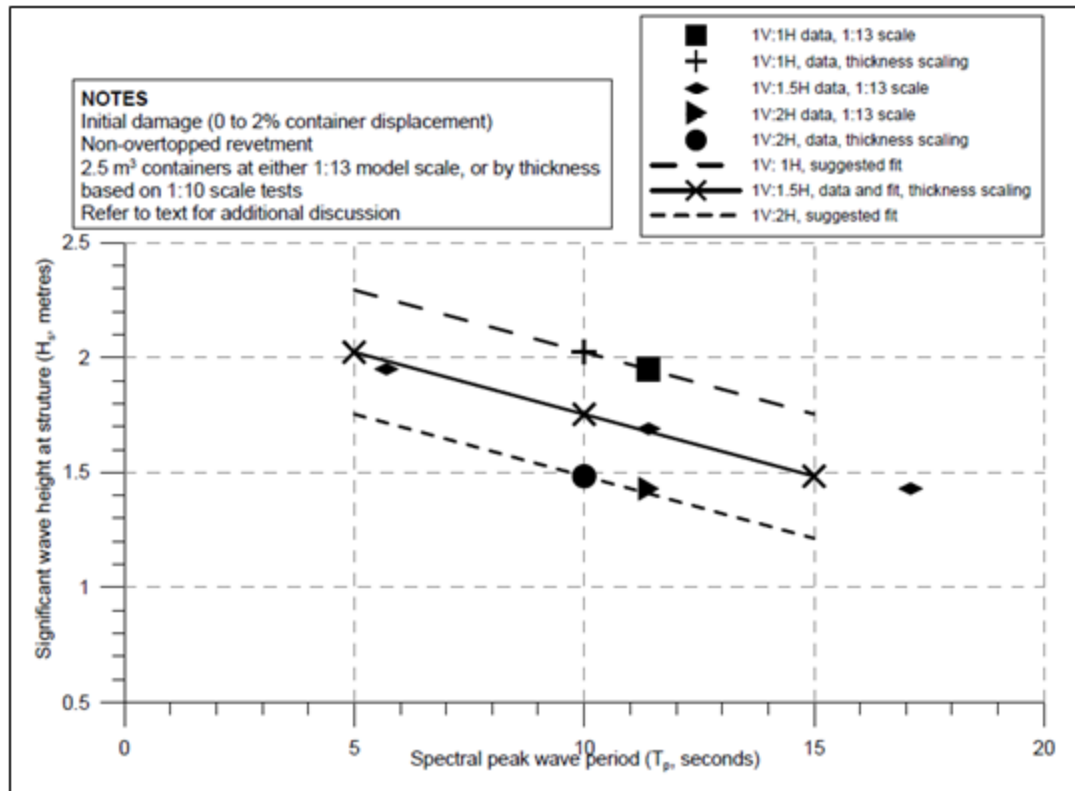
Figure 2-13: Proposed Design Wave Height Relationship with Peak Wave Period for 2.5m³ GSCs (adapted from Coghlan et al. 2008)

Coughlan et al. noted that since the results shown in Figure 2-13 are based on the up scaled results of the 0.75m³ GSCs and indicated wave heights for the 2.5m³ GSCs are approximately 35% greater than those for the 0.75m³ GSCs, further large scale physical modelling was required to validate the design chart before using for using for design purposes.

2.5.2   Stability Equations

The available design charts and stability equations presented in this chapter, display the progress of understanding gained through the years of investigation into the hydraulic stability of GSC revetments. The latest stability equations developed have become more inclusive of factors relevant to hydraulic stability of GSC revetments and are thus more reliable. All the available stability equations are based on the stability number concept and the balance of wave induced forces. Variables common to the stability equations presented in this section are declared:

- α = Angle of structure slope (90˚ is vertical)
- g = gravitational constant 9.81 [m/s²]
- L_0 = Deepwater wave length and is defined as: $L_0 = \frac{gT_p^2}{2\pi}$ [m
- T_p = Peak spectral period [s]

29

- Δ = Relative density of the GSC [-]
- ρ_E = Density of sand container elements [kg/m³]
- ρ_W = Density of water [kg/m³]

The stability equations are now discussed.

2.5.2.1 Hudson (1956)

Hudson Stability Formula is commonly used for armour stone and Hudson (1956) proposed the following:

$$N_s = \frac{H_s}{\Delta D_n} = (K cot\alpha)^{1/3}$$

Where:

- N_s = The stability number
- K = Experimentally derived stability coefficient [-]
- D_n = Equivalent cube length [m]
- H_s = Density of sand container elements [kg/m³]

The K value is determined experimentally and is dependent on roughness, shape and interlocking properties of an armour unit. Although originally designed to be used in the stability calculations of rock armour, K values have been experimentally investigated for a range of other materials and shape of armour. The application of the equation is therefore not limited to rock armour and can be applied to GSC armour. The Hudson formula is simple to use but it is limited in that it does not explicitly consider wave period, inertia forces or storm duration (Recio, 2007)

2.5.2.2 Bouyze and Schram (1990)

Bouyze and Shram proposed a stability equation for GSC structures based on scale model tests as well as on the Hudson equation. The model tests involved geotextile tubes filled with sand being subjected to unidirectional flow (ie no waves). The formula is based on the critical flow that induced movement of the geotextile tube. The formula is as follows:

$$\frac{\mu_{cr}}{g\Delta D^{0.5}} = 0.5 \; to \; 1.0$$

Where:

- μ_{cr} is the critical velocity (averaged over the water column) at the start of movement
- D is the diameter of geotextile tube

Like the Hudson formula the Bouyze formula is simple to use. The limitations are that the empirical values are obtained from unidirectional flow as opposed to waves and that geotextile tubes are used and the applicability to GSCs with finite length is thus questionable.

2.5.2.3 *Wouters (1998)*

Wouters proposed a stability formula based on the Hudson equation and experimental data. The stability equation is developed with balance of moments of the drag force (F_D), lift force (F_L) and the stabilising gravitational force (F_G). The thickness D of the cover layer is calculated as opposed to the previous methods which ultimately calculate the required weight of units. D is defined as $D = l \cdot sin\alpha$. Wouters also incorporated the porosity (n) of the filling material (sand). The stability number is then calculated as follows:

$$N_s = \frac{H_s}{\left(\frac{\rho_E}{\rho_W} - 1\right) D} = \frac{C_W}{\sqrt{\xi_o}}$$

Where:

- N_S = Stability number [-]
- ρ_E = Density of sand container elements [kg/m³] as defined as $\rho_E = (1-n)\rho_s + \rho_w n$
- n = Is the porosity of the filling sand
- D = Characteristic diameter of sand container and defined as: $D = l_c \sin \alpha$ [m]
- l_c = Length of sand container parallel to direction of wave attack [m]
- C_W = 2.0 (empirical parameter based on test results) [-]
- ξ_0 = Surf similarity parameter and defined as: $\xi_0 = \frac{\tan \alpha}{\sqrt{\frac{H_S}{L_0}}}$ [-]

For GSC revetments Wouters suggests a C_W value of 2.0 for this case. This empirical value limits the use of this equation as it can only be calculated experimentally for each case. The advantages however, are that it takes wave period and the porosity of the filling material into account.

2.5.2.4 *Pilarczyk (2000)*

Pilarczyk (2000) used Wouters'(1998) stability equation in combination with data from small scale model tests and proposed a modified equation for GSC revetments. A more accurate empirical parameter C_W is proposed. Pilarczyk (2000) proposed the following:

$$N_s = \frac{H_s}{\left(\frac{\rho_E}{\rho_W} - 1\right) D} = \frac{C_W}{\sqrt{\xi_o}}$$

31

Where:

- N_S = Stability number [-]
- ρ_E = Density of sand container elements [kg/m³] as defined as $\rho_E = (1 - n)\rho_s + \rho_w n$
- n = Is the porosity of the filling sand
- D = Characteristic diameter of sand container and defined as: $D = l_c \sin \alpha$ [m]
- l_c = Length of sand container parallel to direction of wave attack [m]
- C_W = 2.5 (empirical parameter based on test results) [-]
- ξ_0 = Surf similarity parameter and defined as: $\xi_0 = \dfrac{\tan \alpha}{\sqrt{\dfrac{H_s}{L_0}}}$ [-]

2.5.2.5 *Oumeraci et al (2002)*

Oumeraci *et al* went further than Pilarczk (2000) and used Wouters formula in combination with data from large scale model tests and proposed a modified equation for GSC revetments. A distinction is made between different parts of the structure. Crest units are distinguished from slope units and as such new equations were developed. A more accurate empirical parameter C_w is also introduced. Oumeraci *et al* proposed the following:

$$N_{s,slope} = \frac{H_s}{\left(\frac{\rho_E}{\rho_W} - 1\right) D} < \frac{C_w}{\sqrt{\xi_o}}$$

and

$$N_{s,crest} = \frac{H_s}{\left(\frac{\rho_E}{\rho_W} - 1\right) D} < 0.79 + 0.09 \frac{R_C}{H}$$

Where:

- $N_{s,slope}$ = The stability number for a slope elements
- $N_{s,crest}$ = The stability number for a crest element
- C_w = 2.75 (empirical parameter based on test results) [-]
- R_c = The freeboard of the revetment [m]
- D = Characteristic diameter of sand container and defined as: $D = l_c \sin \alpha$ [m]

2.5.2.6 *Recio (2007)*

One of the more recent stability equations is that proposed by Recio (2007). The equation is essentially based on the balance of wave induced forces. Thorough physical model tests investigated the processes that affect the hydraulic stability of GSC revetments and prompted the inclusion of various parameters. The included parameters account for the deformation characteristics of GSCs as

well the empirical force coefficients derived for GSCs. A distinction is made between two common modes of failure for GSCs: sliding and overturning. The stability equations, written in terms of required GSC length are shown below:

a) Sliding Stability Equation:

$$l_c \geq u^2 \left[\frac{(0.5KS_{CD}C_D + 2.5KS_{CL}C_L\mu)}{\left(\mu KS_R\Delta g - KS_{CM}C_M \frac{\delta u}{\delta t} \right)} \right]$$

b) Overturning Stability Equation:

$$l_c \geq u^2 \left[\frac{(0.05KO_{CD}C_D + 1.25KO_{CL}C_L\mu)}{\left(0.5KO_R\Delta g - 0.1KO_{CM}C_M \frac{\delta u}{\delta t} \right)} \right]$$

Where:

- l_c is the length of sand container parallel to direction of wave attack [m]
- u and $\frac{\delta u}{\delta t}$ are the wave induced horizontal particle velocity and the associated horizontal acceleration respectively.
- μ is the friction coefficient between the GSCs
- C_D, C_M and C_L, are the empirically derived force coefficients for Drag , Inertia and Lift forces.
- KS_{CD}, KO_{CD} are the deformation factors that account for the variation of projected area of a GSC normal to wave direction and the subsequent effect on the drag force for sliding and drag moment for overturning
- KS_{CL}, KO_{CL} are the deformation factors that account for the variation of projected area of a GSC in the wave direction and the subsequent effect on the on the lift force for sliding and lift moment for overturning
- KS_R, KO_R are the deformation factors that account for i) the reduction of resisting force and moment due to deformations and ii) the increase of the resisting force and moment due to the contribution of upper GSCs.
- KS_{CM}, KO_{CM} are the deformation factors that account for variations of volume of a GSC on the inertia forces and inertia moments. The volume of a GSC is assumed to stay constant and thus remains as 1.

The equations can also be written in terms of required GSC mass as follows:

c) Sliding Stability Equation:

$$W_{GSC} \geq \rho_s \left(u^2 \left[\frac{(0.5KS_{CD}C_D + 2.5KS_{CL}C_L\mu)}{\left(\mu KS_R \Delta g - KS_{CM}C_M \frac{\delta u}{\delta t} \right)} \right] \right)^3 /10$$

d) Overturning Stability Equation:

$$W_{GSC} \geq \rho_s \left(u^2 \left[\frac{(0.05KO_{CD}C_D + 1.25KO_{CL}C_L\mu)}{\left(0.5KO_R \Delta g - 0.1KO_{CM}C_M \frac{\delta u}{\delta t} \right)} \right] \right)^3 /10$$

Where:

- W_{GSC} is the required mass of the container [kg]
- ρ_s is the bulk density of fill material [kg/m³]

It is important to note that these equations were developed based on certain assumptions. The use of this equation is therefore limited to the assumptions made. The assumptions for the derivation of the equation are (Recio, 2007):

I. The length l_c of the GSC is twice as large as its width and five times as large as its height

II. The GSCs have a sand fill ratio of 80%

III. The font slope of the structure is at 45˚ with the horizontal.

The assumptions stated above are shown graphically in Figure 2-14.
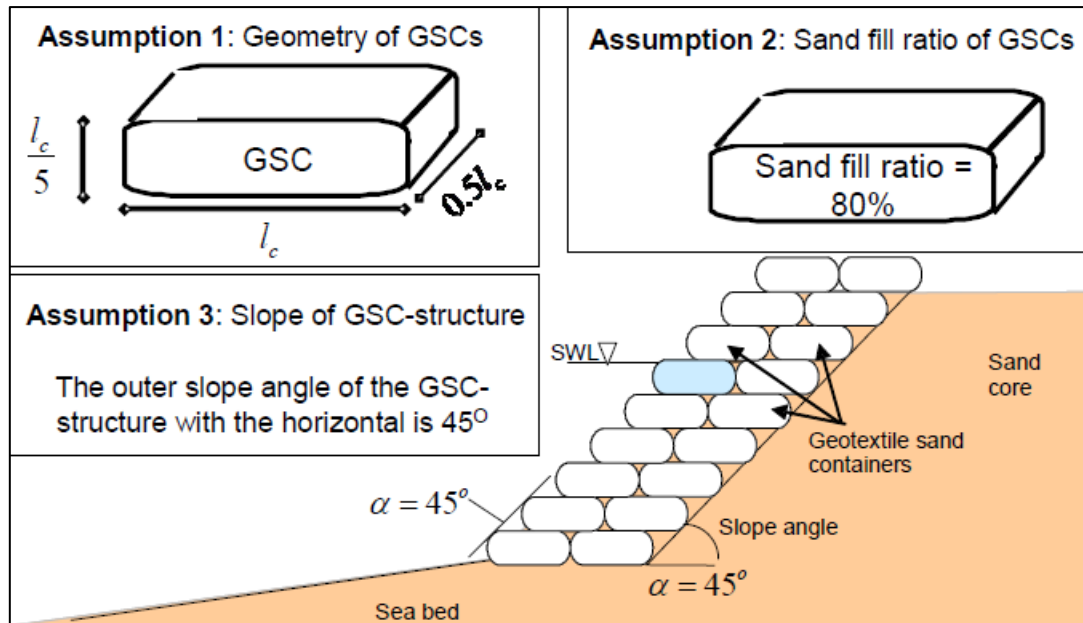
Figure 2-14: Initial Assumptions made for the Derivation of the Stability Equations (Recio, 2007)

The equations can however be modified to suit other geometries of GSCs and GSC revetment structure slopes (refer to section 5.2.2.3)

2.6   Summary

The literature review process has highlighted the complexities involved in understanding the hydraulic stability of GSC revetments. From the literature review it is evident that the following characteristics of GSCs and GSC revetments are considered the most critical in terms of the hydraulic stability:

I.   Sand Fill Ratio of GSCs

II.   Internal movement of sand

III.   Packing arrangement in terms of GSC orientation as well as the number of GSC armour layers

IV.   Structure slope

It is also understood from the literature review that the critical location on the GSC revetment is just below the still water level (SWL) and that the critical phase for stability is on the downrush phase of the wave cycle. The effect of breaking waves on GSC revetments is not as critical as expected when compared to that of non-breaking waves.

The available design charts and stability equations go a long way in assisting in the design of GSC revetments. They are however limited to the permutations of GSC revetments on which they are

based. Unfortunately the GSC revetments found along stretches of the KwaZulu-Natal Beaches do not fall within the range of application for the available design charts and stability equations. As such, large scale physical modelling is required to determine their hydraulic stability. The available design charts and stability equations will also be evaluated to determine if they can be applied to or modified to include GSC revetments outside their range of limitations such as the unique GSC revetment permutation found in KwaZulu-Natal. The physical model test series should thus evaluate different permutations of GSC revetments that include those used for the development of design charts and stability equations. In this way, the hydraulic stability of the KwaZulu-Natal GSC revetment will be made clearer and the applicability of the design charts and stability equations to permutations outside their range of limitations will be better understood.

3   Two-Dimensional Physical Modelling

A fixed bed, two dimensional, physical model test series is undertaken to investigate the effect of packing arrangements and structure slopes on the hydraulic stability of GSC revetments. The details of the physical model setup and permutations of GSC revetments considered for testing are discussed in this chapter.

3.1   Scope of Physical Model

From the literature review process it became evident that physical model testing of the hydraulic stability of various permutations of GSC revetments was necessary. For the purposes of this study only the hydraulic stability of the slope GSC elements are considered. The literature review process identified the critical zone of GSC revetments as just below the still water level (SWL) and the hydraulic stability of the toe and crest elements of the structure are thus not considered. Details on an effective toe designs can however be found in Appendix A.

3.2   Testing Facilities

The physical model testing program was undertaken at the Stellenbosch University's Hydraulic Laboratory. The laboratory has two wave flumes: a glass flume measuring 35m in length, 0.8m in depth and 1.0m in width; as well as a larger concrete flume measuring 60m in length, 2.0m in depth and 2.0m in width. The glass flume is fitted with a rack and pinion piston-type paddle while the concrete flume is fitted with a hinge-type paddle. The wave flumes are both capable of regular and irregular wave and are fitted with dynamic wave absorption systems. The dynamic wave absorption system compensates for the reflected waves that come off of the structure during testing. The system thus allows for structures with high reflection properties to be tested.

For the purposes of this physical model test, the larger concrete wave flume was chosen so as to enable a larger model scale to be chosen. Further details of the concrete flume and its capabilities can be found in Appendix B.

3.3   Physical Model Design

The physical model tests set out to examine the hydraulic stability of various construction permutations of a GSC revetment. The design of the physical model tests was not based on a site specific prototype but rather on a generic GSC revetment. A generic GSC revetment is defined as a structure that would commonly be found where the erosion of a sandy coastline has threatened public or private property. It is placed against a pre-existing dune to provide protection from further erosion and wave attack. Although the revetment itself was not based on a site specific prototype,

the geometry of the GSCs was based on prototype GSCs that are commonly used to construct GSC revetments in South Africa. The prototype GSCs have a length of 2.4m, a width of 2.0m and a height of 0.5m with a mass of approximately 4000 kg.

Different permutations of the GSC revetments were tested in the fixed-bed two-dimensional flume. The same hydraulic conditions tested were the same for each permutation. This was done so that the performance of each revetment permutation could be compared with one another for qualitative analysis. A total of 12 GSC revetment permutations were tested and are summarised in Table 3-1 below. Three fundamental aspects of the GSC revetment were varied: the type of armour layer, the orientation that the GSCs were placed within the GSC revetment and slope at which the GSC revetment was built.

GSC Revetment Number	Structure Slope	Orientation of GSC Containers	GSC Armour Layer
1	α = 45˚	A	Single
2	α = 45˚	A	Double
3	α = 45˚	B	Single
4	α = 45˚	B	Double
5	α = 33˚	A	Single
6	α = 33˚	A	Double
7	α = 33˚	B	Single
8	α = 33˚	B	Double
9	α = 26˚	A	Single
10	α = 26˚	A	Double
11	α = 26˚	B	Single
12	α = 26˚	B	Double

Table 3-1: GSC revetment permutations tested

For the purposes of this study the orientation of the GSC within the GSC revetment is defined as either 'A' or 'B'. The GSC is considered in the 'A' orientation when then length of the GSC is perpendicular to the direction of the wave attack and is considered in the 'B' orientation when the length of the GSC is parallel to the direction wave attack, as shown in Figure 3-1
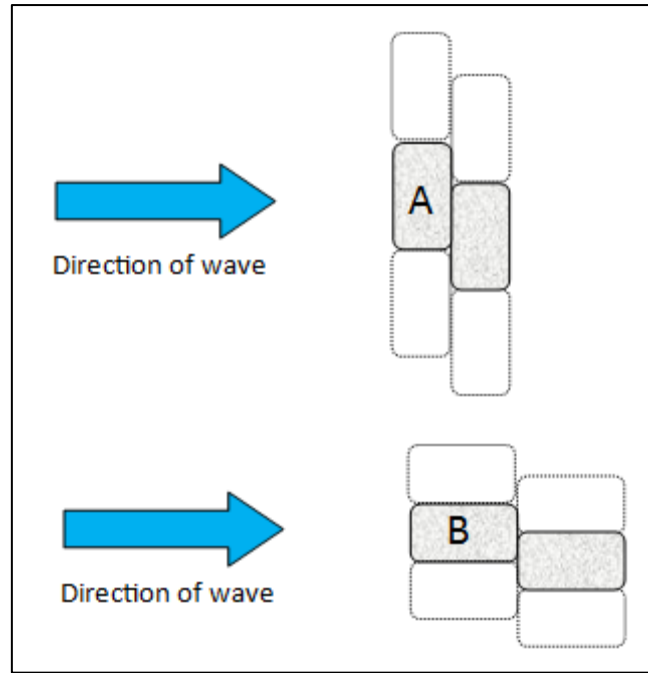
Figure 3-1: Plan View of GSC in 'A' and 'B' Orientation relative to Wave Direction

The concrete wave flume as set up for the physical model test is illustrated in Figure 3-2. The model GSC revetment is constructed opposite to the hinged paddle wave-maker at the top of a 1V:20H concrete lined slope. A movable control station situated above the flume is used to control the input signal to the wave-maker, capture data from the measuring equipment and proved to be a useful observation point during the test runs.
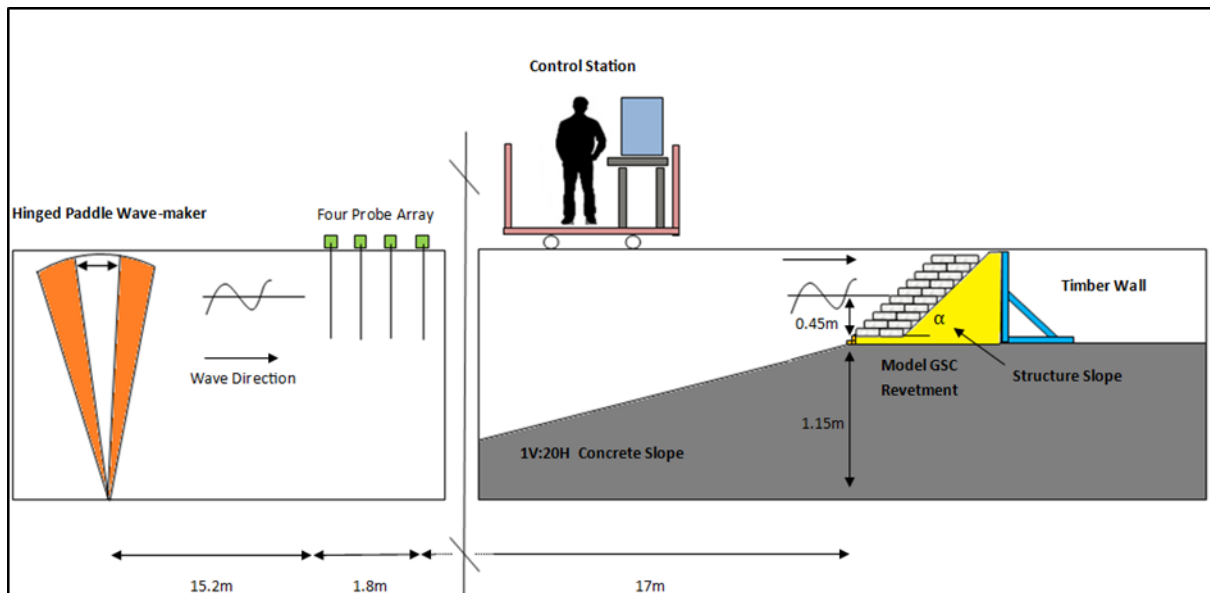
Figure 3-2: Schematic Diagram of Concrete Wave Flume Setup (Not to Scale)

3.3.1 Model Scale

A scale of 10 was chosen for the physical model. The choice of this scale was based on several factors. It was deemed large enough so as to avoid scale effects while small enough that the wave

39

making capabilities of the paddle were not exceeded. This scale was also considered convenient for the construction of the model revetment. At this scale the width of the flume was a multiple of the length of a model GSC, both in the 'A' and 'B' orientation. This meant that the width of the flume did not have to be modified for the model tests. The offset packing arrangement of the model revetment required 'half' model GSCs to be constructed to fill the voids at the model revetment and flume-wall interface.

Froude's scaling law is applied to most wave models as gravity and momentum are the predominant factors in fluid motion. The physical model is thus scaled according to Froude similitude criteria. This means that the Froude number should be the same in the model as it is the prototype (Hughes, 1993). The Froude number gives the ratio of inertial forces to gravitational forces and is defined as follows:

$$F_r = \frac{V}{\sqrt{gL}}$$

Where:

- V: is the velocity [m/s]
- g: acceleration due to gravity [m/s²]
- L: Length [m]

The scale of 10 results in the scale ratios (prototype dimension divided by model dimensions) presented Table 3-2.

Scale Ratio		Value
Length Ratio	L_R	10
Time Ratio	T_R	3.16
Mass Ratio	M_R	1000

Table 3-2: Scaling relationships relevant to the physical model test, as per Froudian Similitude

3.3.2 Modelled GSC Revetment

As mentioned previously, 12 permutations of the GSC revetment were tested as summarised in Table 3-1. The schematic diagrams of cross sections and plan views illustrating the critical variations between the permutations of the GSC revetment are presented below. The schematic diagrams are not to scale and as such the structure slope is simply defined as: α. For the sake of brevity, only the salient differences between the GSC revetments are schematised.
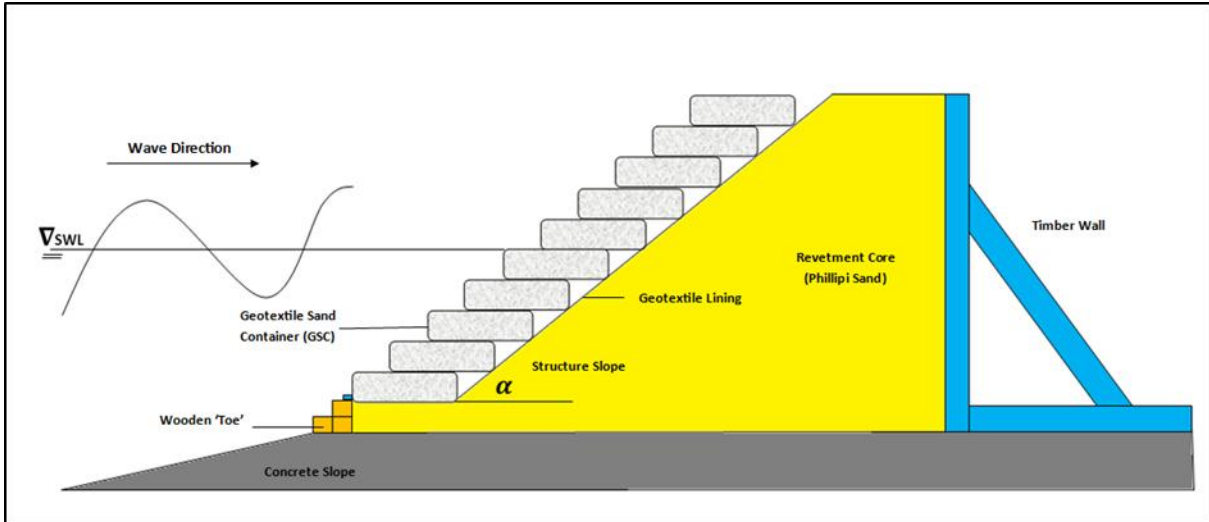
Figure 3-3: Schematic Cross-section of a Single Layer GSC Armour Revetment
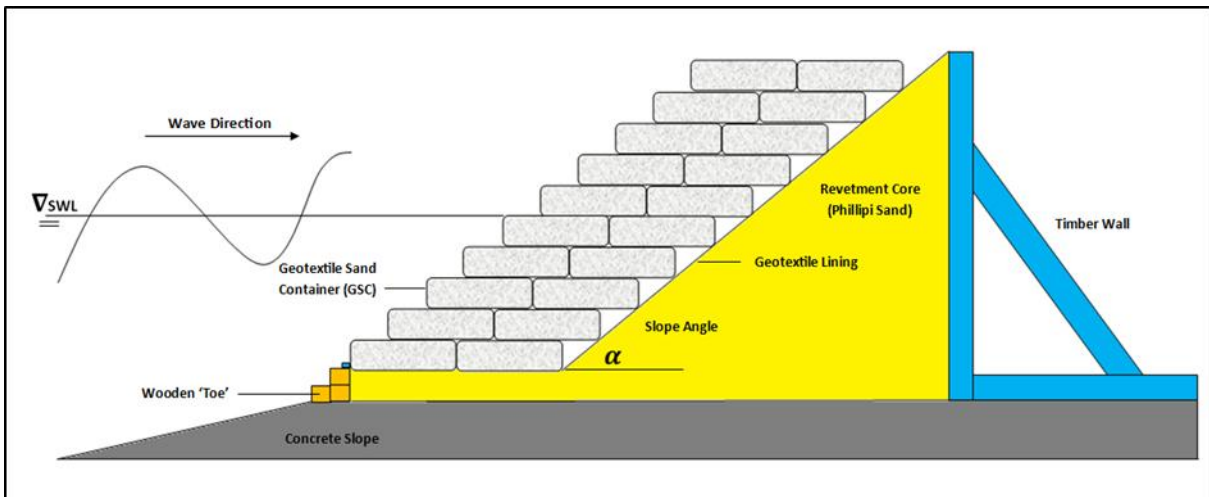
Figure 3-4: Schematic Cross-section of a Double Layer GSC Armour Revetment
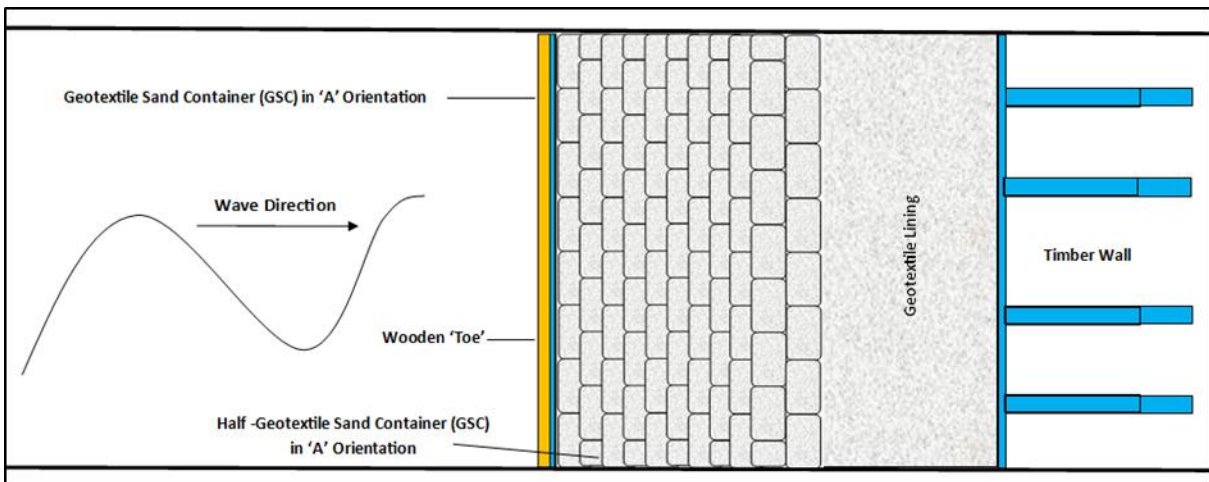
Figure 3-5: Schematic Plan View of a Single Layer GSC Armour Revetment with GSCs placed 'A' Orientation

41
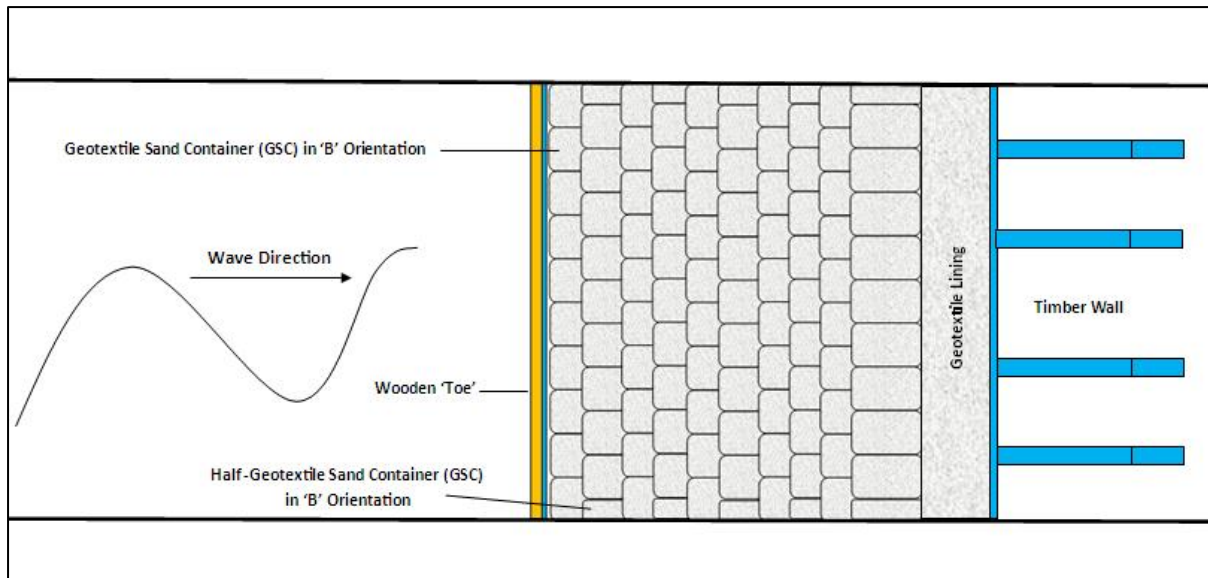
Figure 3-6: Schematic Plan View of a Single Layer GSC Armour Revetment with GSCs placed 'B' Orientation

The model GSC revetments are designed to be constructed on a large sand core, large enough that the boundary effect with the impermeable concrete flume floor and timber wall support structure is avoided. A wooden toe covered in geotextile material was used to replicate an immovable row of GSCs (instead of being buried in sand as per the recommended prototype toe design described appendix A) in order to hold a layer of sand upon which the rest of the model GSC revetment can be constructed. This wooden toe will also prevent the GSC revetment from sliding and thus focus the testing on the slope of the GSC revetment as per the scope of the physical modelling test.

3.3.3   Hydraulic Conditions

As the model GSC revetment was not site specific, an array of wave conditions was used for testing. Irregular waves with a JONSWAP wave spectrum and a peak enhancement factor (γ) of 3.3 was used for all the test runs. The peak enhancement factor (γ) of 3.3 is typically chosen and has been used by most of the physical model testing already done on GSC revetments. (Recio, 2007 and Oumerai et al, 2002). This allows a direct comparison between the results of the model tests to be made.

Stability tests usually consist of approximately 1000 waves in order to represent the duration of a generic storm event. The GSC revetment was initially tested with small wave heights and incremented for each test thereafter. With wave making capabilities of the flume in consideration, three peak spectral periods (Tp) were also tested and a constant water depth was maintained in front of the structure. The following combinations of hydraulic conditions were tested (in prototype dimensions):

- Significant wave heights (Hs) ranging from 0.5m to 1.6m
- Peak spectral periods (Tp) of 5s, 9s and 13s

- Water depth (d) in front of the structure of 4.5m

Calibration of the test waves was necessary in order to calculate the wave characteristics at the toe of the GSC revetment. This was done by measuring the wave conditions at both the section of uniform depth and the location at which the model GSC revetment was to be placed. The waves measured at the uniform depth location represent the offshore waves; while the waves measured at the location at which the model GSC revetment was to be placed represent the incident waves. The input parameters to the wave generation software were saved. Once the GSC revetment was constructed the same input parameters were used. This coupled with the wave absorption capabilities of the paddle maintaining a constant incident wave climate as per the input parameters meant that the characteristics of the incident wave could be known for design purposes.

The software used for wave generation was the HR Wallingford's Wavemaker software. This software allows set-up sea states to be saved. This meant that the sea states set-up for the calibration of the test waves could be used again for the tests when the GSC revetment was in place. This resulted in repeated reliability of the test wave condition.

3.4   Model Construction

The construction of the model began with modifications to the bathymetry of the flume. A smooth 1 in 20 slope was constructed of compacted sand with a thin concrete cap to replicate a steep foreshore beach slope. The model GSC revetment was placed at the top of this slope. The construction of the model GSC revetment was two parts. The GSCs first had to be fabricated after which the supporting structure and sand core of the GSC revetment had to be built.

3.4.1   GSCs

The GSCs were fabricated to replicate as far as possible the prototype GSCs commonly used in South Africa. The fabrication of the GSCs involved measuring and cutting out templates from a roll of geotextile material. The template was then folded in half and sewn closed with a sewing machine. Only a small gap was left open through which the sand was filled with the help of a small funnel. The small gap made it difficult to fill the bag to capacity and so a wooden poker was used to push the sand into the GSC. Once filled to capacity the small gap in the GSC was sewn closed by hand. Photographs of the fabrication progress are shown in Figure 3.7 which follows.

A comparison in made between the geometric properties of the fabricated model containers and the prototype containers in Table 3-3 which follows. It can be seen that the model containers are a good representation of the prototype units.

Dimension	Prototype	Model (Scale 1:10)	Units (Prototype)
Length	2.4	2.5	m
Width	2	2	m
Depth	0.5-0.6	0.5	m
Mass	≈ 4000	4100	kg

Table 3-3: Comparison of Prototype and Model Container (Units in Prototype Dimensions)

Figure 3-7: Photographs Showing the Fabrication Process of GSCs

The GSCs were fabricated using a non-woven polypropylene polymer (PP) which was sponsored by Naue Geotechnics and Geosystems (Germany). The geotextile characteristics as supplied by Naue (2011) are declared in Table 3.4. The material used is not to scale with regards to the prototype GSCs; however it is very difficult to produce appropriately scaled geotextile materials as there are many characteristics of geotextile material to consider. Characteristics of geotextile material such as the porosity, friction coefficients and tensile strength are simply impossible to scale down. It is noted that these characteristics, especially friction coefficients, are significant to the performance of GSC revetment, but a method to scale these geotextile characteristics appropriately remains elusive.

Characteristic	Value	Unit
Mass	180	g/m²
Thickness at 2kPa	≥ 2.2	mm
Max. Tensile Strength: Longitudinal/Transversally	7.2/10.8	kN/m
Elongation at Max strength: Longitudinal/Transversally	45/36	%
Static Puncture Test	1.5	kN/m
Opening Size	0.12	mm
Water permeability	3.E-03	m/s
Friction Angle: GSC-GSC/GSC-Sand	20-25/>30	degrees

Table 3-4: Characteristics of Geotextile used in the Fabrication of Model GSCs (Naue, 2011)

The sand used as fill material in the GSCs is known as "Phillipi" sand and was chosen because of its uniform properties and was readily available. A sieve analysis, shown in Appendix B, found that the median grain size was 0.45mm. As with the geotextile material, the sand is not scaled down due to the complexities in the characteristics of sands Characteristics such as permeability and cohesiveness are not easily scaled down.

The seam used is predominantly the "Prayer" type seam sewn with a sewing machine, except for the small gap which was sewn by hand. Trial model GSCs were roughly handled to test the strength of the seam and it was found to be suitably strong for the purposes of the physical model test.

3.4.2   GSC Revetment

Once the GSCs were fabricated, the construction of the GSC revetment commenced. In order to support the sand core of the revetment, a 'wall' made of reinforced timber was constructed across the width of the flume. This 'wall' was securely bolted to the floor of flume and proved to be very rigid. The same geotextile material used to fabricate the GSCs was used to line the timber 'wall' and the sides of the flume so that fines from the sand core could not escape. The sand core consisted of

the same "Phillipi" sand used as fill material for the GSCs and was properly compacted before being covered with a geotextile lining. The GSCs were then placed on top the geotextile lining to create the final model GSC revetment. Photographs of the construction process are shown in Figure 3.8.

Figure 3-8: Photographs Showing the Construction of the Model GSC Revetment

46

3.5 Measurements

3.5.1 Wave Measurements

Wave measurements in the model were done with common resistance-type probes. A four probe array was located in the deep water section of the flume to measure offshore incident wave heights. The probes were placed at 0.6m spacing, 16m away from the paddle. A wave probe monitor measures the current flowing through the probes. The current flowing between the probe wires is proportional to the instantaneous depth of immersion and is converted to an output voltage proportional to the immersion depth. The probe is calibrated in terms of wave height by varying the depth of immersion in very still water and noting the change in output voltage. During a test the changing output voltage can be captured and stored for post processing. The resistance-type probes are very sensitive to temperature variations in the water. It was thus necessary to calibrate the probes regularly in order negate this effect.

A four probe array is necessary to evaluate the reflective properties of the GSC revetment. Reflection analysis is done with the help HR Wallingford's Data Acquisition Software (DAQ) installed , which calculates the bulk reflection coefficient based on the least squares method developed by Mansard and Funke (1980). The software is also utilised to calculate the necessary wave statistics, such as the maximum wave height (Hmax), the significant wave height (Hs) as well as the wave spectrum analysis.

3.5.2 Structure Measurements

It was necessary to measure the displacements of GSCs to assess the damage incurred by the GSC revetment during a particular test. This was done with a combination of manual measurements, before and after photographs as well as video footage. Manual measurements were simply done with a tape measure in order to quantify the movement of a GSC for damage classification purposes. Cameras were placed in front of the structure and above the structure. Before and after photographs proved particularly useful to compare the performance of various GSC revetment permutations as well as document failure modes. Video footage was not taken of each test and was only used when failure of the revetment began.

3.6 GSC Revetment Damage Classification

In order to assess and classify the damage to the revetment after a particular test, the method of assessment developed by Dassanayake and Oumeraci (2012b) is utilised. This method is designed specifically for GSC structures and comprises two parts. The first part of the assessment requires that the displacement and rotation of each GSC is recorded and classified as either: stable, in

incipient motion or detached. The displacement of a GSC is expressed as a percentage of its unit length, while the rotation is expressed in degrees deviated from the horizontal. The second part of the assessment then considers the GSC structure, specifically the critical GSC-layers of the GSC structure. The individual GSCs that are within the critical GSC layer are binned according to their classification as determined in the first part of the assessment. It is then possible to classify the damage of the GSC structure as either: no damage, in incipient motion, minor damage, medium damage and total failure. Table 3.5 below indicates the damage classification parameters. It is important to note this damage classification is suitable for GSC structures after 100 regular waves during regular wave testing or 1000 waves with a JONSWAP spectrum during irregular wave tests.

Damage Classification I (single GSC): considering only a single GSC in the most vulnerable position (critical GSCs)	
"Stable"	Horizontal displacement < 10% of GSC length (or width) / Upward rotation < 10^0
"Movement"	10% of GSC length, width < Horizontal displacement < 50% of GSC length (or width) 10^0 < Upward rotation < 45^0
"Detachment"	Horizontal displacement > 50% of GSC length, width Upward rotation > 45^0

Damage Classification II (GSC-structure): considering all critical GSC layers of a GSC-Structure				
No Damage [DC 0]	Incipient Motion [DC 1]	Minor Damage [DC 2]	Medium Damage [DC 3]	Total Failure [DC 4]
< 10 % of critical GSCs moved No critical GSCs detached	10% ~ 50% of critical GSCs moved < 5 % of critical GSCs detached	> 50% of critical GSCs moved 5% ~ 20% of critical GSCs detached	20% ~ 40% of critical GSCs detached	> 40% of critical GSCs detached

Table 3-5: Damage classification for individual GSCs and for the GSC Structure (Dassanayake and Oumeraci, 2012b)

3.7 Physical Model Limitations

As in any physical model there are limitations to the physical model. Some of the limitations of the model are discussed.

3.7.1 Model Effects

In order for the results of the physical modelling to have any significant meaning, the limitations imposed by model effects must be taken into account (Hughes, 1993). The expected model effects are discussed below.

3.7.1.1 Influence of side walls

The sides of the model GSC revetment are supported by the flume side walls. These side walls are rigid and have a different friction effect on GSCs placed alongside it than those GSCs found within the model revetment (ie surrounded by other GSCs). Although care was given to make each model GSC as similar as possible, there are some small deviations in the geometric dimensions of individual GSC. These small deviations result in some rows being more tightly packed against the flume side

walls than others. Van Steeg and Klein Breteler (2008) claim that the determined stability of the GSC might be too high because of this effect and should be taken note of when analysing the results.

3.7.1.2   Cross bracing

The flume side walls also have a cross bracing effect on the model GSC revetment. The cross bracing effect is expected to significantly increase the determined stability of the GSC when subjected to a wave load that is not normal to the GSC revetment. However when the wave load is normal to the GSC revetment, as is the case in the Physical model, the effect of this cross bracing is considered negligible.
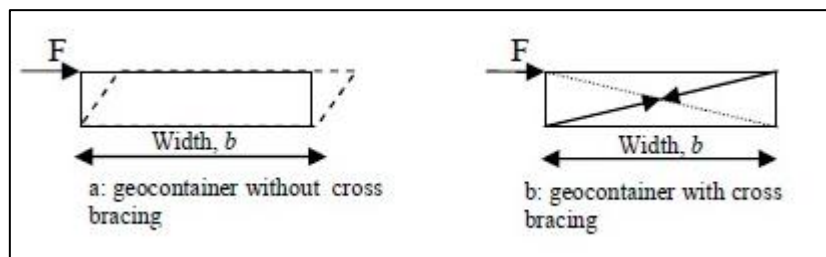
Figure 3-9: Schematisation of a GSC with and without Cross-Bracing(Van Steeg and Klein Breteler, 2008)

3.7.1.3   Scaling sand transport

The internal sand movement which is responsible for the caterpillar mechanism has been highlighted as critical to the stability of a GSC (see Section 2.3.3). The scaling of this phenomenon is thus crucial for the physical model test to be credible.

Van Steeg and Klein Breteler (2008) refined the relationship that Venis (1968) discovered, during physical modelling tests, between the dimensions of a sandbag and the critical velocity required for sand movement. This relationship is shown in Figure 3-11.
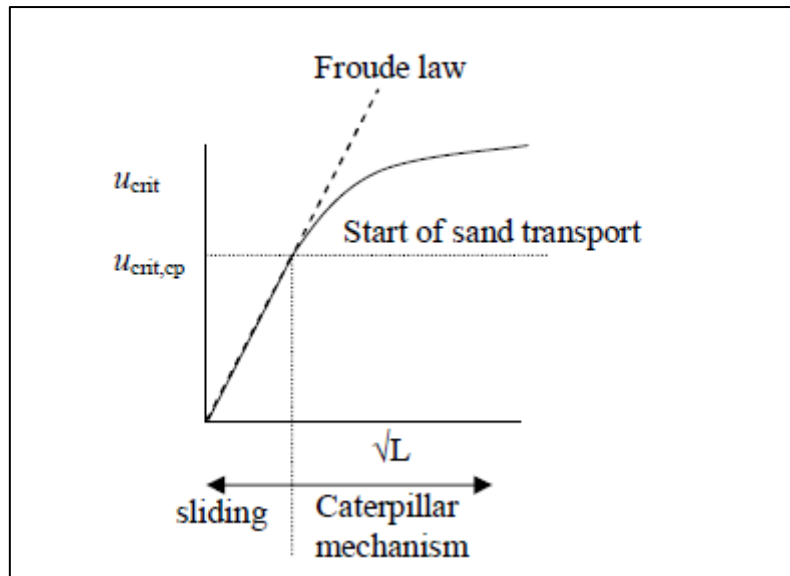
Figure 3-10: Relation between the root of the length of a sandbag ($\sqrt{L}$) and the critical velocity (μ_{crit}) (Van Steeg and Klein Breteler, 2008)

It is evident from Figure 3-10 that The Froude scaling law applies for low velocities as the relationship between the square root of the length ($\sqrt{L}$) of a sandbag and the critical velocity (μ_{crit}) is a straight line. For large scales the velocities are so large that the Froude scaling law is no longer applicable because sand transport inside the GSC occurs (Van Steeg and Klein Breteler, 2008). The point at which the sand starts to shift is almost independent of scale (Venis, 1968). This implies that the scaling is 1:1 regarding the start of movement of sand in the GSCs.

3.7.2   Scale Limitations

As mentioned previously, several parameters of the model could not be scaled suitably, especially with regards to the characteristics of the geotextile material (porosity, tensile strength and friction coefficients). The effect of this needs to be further investigated in future research.

4 Tests and Results

A total of 96 physical model tests were performed on the 12 GSC revetment permutations. Testing began on GSC revetment permutations with steeper slopes and finished with the gentler GSC revetment slope permutations. This was done to limit the amount of sand in the sand core that needed to be re-worked between tests to suit the structure slopes required. A total of 12 wave conditions were used for the tests. Wave conditions varied in wave height (Hs) and period (Tp) and are summarised in Table 4-1 below. Each GSC revetment permutation as described in Table 3-1 was subjected to a series of wave conditions and as such the physical model testing was broken down into 12 test series. Test series began with small wave height (Hs) and period (Tp) wave conditions which were gradually increased until damage to the GSC revetments was observed. In some case it was not possible to inflict damage on the GSC revetment due to the limited wave making capabilities of the hinged paddle wave-maker. The wave making capabilities of the wave-maker were initially over estimated, but due to the dynamic wave absorption system installed and the high reflections of the GSC revetment it quickly became apparent that larger wave heights than the ones summarised in Table 4-1 would not be possible.

Wave Condition	Incident			At Structure		
	Hs (m)	Hmax (m)	Tp (s)	Hs (m)	Hmax (m)	Tp (s)
1	0.49	0.87	4.94	0.47	0.84	4.99
2	1.00	1.76	4.94	0.94	1.85	4.88
3	1.31	2.21	4.94	1.20	2.21	4.88
4	1.46	2.41	4.94	1.35	2.27	4.88
5	1.71	2.95	4.94	1.57	2.63	4.88
6	0.46	0.83	9.15	0.56	0.93	8.79
7	0.93	1.64	9.15	1.13	1.92	8.79
8	1.23	2.14	9.31	1.52	2.56	8.78
9	1.40	2.40	9.03	1.73	3.00	8.71
10	0.51	1.05	12.69	0.68	1.14	11.60
11	0.82	1.59	12.68	1.05	1.97	11.58
12	1.02	2.02	12.69	1.36	2.45	12.69

Table 4-1: Summary of Wave Conditions used for the Physical Model Testing

A discussion of the test series and the results thereof follows.

51

4.1 Test Series: GSC Revetment Permutations with α=45˚

The first four test series were for GSC revetments with a structure slope of α=45˚and were all tested with the same wave conditions, shown in Table 4-2. Being the first tests of the entire test program, testing in these series was done cautiously, particularly for Series 1 and 2. The test series began with small wave heights and short periods and were gradually increased until the maximum wave heights and periods that the wave-maker could produce with the dynamic wave absorption turned on were reached and or damage to the GSC revetment was recorded.

Test Number	Wave Condition	At Structure	
		Hs (m)	Tp (m)
1	1	0.469	4.99
2	2	0.936	4.88
3	4	1.345	4.88
4	5	1.568	4.88
5	6	0.557	8.79
6	7	1.131	8.79
7	9	1.73	8.71
8	10	0.677	11.6
9	12	1.358	12.69

Table 4-2: Wave Conditions Tested for Test Series 1, 2, 3 and 4

The individual test series specifications and results follow.

4.1.1 Test Series 1: Single Armour GSC Revetment (A' Orientation)

The model setup for test series 1 was as follows:
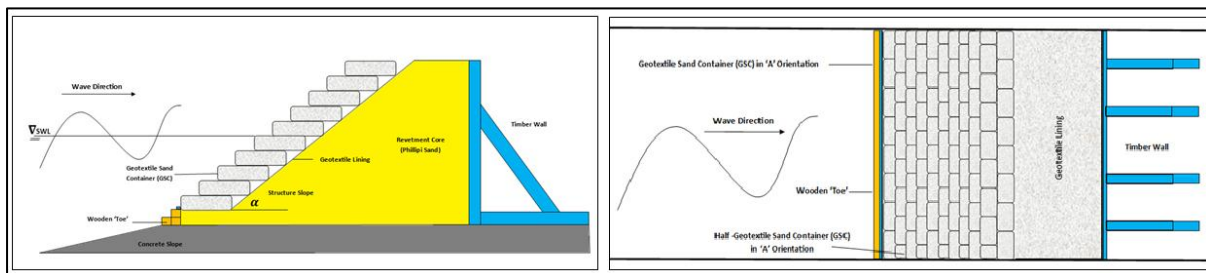
Figure 4-1: Schematic Cross-section (Left) and Plan View (Right) of GSC Revetment for Test Series 1

The first test series proved useful to correct some oversights during the construction and setup of the physical model. This permutation of GSC revetment proved to be stable for all the wave conditions tested and no damage was observed. It was noted that the larger wave heights produced some overtopping but the crest GSCs remained stable

4.1.2 Test Series 2: Single Armour GSC Revetment ('B' Orientation)

The model setup for Test Series 2 was as follows:

Figure 4-2: Schematic Cross-section (Left) and Plan View (Right) of GSC Revetment for Test Series 2

This permutation of GSC revetment proved to be stable for all the wave conditions tested and no damage was observed. It was noted that the larger wave heights produced some overtopping but the crest GSCs remained stable

4.1.3 Test Series 3: Double Armour GSC Revetment ('A' Orientation)

The model setup for Test Series 3 was as follows:
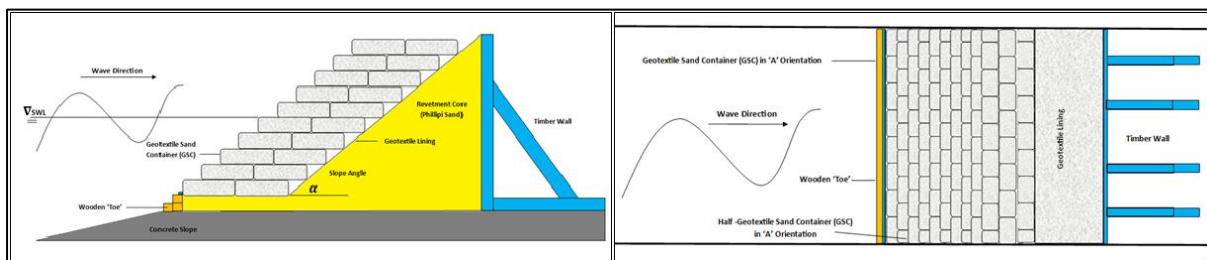
Figure 4-3: Schematic Cross-section (Left) and Plan View (Right) of GSC Revetment for Test Series 3

This permutation of GSC revetment proved to be stable for all the wave conditions tested and no damage was observed. It was noted that the larger wave heights produced some overtopping but the crest GSCs remained stable.

4.1.4 Test Series 4: Double Armour GSC Revetment ('B' Orientation)

The model setup for Test Series 4 was as follows:
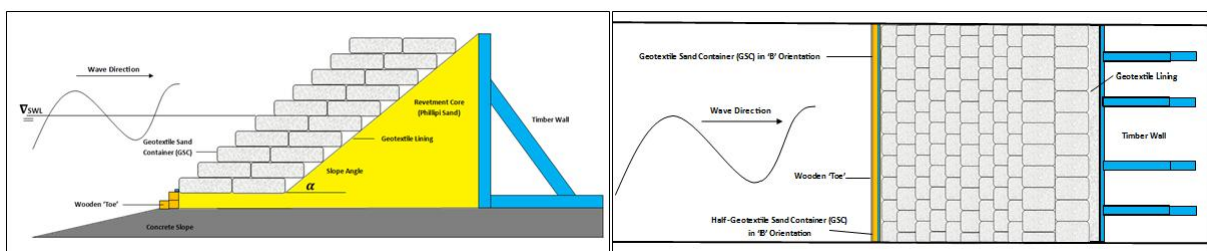
Figure 4-4: Schematic Cross-section (Left) and Plan View (Right) of GSC Revetment for Test Series 4

53

This permutation of GSC revetment proved to be stable for all the wave conditions tested and no damage was observed. It was noted that the larger wave heights produced some overtopping but the crest GSCs remained stable

4.1.5 Comments on Test Series 1, 2, 3 and 4

It was unfortunate that larger wave heights could not be produced to initiate damage to the GSC revetments tested. The knowledge gained through the literature process, did indicate that the steeper slope GSC structures, such as the ones tested, were likely to be the most stable. It was thus decided that testing on the GSC revetments with shallower structure slopes should go ahead. The fact that no damage was observed for these test series is a result in itself and the significance thereof is discussed in Chapter 5.

4.2 Test Series: GSC Revetment Permutations with α=33˚

The GSC revetment permutations with structure slopes of 1V:1.5H (α=33˚) are tested in test series 5, 6, 7 and 8. As with previous test series, they began with small wave heights and short periods and were gradually increased until the maximum wave heights and periods that the wave-maker could produce with the dynamic wave absorption turned on were reached and or damage to the GSC revetment was recorded.

The individual test series specifications and results follow.

4.2.1 Test Series 5: Single Armour GSC Revetment (α=33˚; 'A' Orientation)

The model setup for Test Series 5 was as follows:
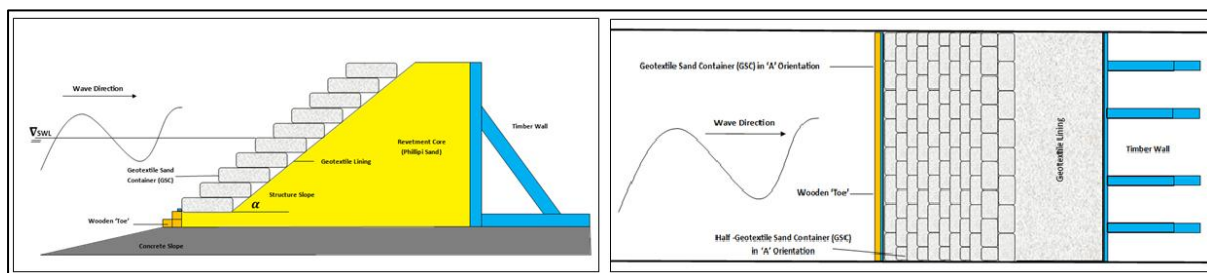
Figure 4-5: Schematic Cross-section (Left) and Plan View (Right) of GSC Revetment for Test Series 5

This permutation of GSC revetment proved to be stable for all but one of the wave conditions tested. One of the "half" GSCs was pull out during Test 5-5 as shown in Figure 4.6. This half GSC was located just below the still water level (SWL). As per the damage classification defined in Section 3.6, the GSC revetment is considered to be in incipient motion (or DC1 according to damage classification in Table 3-5) for the wave condition used in Test 5-5.

Figure 4-6: Photograph Before (Left) and After (Right) of Test 5.5

It was noted that the larger wave heights produced some overtopping but the crest GSCs remained stable. The wave conditions and damage classification of the revetment for each test is summarised in Table 4-3.

Test Number	Wave Condition	At Structure		Damage Classification
		Hs (m)	Tp (m)	
5-1	1	0.469	4.99	No Damage
5-2	2	0.936	4.88	No Damage
5-3	4	1.345	4.88	No Damage
5-4	5	1.568	4.88	Incipient Motion
5-5	7	1.131	8.79	No Damage
5-6	9	1.73	8.71	No Damage
5-7	12	1.358	12.69	No Damage

Table 4-3: Wave Conditions Tested for Test Series 5

Apart from the half bag being pulled out during Test 5-5, there were signs of internal sand movement in the GSCs during other high wave tests (5-6 and 5-7). The evidence of this can be seen by the enlargement of the front ends, or outward facing end, of the GSCs located just above and below the SWL. The structure as a whole also showed some settlement. It was observed that this settlement did not occur at the toe, but rather as a consequence of the internal sand movement reducing the height of the back ends, or inward facing end, of the individual GSCs. This cumulative effect over the 11 rows of GSCs contributes to the total settlement of the GSC revetment.

4.2.2   Test Series 6: Single Armour GSC Revetment (α=33˚; 'B' Orientation)
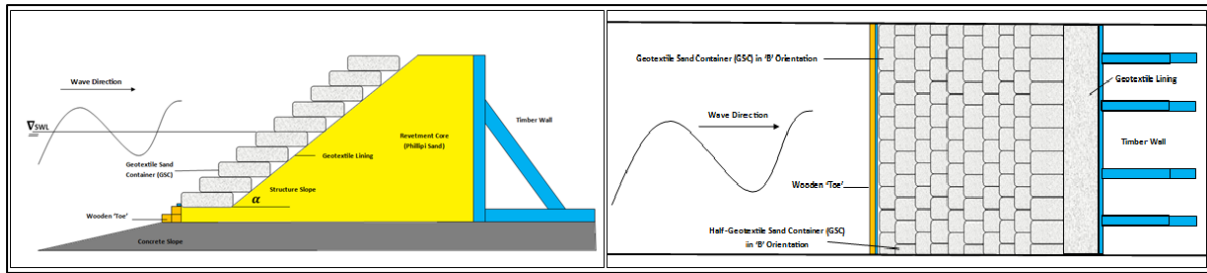
The model setup for Test Series 6 was as follows:

Figure 4-7: Schematic Cross-section (Left) and Plan View (Right) of GSC Revetment for Test Series 6

Based on the results of the previous test series, where initial damage was observed on one of the largest wave conditions, it was decided to focus on just the largest wave conditions for this test series. This was done in order to limit the number of redundant tests, as it was predicted that this test would deliver similar results. This prediction proved correct as this permutation of GSC revetment showed only incipient motion damage during two of the larger wave conditions (6-2 and 6-4). In both tests a "half" GSC was pulled out and the neighbouring GSCs, although not completely detached, had moved outwards (seawards). The damage during Test 6-6 is shown in Figure 4.8
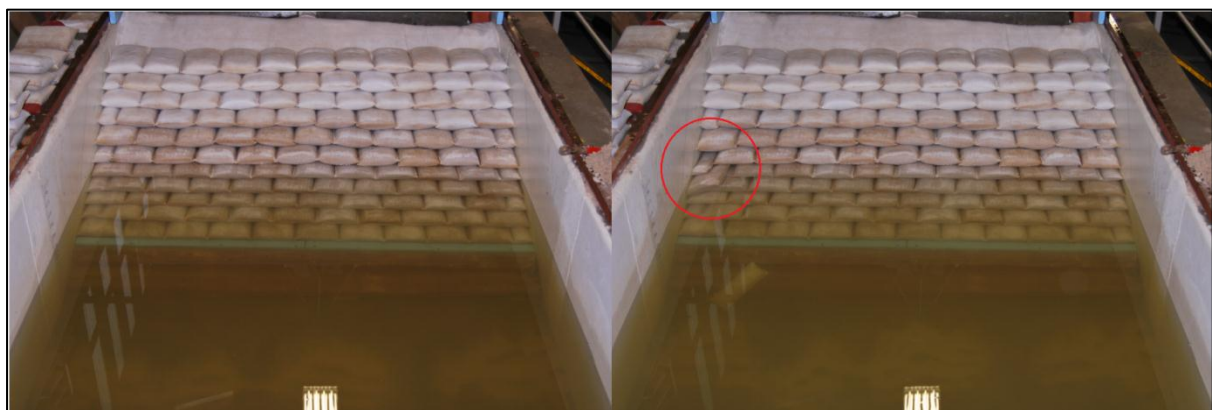
Figure 4-8: Photograph Before (Left) and After (Right) of Test 6.4

It was noted that the larger wave heights produced some overtopping but the crest GSCs remained stable. The wave conditions and damage classification for each test is summarised in Table 4-4

Test Number	Wave Condition	At Structure		Damage Classification
		Hs (m)	Tp (m)	
6-1	4	1.345	4.88	No Damage
6-2	5	1.568	4.88	Incipient Motion
6-3	9	1.73	8.71	No Damage
6-4	12	1.358	12.69	Incipient Motion

Table 4-4: Wave Conditions Tested and Damage Classification for Test Series 6

As with Test Series 5, there were signs of internal sand movement in the GSCs during other high wave tests (6.1 and 5-3). The evidence of this can be seen by the enlargement of the front ends, or outward facing end, of the GSCs located just above and below the SWL. The structure as a whole also showed some settlement. It was observed that this settlement did not occur at the toe, but rather as a consequence of the internal sand movement reducing the height of the back ends, or inward facing end, of the individual GSCs. This cumulative effect over the 11 rows of GSCs contributes to the total settlement of the GSC revetment.

4.2.3 Test Series 7: Double Armour GSC Revetment (α=33˚; 'A' Orientation)

The model setup for Test Series 7 was as follows:
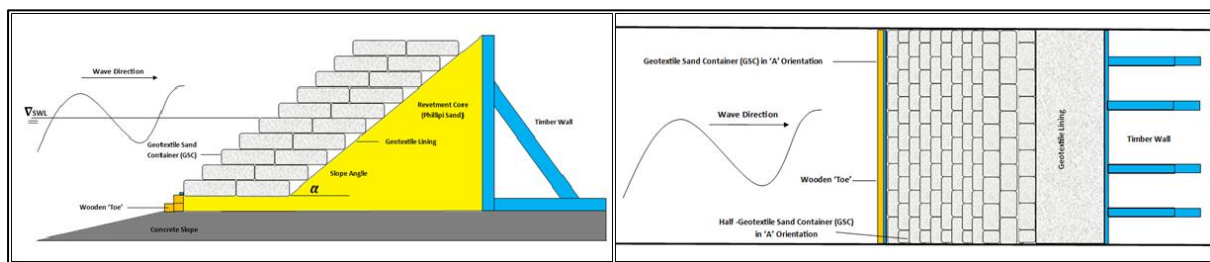
Figure 4-9: Schematic Cross-section (Left) and Plan View (Right) of GSC Revetment for Test Series 7

The results from Test Series 5 and 6 showed very modest signs of damage under the wave conditions considered. From knowledge gained through the literature review process, the performance of a double layer GSC armour revetment, such as the one considered in this Test Series, was expected to perform better than a single layer GSC armour revetment, as in Test Series 5 and 6. In other words, based on the results of Test Series 5 and 6, Test Series 7 was expected to show no damage under the wave conditions considered. Testing went ahead nonetheless to confirm.

This prediction proved to be incorrect and the degrees of damage ranged from incipient motion to total failure of the GSC revetment. The wave conditions and damage classification for each test is summarised in Table 4.5

Test Number	Wave Condition	At Structure		Damage Classification
		Hs (m)	Tp (m)	
7-1	2	0.936	4.88	No Damage
7-2	3	1.2	4.88	Incipient Motion
7-3	4	1.345	4.88	Moderate Damage
7-4	5	1.568	4.88	Total Failure
7-5	7	1.131	8.79	No Damage
7-6	8	1.515	8.78	Incipient Motion
7-7	9	1.73	8.71	Moderate Damage
7-8	10	0.677	11.6	No Damage
7-9	11	1.049	11.58	No Damage
7-10	12	1.358	12.69	Minor Damage

Table 4-5: Wave Conditions Tested and Damage Classification for Test Series 7

It was noted that the larger wave heights produced some overtopping but the crest GSCs remained stable. Tests 7-1 to 7-4 show a gradual progression of damage as the larger wave conditions were tested. The progression of damage from incipient motion to total failure for tests 7-2 to 7-4 respectively is shown in Figure 4-10, no damage was observed for test 7-1 and is thus not shown.
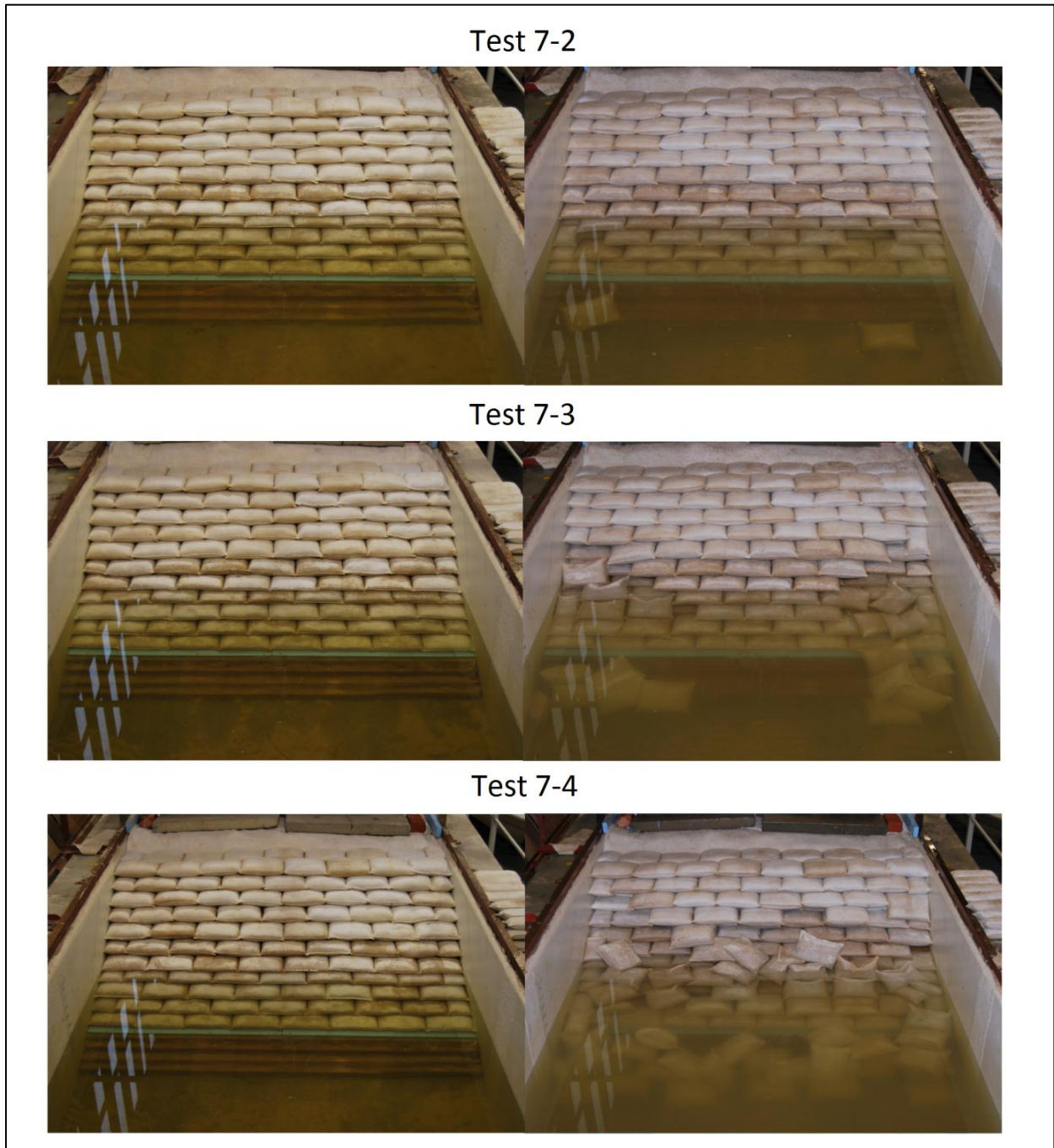
Figure 4-10: Photographs Before (Left) and After (Right) of Tests 7-2, 7-3 and 7-4

The GSCs located just below the SWL are pulled out first, after which the GSCs located just above those that have been pulled out are undermined from the wave attack and eventually slide down the revetment slope and settle at the toe of the structure. This phenomenon works itself up the

revetment slope as the test carries on. Initial displacement of GSCs occurs within the first third of a particular test duration (≈300 waves).

4.2.4   Test Series 8: Double Armour GSC Revetment (α=33˚; 'B' Orientation)
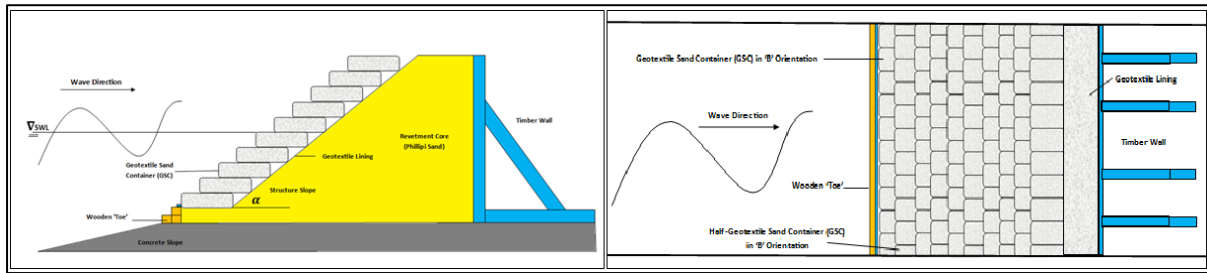
The model setup for Test Series 8 was as follows:

Figure 4-11: Schematic Cross-section (Left) and Plan View (Right) of GSC Revetment for Test Series 8

For Test Series 8, it was decided that the largest wave height wave conditions were to be tested first. This was done as a test number limiting measure. Based on the results from the wave conditions tested, a decision would be made on whether more testing was required. After the wave conditions were tested it was deemed that this was not required as the largest wave height wave conditions resulted in incipient motion. For analysis purposes, this was sufficient. Similar to Test Series 5 and 6, '"half' GSCs located just below the SWL were pulled out for all three tests. The wave conditions and damage classification for each test is summarised in Table 4-6

Test Number	Wave Condition	At Structure		Damage Classification
		Hs (m)	Tp (m)	
8-1	5	1.568	4.88	Incipient Motion
8-2	9	1.73	8.71	Incipient Motion
8-4	12	1.358	12.69	Incipient Motion

Table 4-6: Wave Conditions Tested and Damage Classification for Test Series 8

It was noted that the larger wave heights produced some overtopping but the crest GSCs remained stable.

4.2.5   Comments on Test Series 5, 6, 7 and 8

The results of these test series were quite surprising. At first glance, single layer GSC armour revetment permutations seem to match or even perform better than their double layer GSC armour equivalent permutations. This is analysed further in Chapter 5. Some concerns arose regarding the displacement of the "half' GSC and whether they could be considered in the damage classification as per Section 3.6. A conservative approach was decided upon, and ultimately the "half" bags were included in the damage classification assessment.

4.3   Test Series: GSC Revetment permutations with α=26˚

The GSC revetment permutations with structure slopes of 1V:2H (α=26˚) are tested in test series 9, 10, 11 and 12. As with previous test series, they began with small wave heights and short periods and were gradually increased until the maximum wave heights and periods that the wave-maker could produce with the dynamic wave absorption turned on were reached and or failure of the GSC revetment was observed.

4.3.1   Test Series 9: Single Armour GSC Revetment ('A' Orientation)
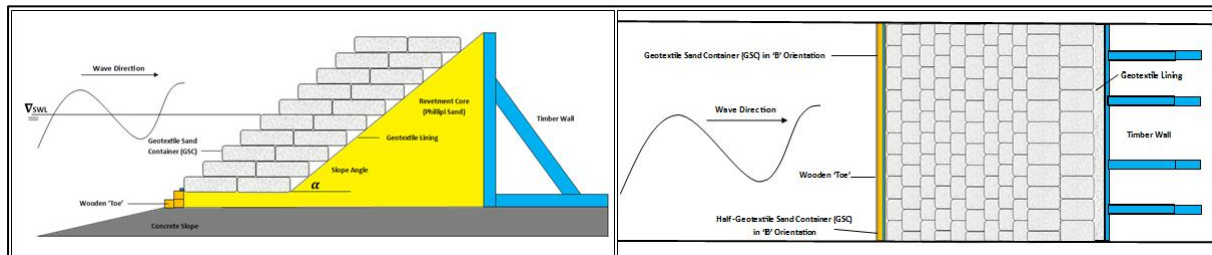
The model setup for Test Series 9 was as follows:

Figure 4-12: Schematic Cross-section (Left) and Plan View (Right) of GSC Revetment for Test Series 9

Test Series 9 was the first test series with the GSC revetment slope of 1V:2H (α=26˚). The results quickly showed that the performance of the GSC revetment was compromised at this slope with moderate damage achieved with relatively smaller wave heights as compared with the previous permutations of this revetment at steeper slopes. Initial GSC displacement occurred just below the SWL, after which the GSCs located just above those that have been pulled out are undermined from the wave attack and eventually slide down the revetment slope and settle at the toe of the structure. This phenomenon works itself up the revetment slope as the test carries on. Initial displacement of GSCs occurs within the first third of a particular test duration (≈300 waves). The wave conditions and damage classification for each test is summarised in Table 4.7.

Test Number	Wave Condition	At Structure		Damage Classification
		Hs (m)	Tp (m)	
9-1	2	0.936	4.88	No Damage
9-2	3	1.2	4.88	Incipient Motion
9-3	4	1.345	4.88	Moderate Damage
9-4	7	1.131	8.79	No Damage
9-5	8	1.515	8.78	Moderate Damage
9-6	9	1.73	8.71	Moderate Damage
9-7	10	0.677	11.6	No Damage
9-8	11	1.049	11.58	Minor Damage

Table 4-7: Wave Conditions Tested and Damage Classification for Test Series 9

Figure 4-13 and Figure 4-14 below illustrates the degrees of damage for Tests 9-3 and 9-5 respectively
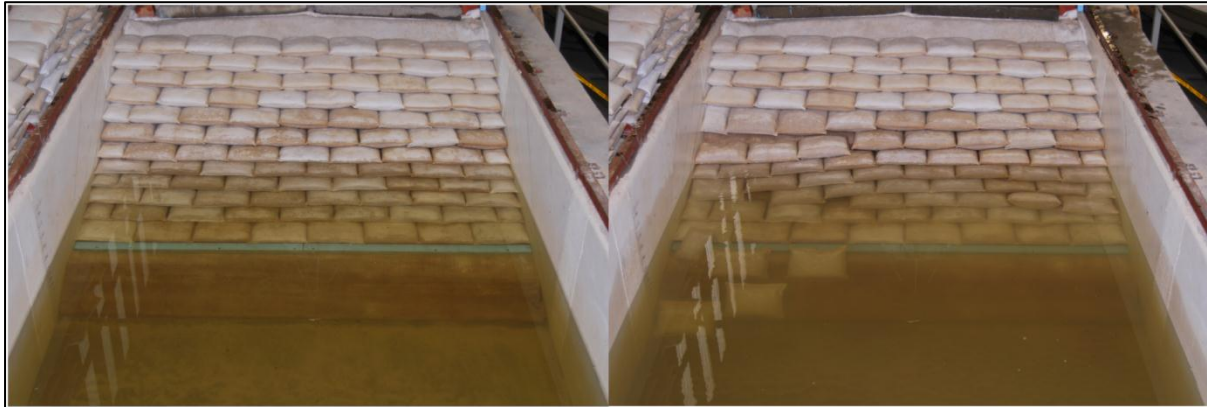
Figure 4-13: Photographs Before (Left) and After (Right) of Tests 9-3

Figure 4-14: Photographs Before (Left) and After (Right) of Tests 9-5

Overtopping of the GSC revetment was observed but did not result in the displacement of crest GSCs.

4.3.2   Test Series 10: Single Armour GSC Revetment ('B' Orientation)

The model setup for Test Series 10 was as follows:

Figure 4-15: Schematic Cross-section (Left) and Plan View (Right) of GSC Revetment for Test Series 10

Test Series 10 showed a similar trend than that of Test Series 9, with this GSC revetment incurring significantly more damage than that seen with the same GSC revetment permutations with steeper

structure slopes. Initial GSC displacement occurred just below the SWL, after which the GSCs located just above those that have been pulled out are undermined from the wave attack and eventually slide down the revetment slope and settle at the toe of the structure. This phenomenon works itself up the revetment slope as the test carries on. Initial displacement of GSCs occurs within the first third of a particular test duration (≈300 waves).The wave conditions and damage classification for each test is summarised in Table 4.8

Test Number	Wave Condition	At Structure		Damage Classification
		Hs (m)	Tp (m)	
10-1	2	0.936	4.88	No Damage
10-2	3	1.2	4.88	Minor Damage
10-3	4	1.345	4.88	Minor Damage
10-4	7	1.131	8.79	No Damage
10-5	8	1.515	8.78	No Damage
10-6	9	1.73	8.71	Moderate Damage
10-7	10	0.677	11.6	No Damage
10-8	11	1.049	11.58	Moderate Damage

Table 4-8: Wave Conditions Tested and Damage Classification for Test Series 10

Figure 4-9 illustrates the damage incurred during Test 10-8.

Table 4-9: Photographs Before (Left) and After (Right) of Tests 10-8

4.3.3   Test Series 11: Double Armour GSC Revetment ('A' Orientation)
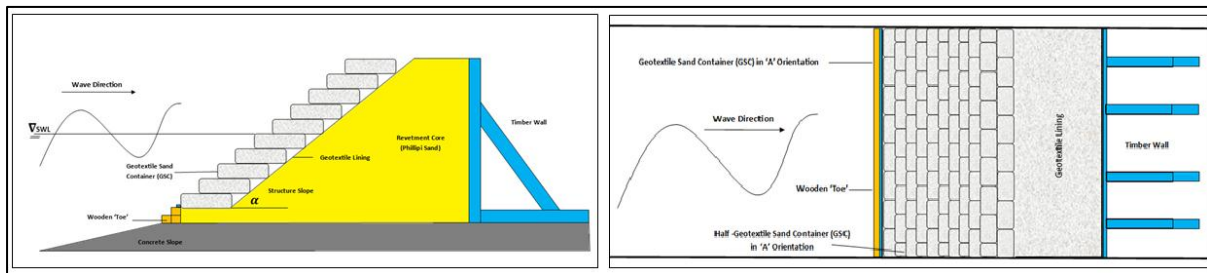
The model setup for Test Series 11 was as follows:
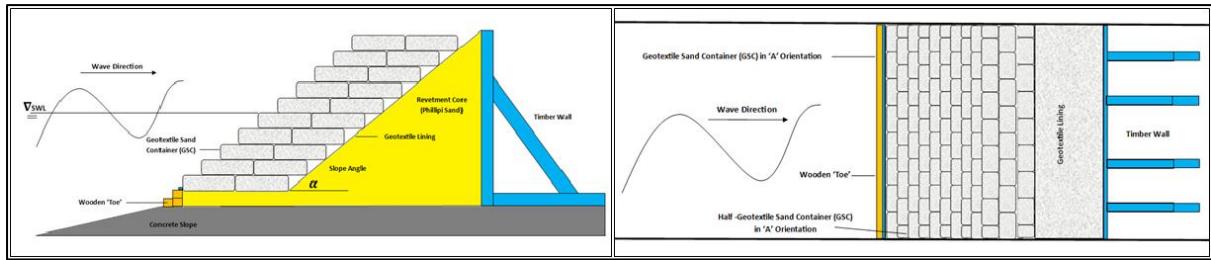
Figure 4-16: Schematic Cross-section (Left) and Plan View (Right) of GSC Revetment for Test Series 11

Test Series 11 GSC revetment incurring more damage than that seen with the same GSC revetment permutations with steeper structure slopes. Initial GSC displacement occurred just below the SWL, after which the GSCs located just above those that have been pulled out are undermined from the wave attack and eventually slide down the revetment slope and settle at the toe of the structure. This phenomenon works itself up the revetment slope as the test carries on. Initial displacement of GSCs occurs within the first third of a particular test duration (≈300 waves).The wave conditions and damage classification for each test is summarised in Table 4-10.

Test Number	Wave Condition	At Structure		Damage Classification
		Hs (m)	Tp (m)	
11-1	2	0.936	4.88	Incipient Motion
11-2	3	1.2	4.88	No Damage
11-3	4	1.345	4.88	Incipient Motion
11-4	5	1.568	4.88	Minor Damage
11-5	7	1.131	8.79	Incipient Motion
11-6	8	1.515	8.78	Minor Damage
11-7	9	1.73	8.71	Total Failure
11-8	10	0.677	11.6	No Damage
11-9	11	1.049	11.58	Moderate Damage

Table 4-10: Wave Conditions Tested and Damage Classification for Test Series 11

The progression of damage from incipient motion in test 11-5 to total failure in test 11-7 is shown in Figure 4-17 below.
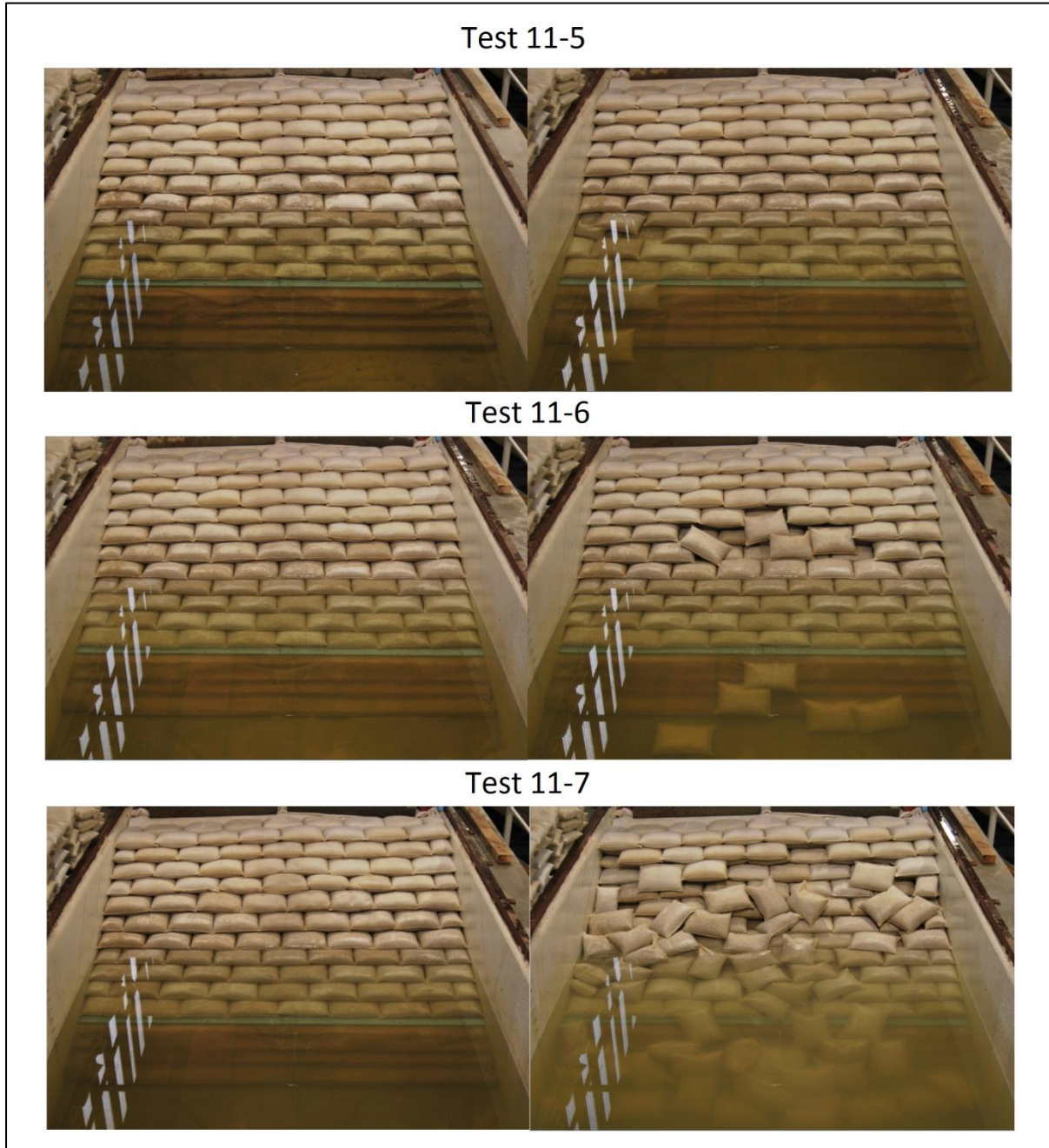
Figure 4-17: Photographs Before (Left) and After (Right) of Tests 11-5, 11-6 and 11-7

4.3.4   Test Series 12: Double Armour GSC Revetment (α=26˚; 'B' Orientation)

The model setup for Test Series 12 was as follows:

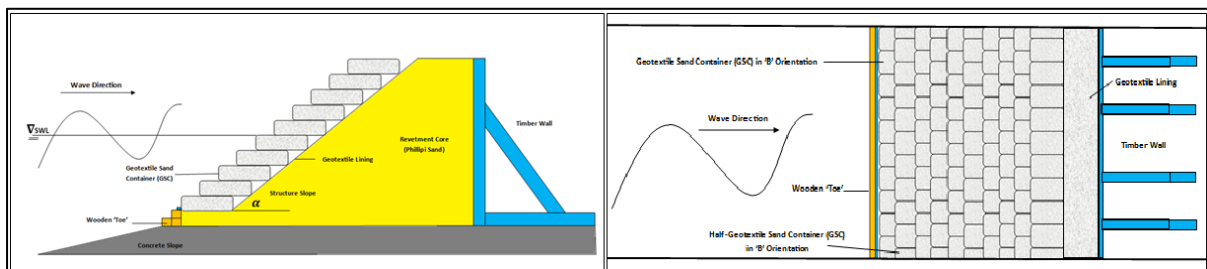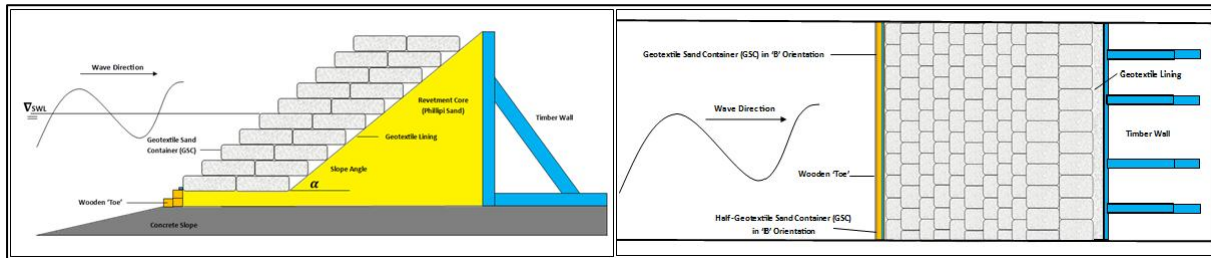**Figure 4-18: Schematic Cross-section (Left) and Plan View (Right) of GSC Revetment for Test Series 11**

Test Series 11 GSC revetment incurring more damage than that seen with the same GSC revetment permutations with steeper structure slopes. Initial GSC displacement occurred just below the SWL , after which the GSCs located just above those that have been pulled out are undermined from the wave attack and eventually slide down the revetment slope and settle at the toe of the structure. This phenomenon works itself up the revetment slope as the test carries on. Initial displacement of GSCs occurs within the first third of a particular test duration (≈300 waves).The wave conditions and damage classification for each test is summarised in Table 4-11.

Test Number	Wave Condition	At Structure		Damage Classification
		Hs (m)	Tp (m)	
12-1	2	0.936	4.88	No Damage
12-2	3	1.2	4.88	Incipient Motion
12-3	4	1.345	4.88	Incipient Motion
12-4	5	1.568	4.88	Incipient Motion
12-5	7	1.131	8.79	No Damage
12-6	8	1.515	8.78	Total Failure
12-7	9	1.73	8.71	Total Failure
12-8	10	0.677	11.6	No Damage
12-9	11	1.049	11.58	Incipient Motion
12-10	12	1.358	12.69	Total Failure

Table 4-11: Wave Conditions Tested and Damage Classification for Test Series 11

65

Figure 4-19 illustrates the damage incurred during Test 12-10.

Figure 4-19: Photographs Before (Left) and After (Right) of Tests 12-10

4.3.5   Comments of Test Series 9, 10, 11 and 12

Upon first glance it is evident that the GSC revetment permutations with a single layer GSC armour performed better than the equivalent double layer GSC armour revetment permutations. The methods of failure appear to differ between the single and double layer permutations however. A slumping mechanism is observed in the failure of single layer GSC armour revetments while a more gradual 'pull-out' effect and undermining of neighbouring GSCs is observed for double layer GSC armour revetment permutations. It was also observed that the sand core of the single layer GSC revetment showed signs of sand movement behind the geotextile lining once the layer of GSC armour was removed during the larger wave condition tests, as to be expected with no primary protection. During the larger wave condition tests on the double layer GSC revetments, the sand core remained largely intact despite some GSCs from the inner layer being pulled out.

4.4   Summary

Over the 96 physical model tests much was discovered about the hydraulic stability of the various GSC revetment permutations. The results of these tests are analysed and discussed in detail in the following chapter. However, first impressions from the physical model testing were as follows:

  I.   Steeper structure slopes offer markedly greater hydraulic stability than gentler slopes.

 II.   Double layer GSC armour revetments permutations incur damage sooner than their single layer GSC armour equivalents.

III.   When significant damage does occur on the single layer GSC revetment permutations the sand core incurs damage as well; while in the case of significant damage occurring on double layer GSC revetments the sand core remains largely intact.

IV.   GSC revetment permutations with 'B' orientation GSCs are marginally more hydraulically stable that those with 'A' orientation, but the difference is marginal.

5   Analysis

In order for the results of the physical model test to bear meaning, a detailed analysis is required. This chapter seeks to accomplish that by:

I.   Interpreting the results of the physical modelling such that answers to the primary objectives may be found.

II. Evaluate the available design charts and stability equations with the results of the physical modelling

III. Discuss the implications of the physical model results on the design of GSC revetments along the KwaZulu-Natal coastline and the reliability of available design charts and stability equations.

5.1   Physical Model Results

The primary objective of the physical modelling was to investigate the effect of various packing arrangements on the hydraulic stability of a GSC revetment. Specifically, the effect of the orientation of the GSC with respect to the direction of wave attack, the effect of single versus double layer GSC armour and the effect of different structure slopes on the hydraulic stability of GSC revetment was to be investigated.

As mentioned in Chapter 4, the limited wave making capabilities of the wave flume at the chosen length scale (10) meant that it was not possible to create a large enough waves in order for damage to occur on the GSC revetment with a slope of 1V:1H (α=45˚), for both single and double armour layer permutations. This in itself is a meaningful result; however, the effect of the GSC orientation and the effect of single versus double layer GSC armour on the hydraulic stability could not be investigated for this slope. The 1V:1.5H (α=33˚) and 1V:2H (α=26˚) slopes will thus form the basis for this investigation. This is not too great a concern as the structure slope in prototype situations are rarely 1V:1H (α=45˚) due to the difficulty involved in construction. The difficulty of constructing such a slope is brought on by the angle of repose of dry sand, approximately 1V:1.5H (Coughlan *et al*, 2008). Retaining structures are necessary, leading to unwanted increased cost and complexity issues.

5.1.1   'A' Orientation versus 'B' Orientation

The effect of different orientations (orientations defined in Figure 3-1) of the GSCs on the hydraulic stability of the revetments is analysed by comparing the largest significant wave height (Hs) and the corresponding peak period (Tp) that was measured before incipient motion occurred, as per the damage classification defined in Section 3.6, on each of the GSC revetment permutations. The results are shown graphically in the Figures 5-1 to 5-4 below.

Figure 5-1: Comparison of single layer GSC revetment (α=33˚) performance with GSCs placed at 'A' and 'B' orientations
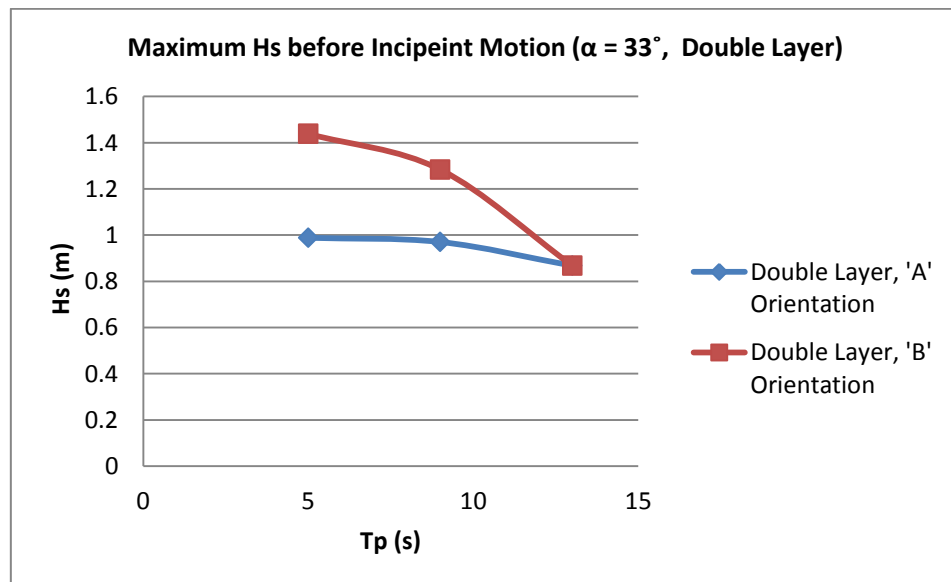
Figure 5-2: Comparison of double layer GSC revetment (α=33˚) performance with GSCs placed at 'A' and 'B' orientations
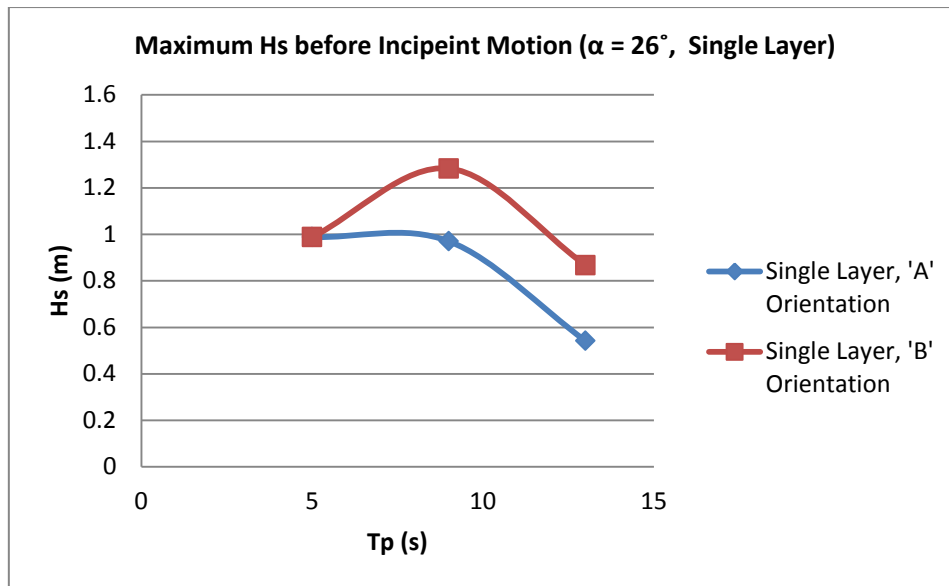
Figure 5-3: Comparison of single layer GSC revetment (α=26˚) performance with GSCs placed at 'A' and 'B' orientations
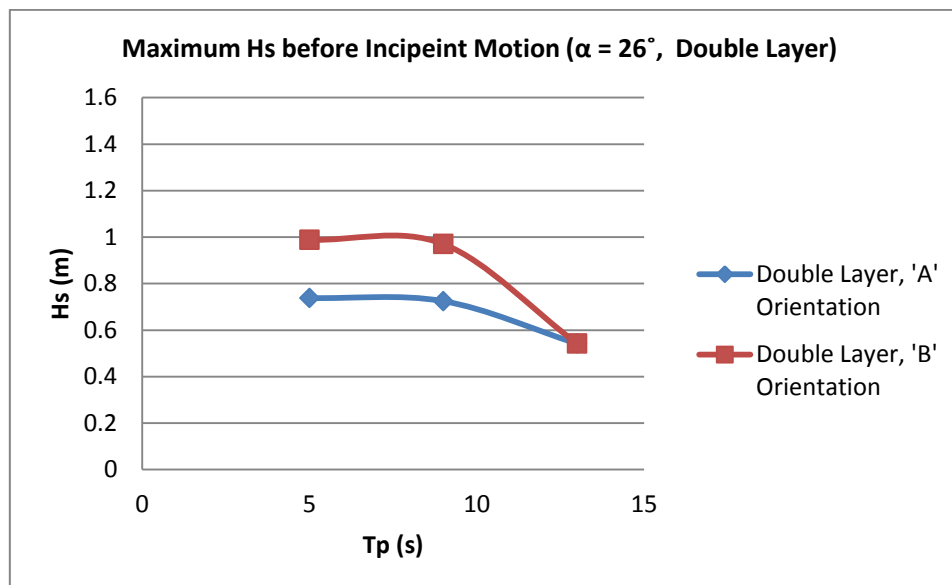
Figure 5-4: Comparison of double layer GSC revetment (α=26˚) performance with GSCs placed at 'A' and 'B' orientations

It is evident from the figures above that the trend for GSC revetments is to perform better, which is to resist larger wave heights, when placed in the 'B' orientation as opposed to the 'A' orientation (The only exception being that of the single GSC armour layer at a slope of 1V:1.5H (α=33) as seen in figure 5-1, which is within the margin of experimental error. This result is to be expected as there is a greater overlap length of the individual GSCs within the 'B' orientated revetment permutations. It is also interesting to note that for single layer permutations the longer periods perform better in the 'B' orientation than the 'A' orientation, while there is no difference in performance for the shorter periods. The double layer permutations show a different trend: there is no difference in

performance for the longer periods, while 'B' orientated permutations perform better than 'A' orientated permutations for the shorter periods.

5.1.2   Single Layer GSC Armour versus Double Layer GSC Armour

The effect of single layer GSC armour and double layer GSC armour on the hydraulic stability of the revetments is analysed by comparing the largest significant wave height (Hs) and the corresponding peak period (Tp) that was measured before incipient motion occurred, as per the damage classification defined in section 3.6, on each of the GSC revetment permutations. The results are shown graphically in Figures 5-5 to 5-8 below.

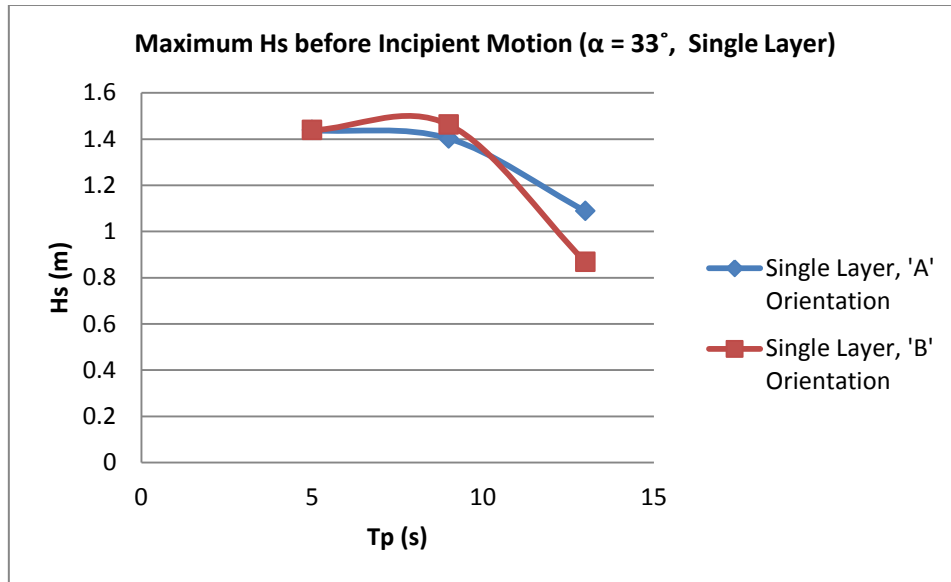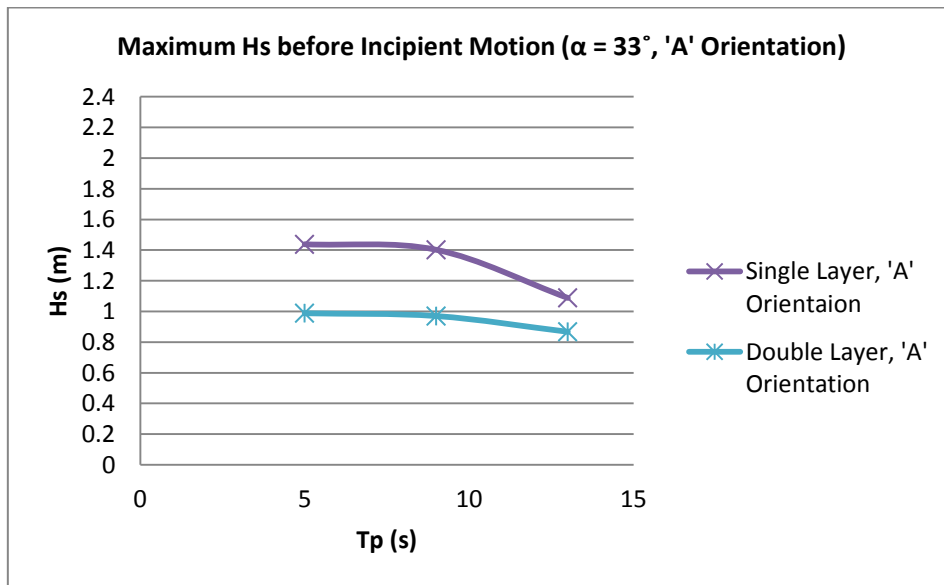**Figure 5-5: Comparison GSC revetment performance with single and double layer GSC armour layers (α=33˚, 'A' orientation)**
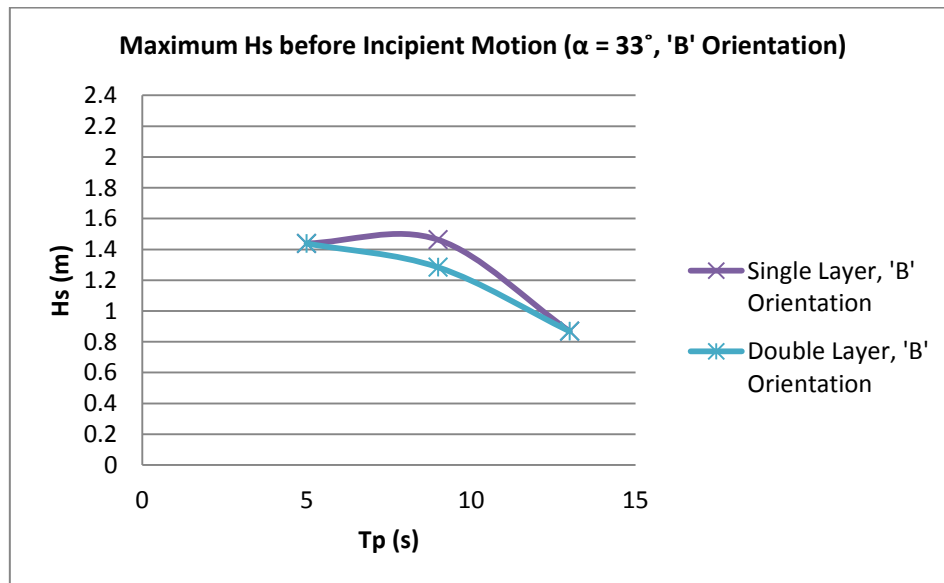
Figure 5-6: Comparison GSC revetment performance with single and double layer GSC armour layers (α=33˚, 'B' orientation)
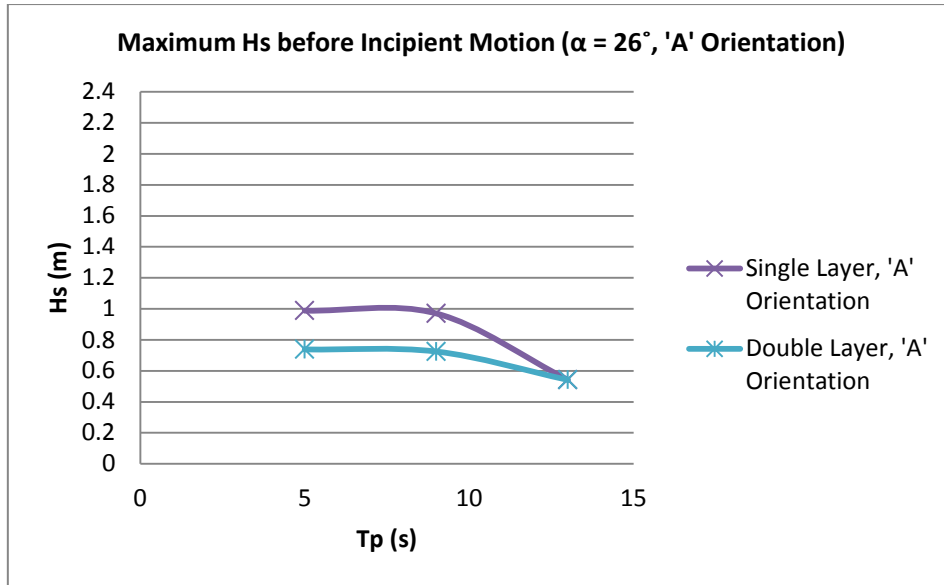
Figure 5-7: Comparison GSC revetment performance with single and double layer GSC armour layers (α=26˚, 'A' orientation)
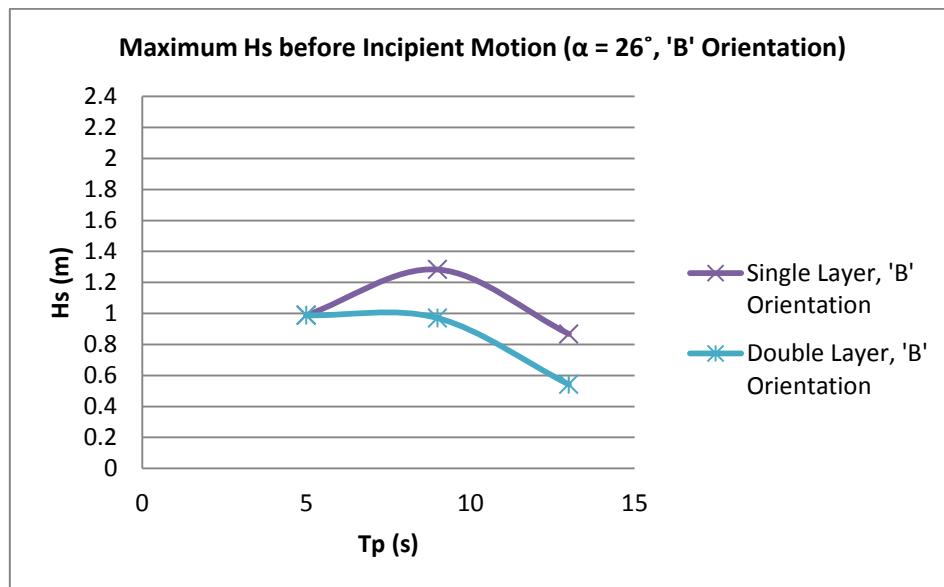
Figure 5-8: Comparison GSC revetment performance with single and double layer GSC armour layers (α=26˚, 'B' orientation)

It is evident form the figures above that the trend is for single layer GSC armour revetment to perform better, which is to resist larger wave heights, or at least match that of double layer GSC armour revetments. This result is not expected as the literature review process identified as double layer GSC armour revetments to be more hydraulically stable. The reason for this discrepancy is discussed at the end of this chapter.

71

5.1.3   GSC Revetment Slope

The effect of different structure slope on the hydraulic stability of the revetments is analysed by comparing the largest significant wave height (Hs) and the corresponding peak period (Tp) that was measured before incipient motion occurred, as per the Damage Classification defined in Section 3.6, on each of the GSC revetment permutations. Although no damage was recorded on the steepest slope of 1V:1H (α = 45˚), the largest significant wave heights that the slope was subjected to is included in the comparison for illustrative purposes. The results are shown graphically in Figures 5-9 to 5-12 below.
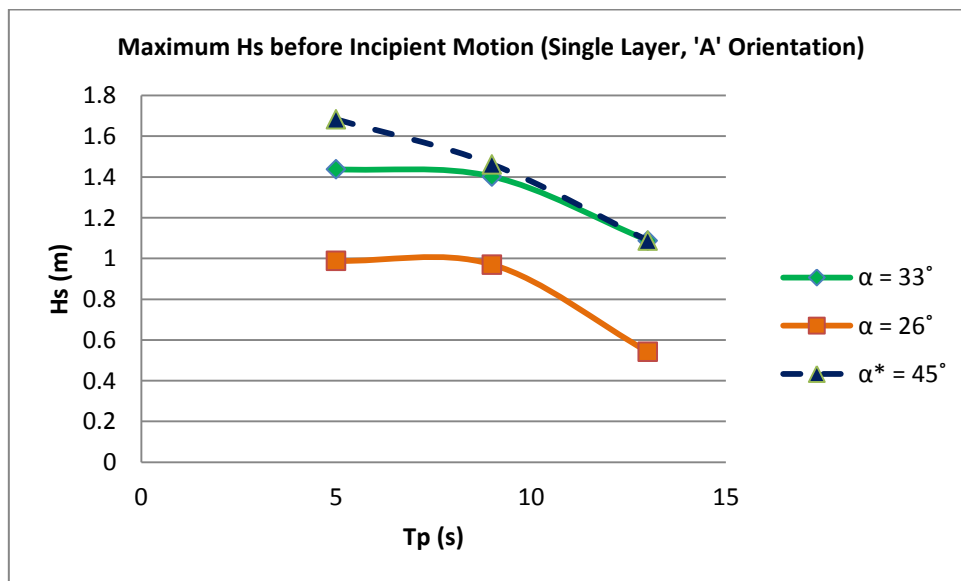
Figure 5-9: Comparison GSC revetment performance with varying structure slopes (Single Layer, 'A' Orientation)
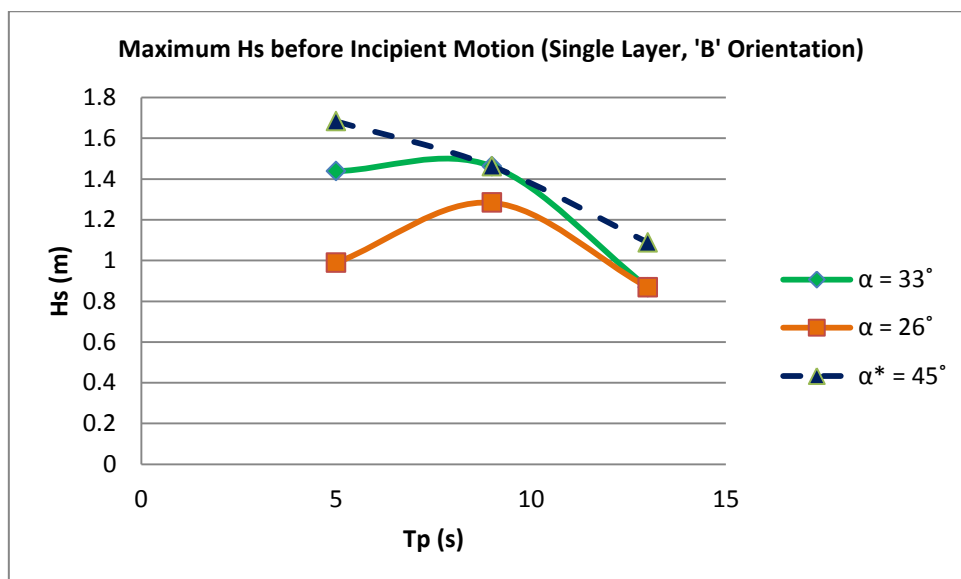
Figure 5-10: Comparison GSC revetment performance with varying structure slopes (Single Layer, 'B' Orientation)

72
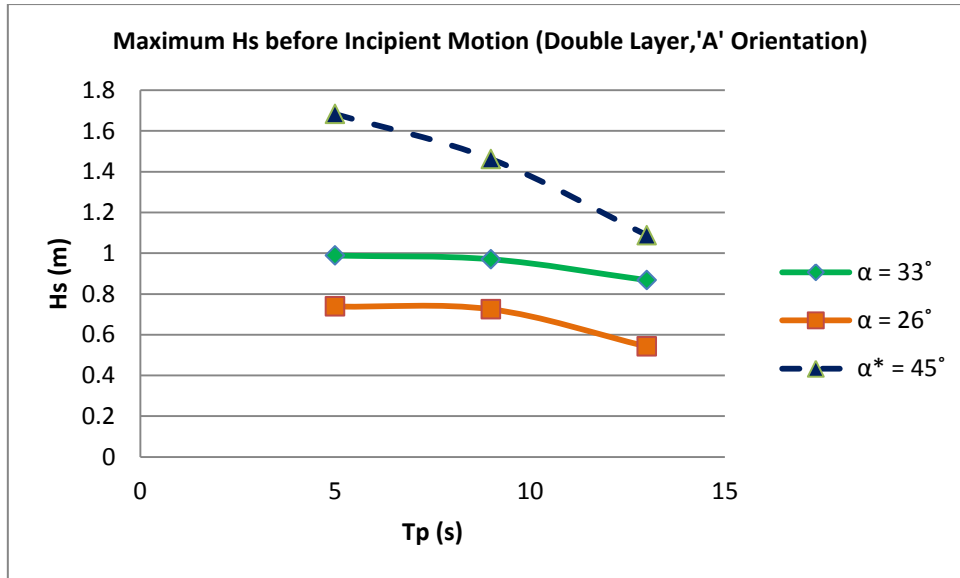
Figure 5-11: Comparison GSC revetment performance with varying structure slopes (Double Layer, 'A' Orientation)
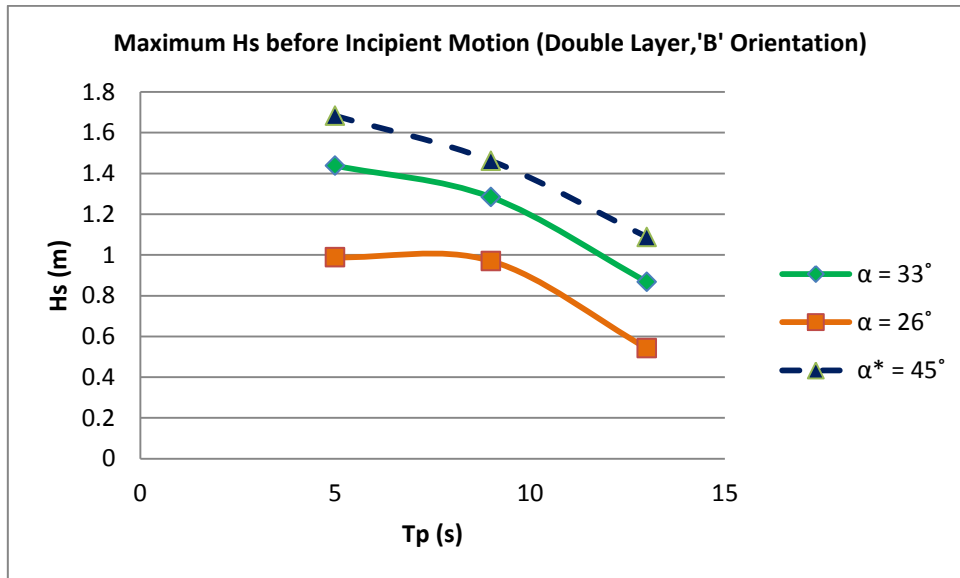
Figure 5-12: Comparison GSC revetment performance with varying structure slopes (Double Layer, 'B' Orientation)

It is evident from the figures above that the trend for GSC revetments is to perform better, which is to resist larger wave heights, when constructed at steeper slopes. Even though for the 1V:1H (α = 45˚) slope no damage was recorded, it remained stable against wave heights larger than when instability had already occurred on the other two shallower slopes.

5.1.4 Summary of Findings

By investigating the point of incipient motion on each of the GSC revetment permutation the primary objectives of the physical model have been met with the following findings:

a) The hydraulic stability of a GSC revetment is greater when the GSCs are placed in the 'B' orientation or when the longest side of the GSC is parallel to the direction of wave attack.

73

b) The hydraulic stability of a GSC revetment is greater when constructed with a single layer GSC armour.

c) The hydraulic stability of a GSC revetment is greater when constructed at steeper slopes such as 1V:1H (α = 45˚).

5.2   Evaluation of Available Design Charts and Stability Equations

In order to evaluate the available design charts and stability equations a comparative analysis is carried out with the physical model results. In this way, the applicability of the design charts and stability equations outside their respective range of limitations can be assessed. It also serves as a method to validate the results of the physical model tests, provided of course there is some correlation between the two.

5.2.1   WRL Design Chart

The WRL design chart is based on the findings of their own physical model tests. The details of these tests are summarised in Section 2.5, however the principal findings of the tests are briefly mentioned:

a) The hydraulic stability of a GSC revetment is greater when constructed with a double layer GSC armour

b) The hydraulic stability of a GSC revetment is greater when constructed at steeper slopes such as 1V:1H (α = 45˚).

These WRL test findings are based on GSC revetments with GSCs placed in an 'A' Orientations and tested under similar wave conditions to the physical model under consideration. Although the physical model tests agree that steeper slopes enhance the hydraulic stability of a GSC revetment, there is disagreement as to whether single or double layer GSC armour offers more hydraulic stability.

The WRL physical model tests base the finding of double layer GSC revetment being more hydraulically stable on a limited amount of monochromatic wave tests, tested on both single and double layer GSC armour revetments at a slope of 1V:1H (α = 45˚). The physical model testing under consideration in this report however indicates that a single layer GSC revetment is more hydraulically stable than a double layer, based on a more extensive random wave test program. The random wave versus regular wave could account for the discrepancy between the physical model results. The random wave stability test is also considered to be more representative of prototype conditions.

The greater stability of a single layer GSC revetment could be explained with help of permeability tests performed by Recio, (2007). One of the main findings of the tests is that the permeability of a GSC structure is considerably reduced if there is a second layer of overlapped containers that obstructs the flow coming out of the gaps of the first layer. The permeability of a revetment is critical to its hydraulic stability as higher permeability reduces the seepage forces and pressure 'build-up' in the structure and thus leading to greater hydraulic stability (Recio, 2007).

The WRL did do extensive random wave tests on double layer GSC armour revetments with varying structure slopes and used the results to develop a design chart. The results obtained using this design chart are compared to the results for a double layer GSC armour revetment with GSCs placed in an 'A' orientation in table 5-1 below.

GSC Revetment: Double Armour Layer with GSCs placed in 'A' Orientation			
Revetment Structure Slope	Peak Wave Period, Tp (s)	Design Significant Wave Height, Hs (m)	
		WRL Design Guide	Physical Model Results
1V:1.5H (α=33°)	5	1.75	0.99
	9	1.55	0.97
	13	1.38	0.87
1V:1.5H (α=26°)	5	1.50	0.74
	9	1.30	0.72
	13	1.15	0.54

Table 5-1: Comparison of design wave heights between WRL Design Guide and physical model results

It is evident that the WRL design chart over predicts the design wave height (Hs) of the physical model test by a factor of between 1.5 and 2. It is important to note that this design chart is based on the results of a GSC revetment with GSCs much smaller (0.75m³) than those considered in the physical model test (2.5m³). The design wave heights for the 0.75m³ GSCs were increased by 35% for the 2.5m³ GSCs. This was never validated by large scale physical modelling and could possibly offer a reason for the over prediction.

5.2.2   Stability Equations

Much work has been done to develop hydraulic stability equations for GSC revetments and are described in detail in Section 2.5. The stability equations used for the comparative analysis of the results obtained in the physical model test are:

1. Wouters (1998)
2. Oumeraci *et al* (2002)
3. Recio (2007)

75

These stability equations have been developed on different principals and require different input parameters. These stability equations represent the most relevant and fundamental equations available and are thus deemed ideal for a comparative analysis.

5.2.2.1 *Stability Equation of Wouters (1998)*

The stability equation proposed by Wouters is based on physical model tests of a single layer GSC armour revetment and is thus only applicable to the results of the physical model test concerned with the single layer GSC armour revetment permutations. For the purposes of this analysis the stability equation as defined in Section 2.5 is re-written in terms of significant wave height as follows:

$$H_s = \left[\frac{2\pi}{gT_p{}^2} \left(\frac{\left\{ C_w D \left(\frac{\rho_E}{\rho_W} - 1 \right) \right\}^2}{\tan\alpha} \right)^2 \right]^{1/3}$$

Where

- H_S = Incident significant wave height [m]
- ρ_E = Density of sand container elements where: $\rho_E = {M_{GSC}}/{V_t}$ [kg/m³]
- M_{GSC} = Mass of GSC unit [kg]
- V_t = Volume of GSC unit as defined in Section 2.1.4
- ρ_W = Density of water [kg/m³]
- D = Characteristic diameter of sand container and defined as: $D = l_c \sin\alpha$ [m]
- l_c = Length of sand container parallel to direction of wave attack [m]
- α = Angle of structure slope (90˚ is vertical)
- C_W = 2.0 (empirical parameter based on test results) [-]
- T_p = Peak spectral period [s]
- g = gravitational constant 9.81 [m/s²]

The design wave height can now be determined for different peak periods (Tp) and GSC lengths. This equation was used to calculate the design wave height for the same peak periods and GSC dimensions as used in the physical modelling tests. The input values used in the equation are as follows:

- Tp   = 5,9,13 (s) and the corresponding L_0 (m)

- α = 33˚ and 26˚

- ρ_E = 1900 [kg/m³]

- ρ_W = 1000 [kg/m³] for the fresh water used in the physical model

- l_c = 2 [m] for 'A' Orienation and 2.5 [m] for 'B' Orientation

- C_W = 2.0[-]

The results are shown in Table 5.2 and shown graphically in Figure 5-13.

GSC Revetment: Single Layer GSC Armour				
Revetment Structure Slope	Peak Wave Period, Tp (s)	GSC Orientation	Design Significant Wave Height, Hs (m)	
			Wouters Stability Equation	Physical Model Results
1V:1.5H (α=33˚)	5	A	1.28	1.44
	9		0.86	1.40
	13		0.68	1.09
1V:1.5H (α=26˚)	5		1.17	0.99
	9		0.79	0.97
	13		0.62	0.54
1V:1.5H (α=33˚)	5	B	1.73	1.44
	9		1.17	1.46
	13		0.92	0.87
1V:1.5H (α=26˚)	5		1.58	0.99
	9		1.07	1.28
	13		0.84	0.87

Table 5-2: Comparison of Design Wave Heights between Wouters Stability Equation and the Physical Model Results
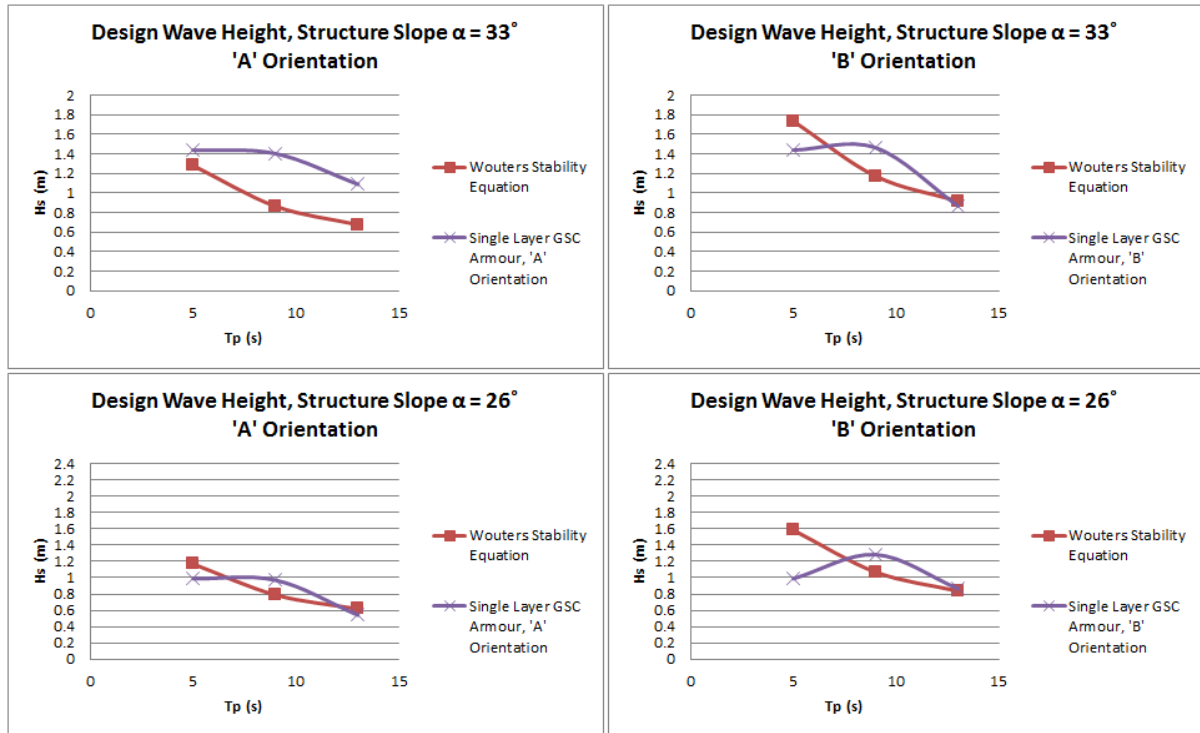
Figure 5-13: Comparison of Design Wave Heights between Wouters Stability Equation and the Physical Model Results

It is evident that there is only a weak correlation between the Wouters stability equation and the results of the physical model test. Wouters stability equation is based on empirical data which could explain the reason for the discrepancy between the results. This stability equation is therefore considered not to be applicable to GSC revetment permutations outside its range of limitations.

5.2.2.2   Stability Equation of Oumeraci et al. (2003)

The OumeracI *et al.* stability equation is largely based on the equation developed by Wouters (1998). The only difference being that Oumeraci *et al.* derived the empirical value C_W = 2.75 for double layer GSC armour revetments as opposed to that of C_W= 2.0 for single layer GSC armour derived by Wouters (1998). This equation is thus relevant to the physical model results concerned with double layer GSC revetment permutations. The input values used in the equation are as follows:

- Tp   = 5,9,13 (s) and the corresponding L_0 (m)
- α = 33˚ and 26˚
- ρ_E = 1900 [kg/m³]
- ρ_W = 1000 [kg/m³] for the fresh water used in the physical model
- l_c = 2 [m] for 'A' Orientation and 2.5 [m] for 'B' Orientation
- C_W = 2.75[-]

78

The results are shown in Table 5-3 and shown graphically in Figure 5-13.

GSC Revetment: Double Layer GSC Armour				
Revetment Structure Slope	Peak Wave Period, Tp (s)	GSC Orientation	Design Significant Wave Height, Hs (m)	
			Oumeraci *et al*. Stablilty Equation	Physical Model Results
1V:1.5H (α=33˚)	5	A	1.45	0.99
	9		0.98	0.97
	13		0.77	0.87
1V:1.5H (α=26˚)	5		1.33	0.74
	9		0.90	0.72
	13		0.70	0.54
1V:1.5H (α=33˚)	5	B	1.97	1.44
	9		1.33	1.28
	13		1.04	0.87
1V:1.5H (α=26˚)	5		1.80	0.99
	9		1.21	0.97
	13		0.95	0.54

Table 5-3: Comparison of Design Wave Heights between Oumeraci et al Stability Equation and the Physical Model Results
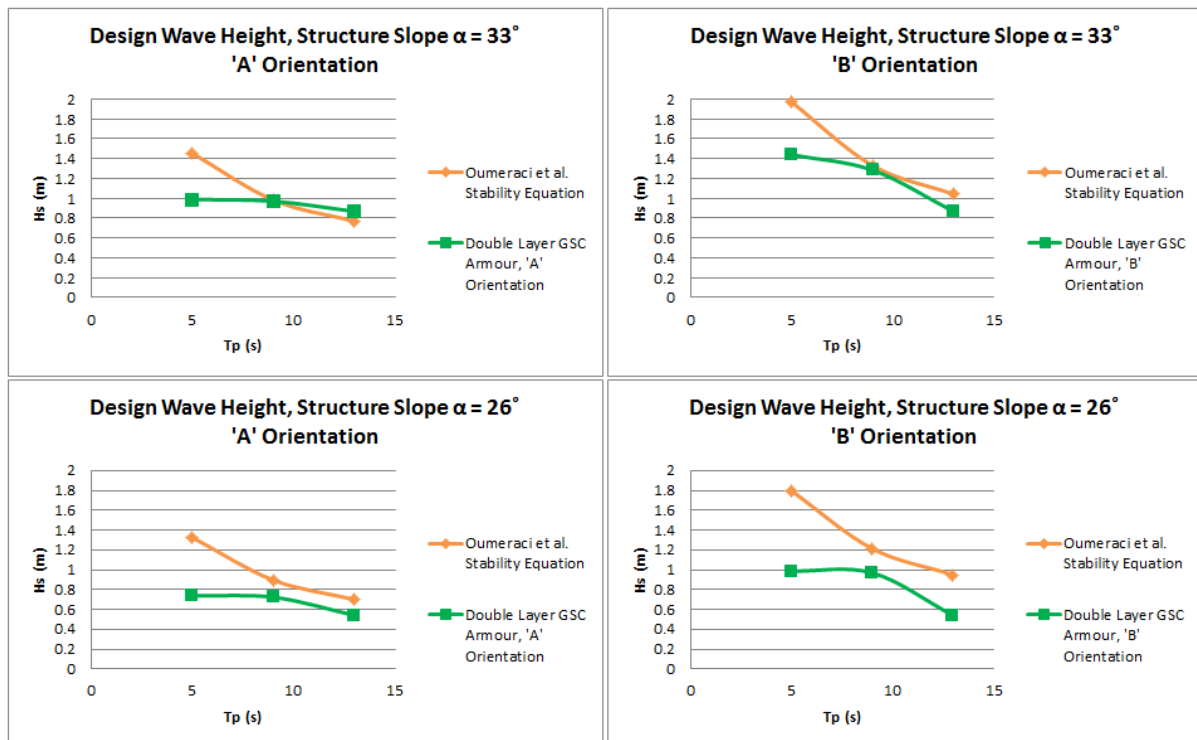
Figure 5-14: Comparison of Design Wave Heights between Oumeraci et al Stability Equation and the Physical Model Results

As with Wouters equation, there is only a weak correlation between the Oumeraci equation and the results of the physical model tests. The empirical nature of these equations appears to be the reason

for the discrepancy and they are therefore not considered suitable to GSC revetments outside their range of limitations.

5.2.2.3   Recio Stability Equation (Recio, 2007)

The Recio stability equation is described in detail in Section 2.5 and is applicable to double layer GSC armour revetments. The equation is valid subject to the following:

- GSCs are made with non-woven geotextile material
- GSCs have an 80% sand fill ratio
- GSCs have a geometry for which the length is twice as large as the width and five times as large as its height
- The GSC structure is constructed at a slope angle of $\alpha = 45°$.

Recio (2007) states that modifications to the equations to adapt them for GSCs with other geometries and GSC revetments with other structure slopes is possible, provided the proposed approach is followed from first principles. In order to adapt the equation to be valid for the physical model test the following variables must be considered:

I.   The effect of the different GSC geometries on the stability equation
II.   The effect of the different GSC geometries on the force coefficients
III.   The effect of the different GSC geometries and structure slopes on the deformation factors

The physical model testing was done on GSC revetments with GSCs placed in an 'A' orientation and in a 'B orientation, as defined in Section 3.3, and at structure slopes varying from $\alpha = 45°$ to $\alpha = 26°$. The geometry of a typical GSC is shown in Figure 5-13 and defined for the GSC revetment permutations tested in the physical model testing in Table 5.4 below.
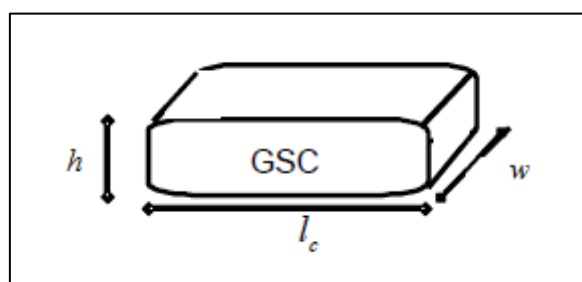
Figure 5-15: Geometry of a typical GSC used in coastal structures, l_c being the length of GSC parallel to the direction of wave attack.

Parameter	Recio	Physical Model 'A' Orientation	Physical Model 'B' Orientation
Length	l_c	l_c	l_c
Width	$w = 0.5 \times l_c$	$w = 1.25 \times l_c$	$w = 0.8 \times l_c$
Height	$h = 0.2 \times l_c$	$h = 0.2 \times l_c$	$h = 0.2 \times l_c$
Volume	$V = 0.1 \times l_c$	$V = 0.25 \times l_c$	$V = 0.16 \times l_c$
Application Area of Drag Force	$A_s = 0.1 \times l_c{}^2$	$A_s = 0.25 \times l_c{}^2$	$A_s = 0.16 \times l_c{}^2$
Application Area of Uplift Force	$A_T = 0.5 \times l_c{}^2$	$A_T = 1.25 \times l_c{}^2$	$A_T = 0.8 \times l_c{}^2$

Table 5-4: GSC parameters defined in terms of l_c, the length of GSC parallel to the direction of wave attack

1) The approach used by Recio (2007) to develop the stability equation was followed using the parameters suitable for each orientation used in the physical model. It is interesting to note that this led to equations identical to that of Recio. This is due to the cross cancelling of the width and length parameter coefficients during the simplification process as well as the same height parameter coefficient remaining constant.

The stability equation (see section 2.5.2.5) thus remains as:

$$l_c \geq u^2 \left[\frac{(0.5 KS_{CD} C_D + 2.5 KS_{CL} C_L \mu)}{\left(\mu KS_R \Delta g - KS_{CM} C_M \frac{\delta u}{\delta t} \right)} \right]$$

2) The force coefficients, C_D, C_M and C_L, are strongly affected by the relation between depth and wave length (*d/L*) (Dean and Dalrymple, 1998) and as such are only valid for shallow water conditions ($\frac{d}{L} \leq 0.10$) as used in the experimental tests conducted by Recio (2007). The geometry of the GSC is not important in the derivation of these force coefficients. The force coefficients derived by Recio (2007) were done so as a function of horizontal flow velocity or considering the GSC structure as "hydraulically transparent". The implication thereof is that the force coefficients can be applied to structures with slope angles different to α = 45˚ provided the following criteria are met:

- Shallow water conditions ($\frac{d}{L} \leq 0.10$)

- Reynolds Number in the range of $10^4 < Re < 10^6$

3)   The derivation of the deformations factors used in the stability equation is discussed in section 2.5. These deformation factors are influenced by the geometry of the GSC and as such must be adapted the geometries of the GSCs used in the physical model. The approach that Recio (2007) utilised to derive the deformation factors was used to determine the deformation factor suitable for the geometry of the GSCs used in the physical model tests. The adapted deformation factors are presented in Table 5.5 below.

Deformation Factor	Slope Angle	Value
KS_{CD}	26˚	2.15
KS_{CL}	26˚	0.88
KS_R	26˚	0.4244
KS_{CM}	26˚	1
KS_{CD}	33˚	1.8
KS_{CL}	33˚	0.91
KS_R	33˚	0.775
KS_{CM}	33˚	1

Table 5-5: Adapted Deformation Factors to be used in the Recio Stability Equation

Where the deformation factors are (as defined by Recio, 2007):

- KS_{CD} is the deformation factor that accounts for the variation of projected area of a GSC normal to wave direction and the subsequent effect on the drag force.
- KS_{CL} is the deformation factor that accounts for the variation of projected area of a GSC in the wave direction and the subsequent effect on the on the lift force
- KS_R is the deformation factor that accounts for i) the reduction of resisting force due to deformations and ii) the increase of the resisting force due to the contribution of upper GSCs.
- KS_{CM} is the deformation factor that accounts for variations of volume of a GSC on the inertia forces. The volume of GSC is assumed to stay constant and thus remains as 1.

The input parameters of the equation are as follows:

- Deformation factors as per Table 5.4
- C_D = 9
- C_M = 1

82

- C_L = 0.3
- μ = 0.48 for a non-woven geotextile
- g = 9.81 m/s² (Gravitational Constant)
- Δ = 0.9 (for ρ_E = 1900 kg/m³ and ρ_w = 1000 kg/m³)
- u = maximum wave-induced horizontal velocity at the location of the critical container
- $\dfrac{\delta u}{\delta t}$ = maximum wave-induced horizontal accelerations at the same location.

The maximum wave-induced horizontal velocities and accelerations are calculated using linear wave theory and summarised in Appendix D. The stability equation is very sensitive to horizontal velocity due to the presence of the square function (u^2) and is therefore more important than the horizontal acceleration (Recio, 2007). In addition, Recio (2007) suggests that using the maximum horizontal acceleration is very conservative. Due to the phase shift between horizontal acceleration and horizontal velocity, the horizontal acceleration tends to zero when the horizontal velocity reaches a maximum and vice versa. To solve these issues, Recio (2007), recommends that the maximum horizontal velocity should be used in conjunction with 10% of the maximum horizontal acceleration and this was applied in the calculations for Table 5-6.

The force coefficients used for calculation purposes are typical values used in such calculations. Ideally suitable empirical values for the GSCs under consideration in this report should be determined; however this is beyond the scope of this study.

The results of the stability equations are as follows

GSC Revetment: Double Layer GSC Armour				
Revetment Structure Slope	Peak Wave Period, Tp (s)	GSC Orientation	Design Significant Wave Height, Hs (m)	
			Recio Stability Equation	Physical Model Results
1V:1.5H (α=33˚)	5	A	1.16	0.99
	9		0.96	0.97
	13		0.93	0.87
1V:1.5H (α=26˚)	5		0.78	0.74
	9		0.67	0.72
	13		0.65	0.54
1V:1.5H (α=33˚)	5	B	1.30	1.44
	9		1.07	1.28
	13		1.03	0.87
1V:1.5H (α=26˚)	5		0.87	0.99
	9		0.74	0.97
	13		0.73	0.54

Table 5-6: Comparison of design wave height between Recio stability equation and physical model results.
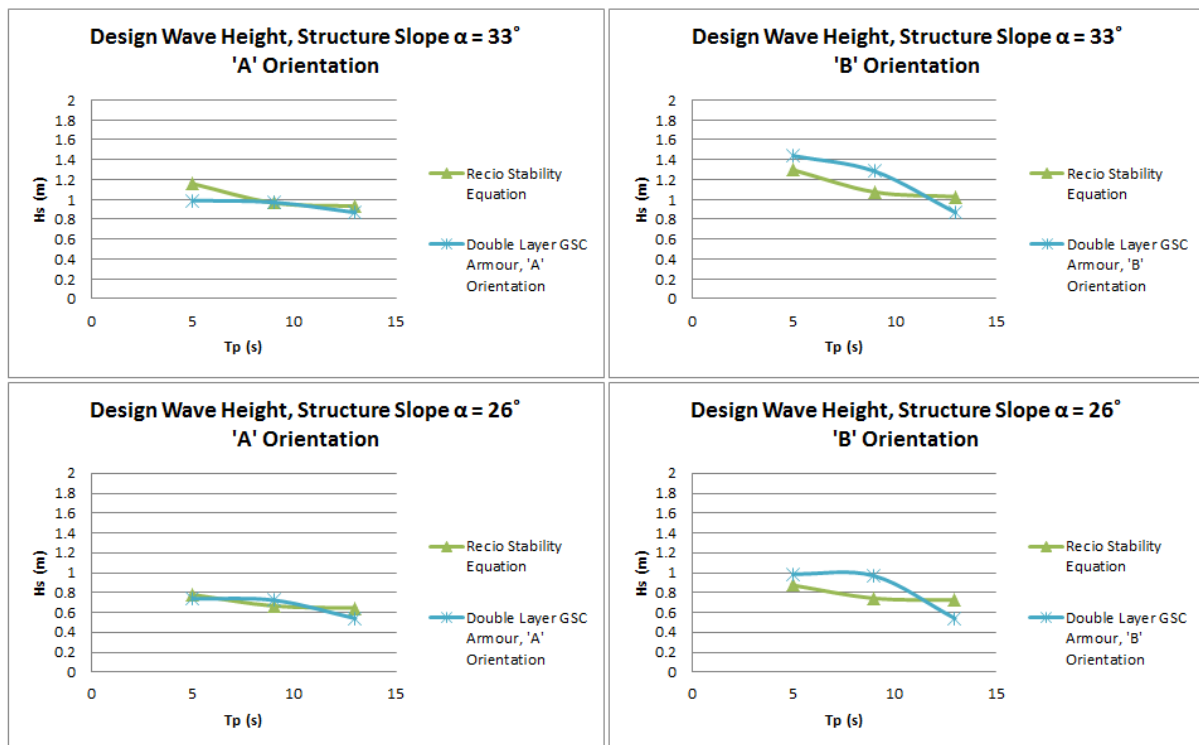
Figure 5-16: Comparison of design wave height between Recio stability equation and physical model results.

84

There is distinct improvement in the correlation between the stability equation and the results of the physical model test in contrast to previous stability equations with values within a factor of 1.2. The Recio stability equation is based on thorough process orientated physical model tests combined with analytical balances of acting forces calculations. It includes the effect of deformation of GSCs and empirical force coefficients as well as taking the friction factor of the geotextile material into account. The inclusion of these variables allows it to be adapted to a greater range of GSC permutations with confidence. It must be remembered that the empirical force coefficients were derived for GSCs with 80% fill ratio as opposed to the 109% and it is suspected that the correlation between the results could be further improved if the empirical values (force coefficients) for these GSCs were available.

5.3   Hydraulic Stability Curves

As is evident from the analysis of the physical model tests with respect to available design charts and stability equations there are many variables to consider when reflecting on the hydraulic stability of GSC revetments. Dassanayake and Oumeraci (2012b) used hydraulic stability curves based on the principal of incipient motion (as defined in Section3.6) to analyse the hydraulic stability of low crested /submerged GSC structures. An example of Dassanyake and Oumeraci (2012b) using hydraulic stability curves in assessing the hydraulic stability of GSCs with different sand fill ratios is presented in Figure 5-17 below.

Figure 5-17: Effect of Sand Fill Ratio on the Hydraulic Stability of GSCs: comparison between 80% (NW80H) and 100% (NW100) , (Dassanayake and Oumeraci, 2012b)

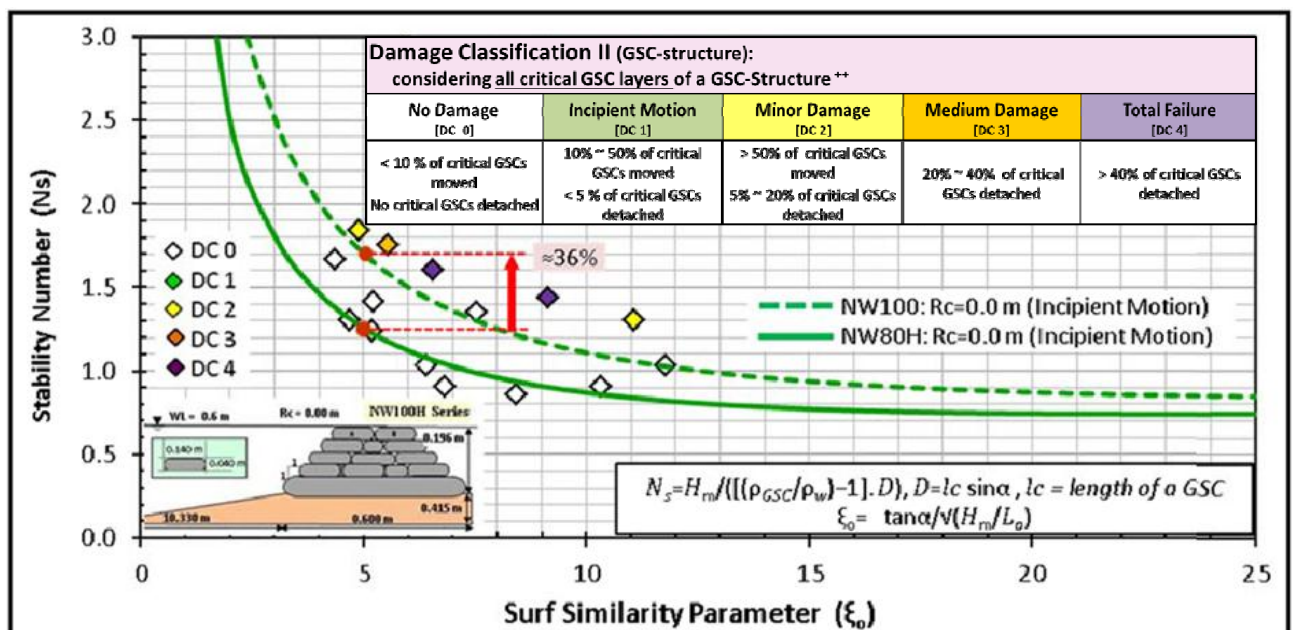By comparing the hydraulic stability curves it is quickly evident that 100% fill GSCs are more hydraulically stable (by 36% as indicated in the Figure). This method of analysis is concise and particularly useful when investigating the effect of a specific variable on the hydraulic stability of a structure, as is the case with the physical model tests undertaken. The hydraulic stability curve for each permutation of the GSC revetment can be derived and compared with one another and an assessment on the performance of each permutation can easily be made.

The process of deriving this stability curves is two parts. The first part requires that the damage to the structure from each physical model test be classified according to the damage classification table described in detail in Section 3.6. The second part requires that the stability number (Ns) and surf similarity parameter (ξ) for each test be calculated according to the following (Dassanyake and Oumeraci, 2012b):

$$N_s = \frac{H_s}{\left(\rho_{GSC}/\rho_w - 1\right) \cdot D}$$

Where:

- H_s = Density of sand container elements [kg/m³]
- ρ_{GSC} = Density of sand container elements [kg/m³]
- ρ_w = Density of water [kg/m³]
- D = Characteristic diameter of sand container and defined as: $D = l_c \sin \alpha$ [m]

And

$$\xi = \frac{\tan \alpha}{\sqrt{\dfrac{H_s}{L_0}}}$$

Where:

- α = Angle of structure slope (90˚ is vertical)
- H_s = Density of sand container elements [kg/m³]
- L_0 = Deepwater wave length and is defined as: $L_0 = \frac{gT_p^2}{2\pi}$ [m]
- T_p = Peak spectral period [s]

The values are plotted against each other and demarcated according to the damage classification. A best fit curve is then drawn to visually delineate between the tests resulting in no damage and those showing incipient motion.

86

The method of hydraulic stability curves as defined by Dassanayake and Oumeraci (2012b) inspired a similar method of analysis of the physical modelling results presented in Chapter 4. Due to the limited number of tests, hydraulic stability curves were not deemed accurate, as there were not enough data points to define a hydraulic stability curve with confidence. The method still showed potential however, and it was decided to use hydraulic stability lines instead. The hydraulic stability line can be defined as:

$$N_s = C_1 \xi + C_2$$

Where:

- N_s = Stability Number
- ξ = Surf Similarity Parameter
- C_1 = Empirical Coefficient (equation slope coefficient)
- C_2 = Empirical Coefficient (equation y-intercept coefficient)

The definition of the stability number had to be adapted to accommodate the different permutations of GSC revetments under consideration. Specifically, the characteristic length parameter (D) as defined by Dassanayake and Oumeraci (2012b) had to be modified as it did not allow more than one GSC orientation as was tested in the physical model test series. A characteristic length parameter (D) defined as an equivalent cube length is considered. This is similar to the equivalent cube length parameter used for traditional rock armour stability analysis. The characteristic length parameter is thus defined as:

$$D = (V_{GSC})^{1/3} \cdot \sin \alpha$$

Where:

- D = Characteristic length parameter [m]
- V_{GSC} = Volume of GSC as defined in Section 2.1.4[m³]
- α = Angle of structure slope (90˚ is vertical)

The hydraulic stability lines determined for each GSC revetment permutation are presented in Figures 5-18 to5-21 which follows.

Figure 5-18: Hydraulic Stability Lines for Single Layer GSC Armour Revetments with GSCs placed in 'A' Orientation
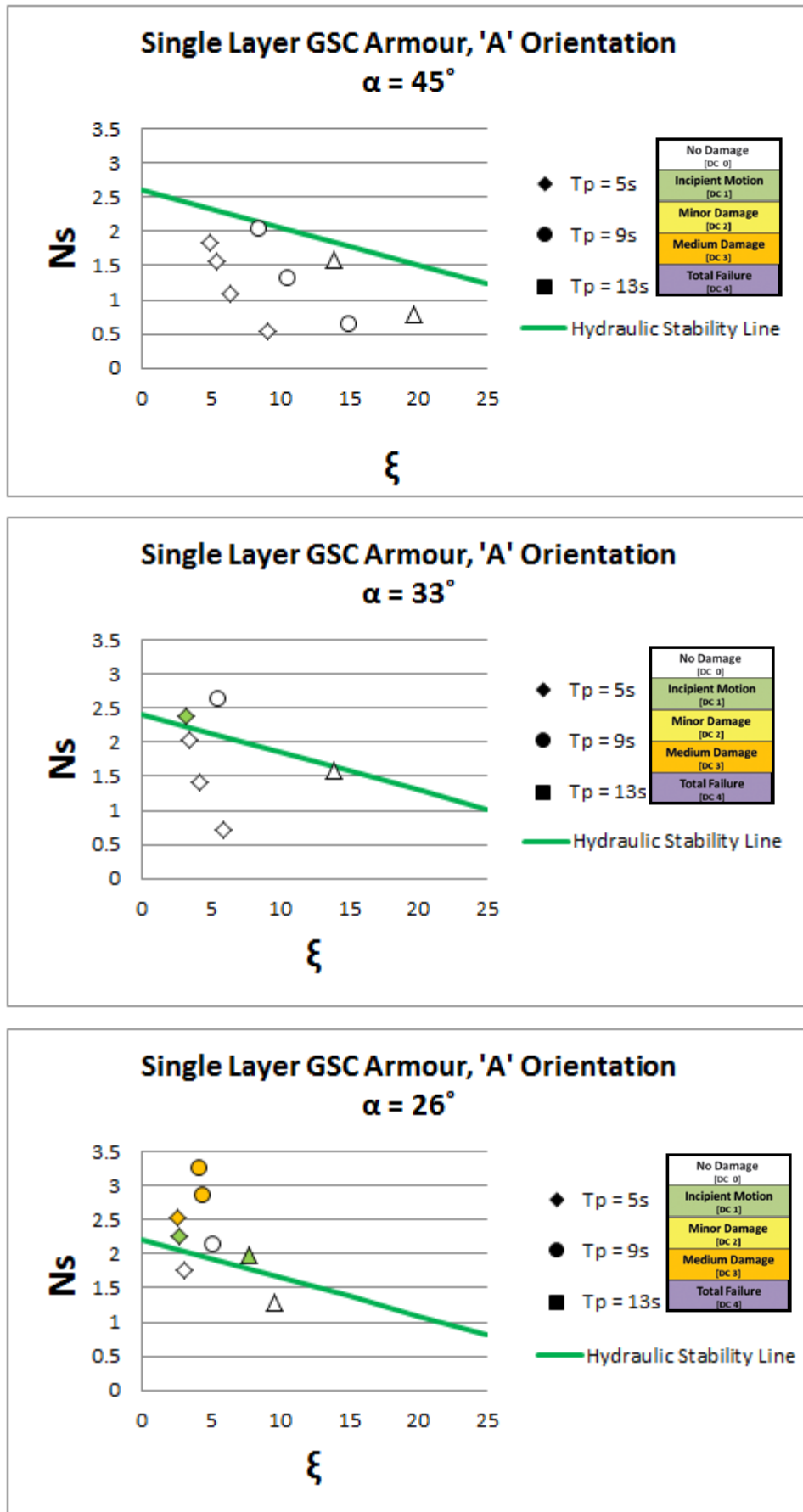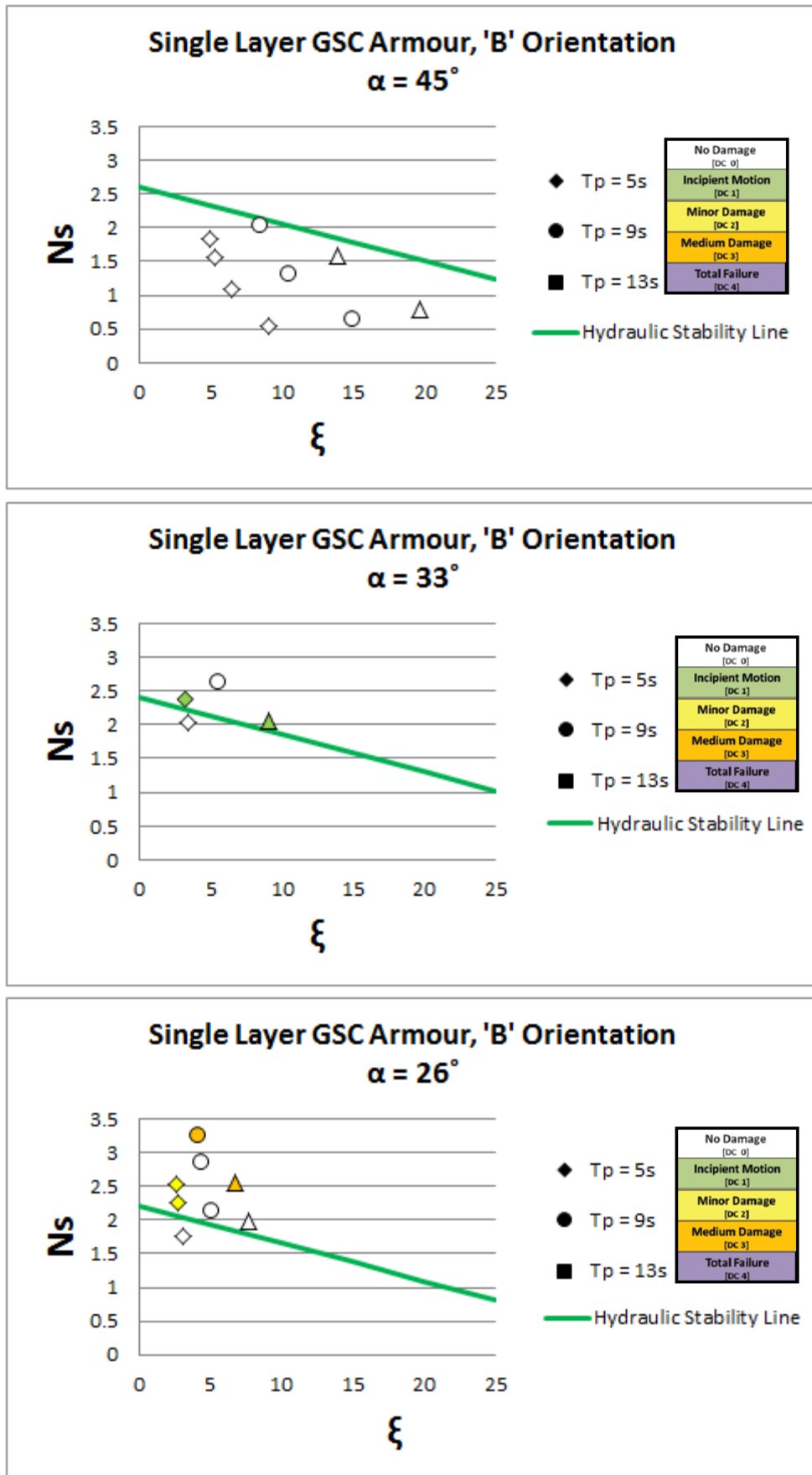
Figure 5-19: Hydraulic Stability Lines for Single Layer GSC Armour Revetments with GSCs placed in 'B' Orientation
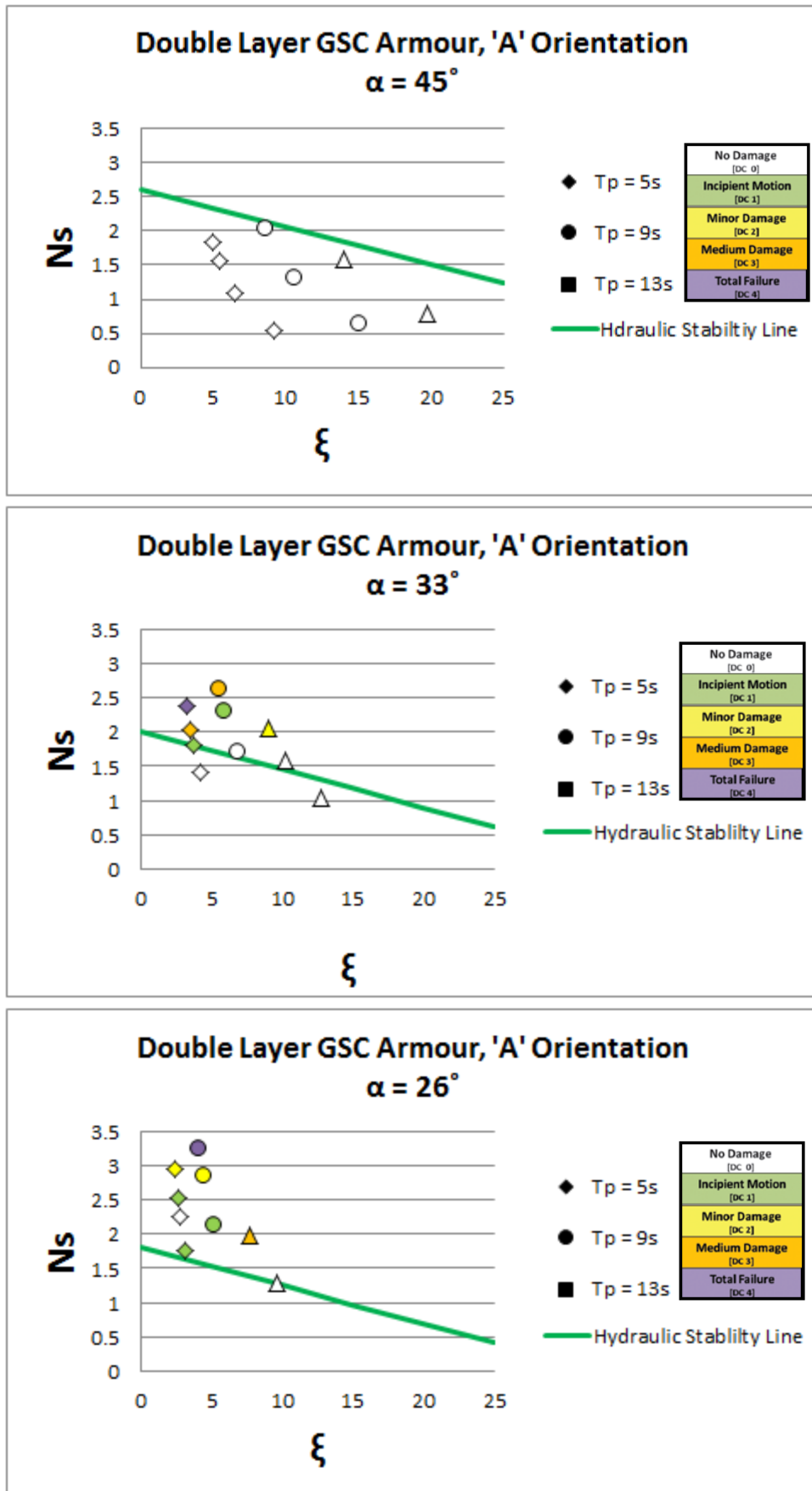
Figure 5-20: Hydraulic Stability Lines for Double Layer GSC Armour Revetments with GSCs placed in 'A' Orientation
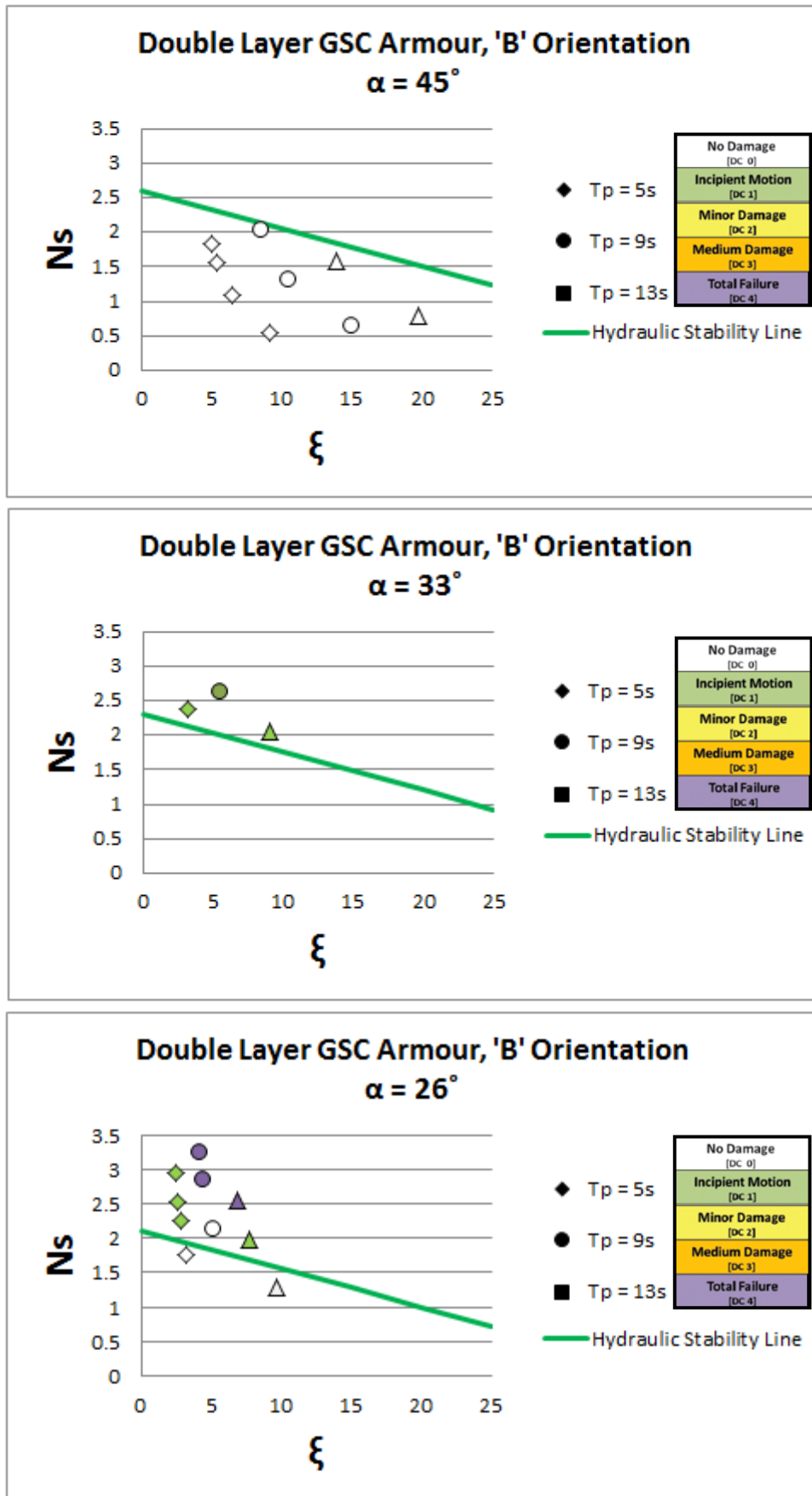
Figure 5-21: Hydraulic Stability Lines for Double Layer GSC Armour Revetments with GSCs placed in 'B' Orientation

From Figures 5-18 to 5-21, the empirical coefficients C_1 and C_2 can be determined and are presented in Table 5-7 below.

GSC Revetment Permutation	α = 45˚		α = 33˚		α = 26˚	
	C_1	C_2.	C_1	C_2.	C_1	C_2.
Single Layer GSC Armour, 'A' Orientation	-0.55	2.6	-0.55	2.4	-0.55	2.2
Single Layer GSC Armour, 'B' Orientation	-0.55	2.6	-0.55	2.4	-0.55	2.2
Double Layer GSC Armour, 'A' Orientation	-0.55	2.6	-0.55	2	-0.55	1.8
Double Layer GSC Armour, 'B' Orientation	-0.55	2.6	-0.55	2.3	-0.55	2.1
Average	-0.55	2.6	-0.55	2.3	-0.55	2.1

Table 5-7: Empirical Coefficients C_1 and C_2 for Hydraulic Stability Lines

The empirical coefficient C_1 is constant across all GSC revetment permutations allowing a direct comparison of hydraulic stability between the GSC revetment permutations based purely on the empirical coefficient C_2. A larger C_2 value indicates a greater hydraulic stability. With this in mind the empirical coefficients C_2 presented in Table 5-7, suggest the following:

I.   Single Layer GSC revetments generally match or perform better than Double layer GSC revetments.

II. GSC revetment permutations with GSCs placed in 'B' orientation perform marginally better than GSC revetment permutations placed in the 'A' orientation.

III. Steeper slopes GSC revetment permutations perform better than gentler sloping GSC revetments permutations

These observations are consistent with the observations made with the analysis summary in section 5.1.4. The method shows good potential, but requires more data points for confirmation of the trends which were revealed.

5.4   Discussion of Results

From the analysis of the physical model tests and the evaluation of the available design charts and stability equations much has been learnt about the hydraulic stability of GSC revetments and the various permutations thereof.

5.4.1   Recio Stability Equation

The correlation between the results of the physical model tests and Recio stability equation is good and validates its use as a design tool for future GSC revetment designs. The Recio stability equation is based on the latest process oriented physical model tests and is considered to supersede previous

stability equations. The input parameters of the Recio stability equation are numerous thus allowing its application to a wide range of GSC permutations, provided the approach derived by Recio (2007) is followed and the limitations imposed considered in the final design.

5.4.2   Physical Model Results

The most significant outcome of the physical model test and the analysis thereof is the performance of single layer GSC armour revetments. The literature review process identified single layer GSC revetments as being significantly less hydraulically stable than their double layer GSC revetment equivalents (Coughlan *et al*, 2008). Upon analysis, the inverse of this was the case during the physical model test considered in the present study. The reason for this discrepancy is attributed to the greater porosity of single layer GSC revetments. As Recio (2007) surmised, the greater the porosity of the structure the more hydraulically stable it will be. The greater porosity of the single layer GSC is due to the large gaps between the GSC units and the geotextile lining. In a double layer GSC revetment these gaps are blocked by the inner layer of GSCs, making the structure less permeable. In prototype situations it is expected that due to the elongation properties of geotextile material, the geotextile lining is expected to mould to the step back structure of the GSC revetment. In doing so, it will limit the available gaps between the GSCs and the geotextile lining and thus limit the permeability of the revetments. This moulding of the geotextile lining was artificially reduced in the physical model tests due the difficulty in scaling the geotextile material. The geotextile material in the physical model test is considerably stronger than would be found in prototype situations. This will negate the porosity advantage of single layer GSC revetments porosity as seen in the physical model tests. At the very least the hydraulic performance of single layer GSC revetments is not as poor as initially suspected.

5.4.3   Mechanisms of failure

The mechanisms of failure, as described in Chapter 4, differ between single layer GSC revetments and double layer GSC revetments. Single layer GSC revetments tend to slump when failure occurs, while double layer GSC revetments fail more gradually with GSCs being pulled out from the critical zone just beneath the still water level (SWL) and slowly undermining neighbouring GSCs. This phenomenon gradually works its way up the revetments slope. Once a single layer GSC revetment has failed the sand core is left exposed to wave attack. Deformations of the sand core during the physical model tests suggest that if it were not for the artificially strong geotextile lining, the same geotextile lining would rupture allowing unabated erosion of the sand core. When a double layer GSC revetment failed, the sand core was left intact as the inner layer of GSCs continued to protect the sand core. From a risk analysis point of view, single layer GSC revetments are thus not

considered to be ideal even though the physical model results show that single GSC revetments can outperform double layer GSC revetment equivalents.

6 Conclusion and Recommendations

The hydraulic stability of GSC revetments is better understood following the physical model results with regards to the effect of packing arrangement and structure slope. Analysis of the physical modelling results revealed three principal trends. Firstly, single layer GSC revetments generally match or perform better than double layer GSC revetments. Secondly, GSC revetment permutations with GSCs placed with the long axis of the GSC parallel to the direction of wave attack perform marginally better than GSC revetment permutations placed with the long axis of the GSC perpendicular to the direction of wave attack. Lastly, steeper slopes GSC revetment permutations perform better than gentler sloping GSC revetments permutations

Through the testing in this report a method of design has evolved for both single layer and double layer GSC revetment permutations. For double layer GSC revetments the tests in this report agree well with the Recio stability equation which is considered to be suitable for the design purposes of double layer GSC armour revetments, provided care is taken to accurately determine the input parameters.

Although progress has been made with the knowledge available on the hydraulic stability of GSC revetments, much more research is still required. This study has highlighted the great number of variables that affect the hydraulic stability of GSC revetments. Further systematic investigation into these variables, such as sand fill ratio of the GSCs and type of sand fill material in GSCs is necessary. Additional studies are required on scale effects of some material parameters of the geotextile material such as porosity, tensile strength and friction coefficients. Further validation of existing design guides and stability equations will broaden their range of applicability and entrench GSC revetments as a reliable coastal protection solution.

Although not intended as a definitive design guide, through the observations made during this study several tentative recommendations on the design of GSC revetments are made and should be used cautiously. The cost effectiveness of single layer GSC armour versus double layer GSC armour is evident; as such it is recommended to use single layer GSC armour revetments where suitable. If critical infrastructure is to be protected, double layer GSC armour is recommended to reduce the risk of core material being exposed if the structure does fail. GSC revetments should be constructed with a structure slope as close to 1V:1H as practical, keeping in mind constructability issues. GSCs should have a sand fill ratio of 100% and placed with the long axis of the GSC parallel with the direction of wave attack (this is more important when dealing with GSCs with more pronounced rectangular dimensions than those tested in this study).

7 References

Blacka, M.J., Carley, Cox, R.J., Hornsey, W. and Restall, S. 2007. Field Measurements of Full Sized Geocontainers. In *Coasts and Ports 2007,* July 18-20, Melbourne, Australia.

Bouyze J. G. and Schram A. R. 1990, Stabiliteit van Grondkribben en Onderwatergolbrekers Opgebouwd uit Zandworsten, TU-Delf, Studentarbeit (Master Student Project Report) (in Dutch).

Coghlan, I.R., Carley, J.T., Mariani, A. and Cox, R.J. 2008. Research and Development studies for Elcomax and Elcorock Geotextile Sand Containers, *WRL Technical Report No 2008/05.*

Dassanayake, D.T., Oumeraci, H. 2012a. Important engineering properties of geotextile sand containers and their effect on the hydraulic stability of GSC-structures, Terra et Aqua Journal, Issue 127, International Association of Dredging Companies, The Netherlands, 3-11.

Dassanayake, D.T., Oumeraci, H. 2012b. Engineering properties of geotextile sand containers and their effect on hydraulic stability and damage development of low-crested / submerged structures, The International Journal of Ocean and Climate Systems, Vol. 3, Issue 3, Multi Science Publishing, Essex, UK, 135-150.

Dean, R. G., and Dalrymple R. A. 1998, Water Wave Mechanics for Engineers and Scientists, World Scientific, Advanced Series on Ocean Engineering, Singapore.

Geofabrics Australasia Jumeirah Beach Seawall Case Study. 2003. [Online]. Available: http://www.geofabrics.com.au/documents/ELCOROCK-JUMAIRAH-BEACH.pdf. [2012, December 8].

Geofabrics Australasia Narrowneck Reef Case Study. 2000. [Online]. Available: http://www.geofabrics.com.au/documents/ELCOROCK-NARROWNECK.pdf. [2012, December 8].

Geofabrics Australasia Kingscliff Seawall Case Study. 2011. [Online]. Available: http://www.geofabrics.com.au/documents/ELCOROCK-Kingscliff-case-study-09-12.pdf. [2012, December 8].

Geosintex Nonwoven Geotextiles. 2012. [Online]. Available: www.geosintex.com/en. [2012, December 8]

Geosintex Woven Geotextiles. 2012. [Online]. Available: www.geosintex.com/en. [2012, December 8]

Hudson, R. 1956. Laboratory investigation of rubble-mound breakwaters. *Journal of the Waterways and Harbour Division*, 93-118.

Hughes, S.A. (1993) *Physical models and laboratory techniques in coastal engineering*, World Scientific.

Krahn, T., Blatz, J., Alfaro, M., Bathurst, R. J. 2007. Large-scale interface shear testing of sand bag dyke materials. *Geosynthetics International*, 14, No. 2, 119–126.

Mansard, E.P.D. and Funke, E.R. (1980) ‗The measurement of incident waves and reflected spectra using a least square method', 17th Int. Conf. of Coastal Engineering, Proc. ICCE'80, ASCE, pp.154-172, Sydney.

Marth R., Mueller G. and Wolters G., 2005. Damages of Blockwork Coastal Structures due to Internal Wave Impact Induced Pressures, Proceedings of the International Coastal Symposium, Ireland.

Naue Fasetechnik 2011, Characteristics of Geotextile Material, Email Correspondance.

Oumeraci H., M. Bleck, Hinz M. and Kuebler S.2002. Großmaßstabliche Untersuchungen zur Hydraulischen Stabilität geotextiler Sandcontainer unter Wellenbelastun (Large-scale Model Tests for the Hydraulic Stability of Geotextile Sand Containers under Wave Attack. Research Report no. 878. Leichtweiss Intitute for Hydraulic Engineering and Water Resources, 62 pages (in German).

Phelp, D., Rossouw, M., Mather, A. and Godfrey, V. 2009. Storm Damage and Rehabilitation of Coastal Structures on the East Coast of South Africa. Proceedings of the ninth international conference organised by the Institution of Civil Engineers, Edinburgh.

PIANC (2011) *Report no. 113 - 2011: The Application of Geosynthetics in Waterfront Areas*

Pilarczyk, K.W., 2000, Geosynthetics and Geosystems in Hydraulic and Coastal Engineering, A.A. Balkema, Rotterdam (balkema@balkema.nl; www.balkema.nl).

Recio J. and Oumeraci H. 2005b, Processes Affecting the Hydraulic Stability of Geotextile Sand Containers -Experimental Studies-, Leichtweiss Institute for Hydraulic Engineering and Water Resources, Research Report No 944, 78 pages.

Recio, J. (2007) Hydraulic Stability of Geotextile Sand containers for Coastal Structures - Effect of Deformations and Stability Formulae. PhD Thesis, Leichtweiss Institute for Hydraulic Engineering and Water resources, www.digibib.tu-bs.de/?docid=00021899

Recio, J., Oumeraci, H., 2009. Processes affecting the hydraulic stability of coastal revetments made of geotextile sand containers. Coastal Engineering 56 (3), 260-284.

Robin, A.C. 2004, Paper bag problem, Mathematics Today, Bulletin of the Institute of Mathematics and its Applications, 40 (June 2004), 104-107.

Theron, A K, Coppoolse, R C and Schoonees, J S (1994). Low-cost coastal protection measures using textiles. 28 PIANC, Section II, Subject 4, pp. 109-118, Seville, Spain

Theron, A K, Schoonees, J S and Manini, D (1999). Successful prototype testing of low-cost dike/beachwall protection. Coastal Structures '99, ASCE, Santander, Spain. Vol. 2: 1027 – 1035

Schoonees, J S, Theron, A K and Coppoolse, R C (1999). Temporary groynes for measuring longshore transport in False Bay. Coastal Sediments '99, ASCE, Long Island, New York. Vol. 2: 971 – 986.

U.S. Army Corps of Engineers (2006) *Coastal Engineering manual (CEM)*.

Van Steeg, P. & Klein Breteler, M. (2008) *Large scale physical model tests on the stability of geocontainers*, Deltares report no H4595, Delft.

Venis W.A. 1967, Closure of Estuarine Channels in Tidal Regions, Behaviour of Dumping Material when Exposed to Currents and Wave action. De Ingenieur Vol. 50.

Wouters, J. 1998, Open Taludbekledingen; stabiliteit van geosystems (Stability of Geosystems) Deftt Hydraulics Report H1930, Annex 7 (in Dutch).

Appendix A: Effective GSC Revetment Toe Design

A recommended effective GSC revetment toe design by WRL Technical Report (2008) is presented in the figure below. The dimensions in the figure are relevant to 0.75m³ GSCs as opposed to 2.5m³ GSCs considered in this study, however the technique remains valid. The technique involves burying the toe of the structure in the foreshore slope, adding a third row of GSCs to the bottom layer (second row in the case of single layer GSC armour revetment) and wrapping this third layer to form an "encapsulated self-healing toe". WRL (2008) found this toe restraint arrangement to be very strong and prevented slip failures.
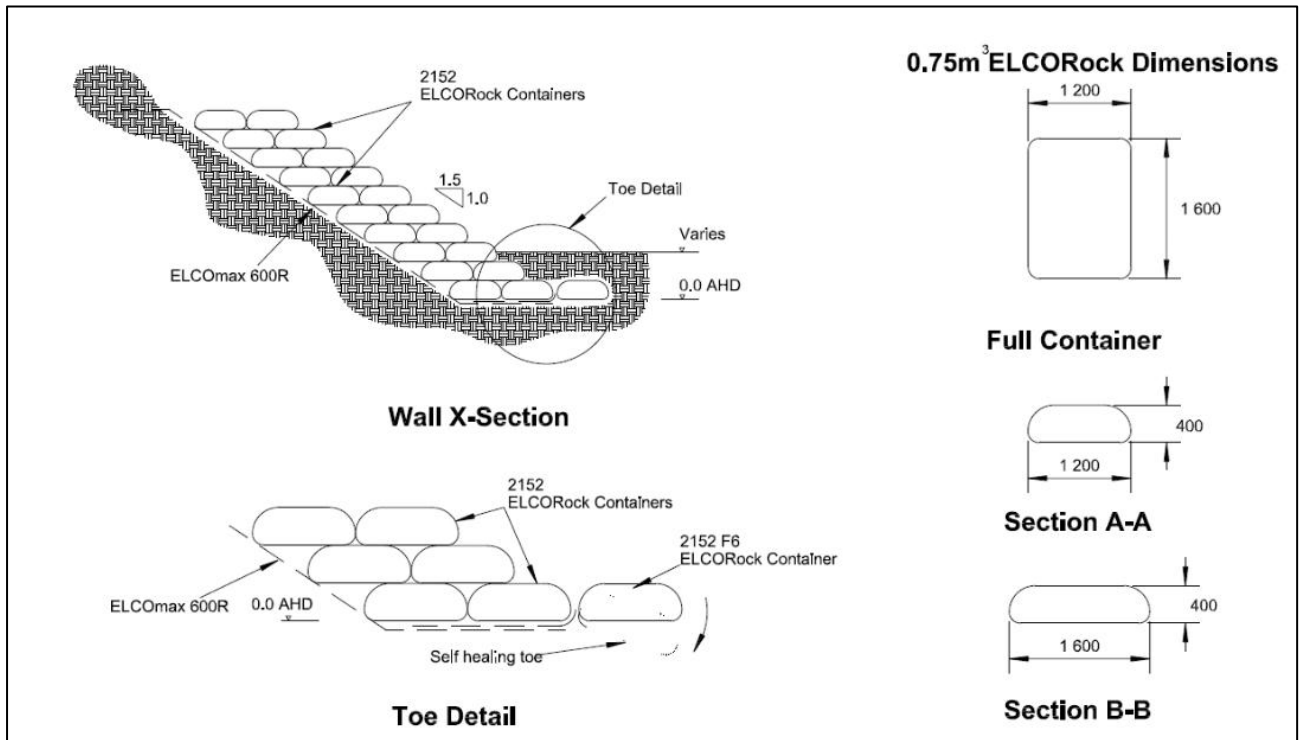
Appendix B: Details of Large Wave Flume

The 2m wide US large flume is used for large scale wave/current structure interaction tests, design optimization and hydrodynamic studies of coastal and offshore structures and wave energy conversion devices. The concrete flume is 50m long of which 6.5m has glass walls on both sides. If required a 1t overhead gantry crane may be used to build the models. A hinged type wave maker was upgraded with Dynamic Absorption System and now receives HR Wave Maker input signals, enabling fully irregular waves and design spectra on demand.

Wave Maker:

The flume is equipped with a hinged type wave maker with Dynamic Wave Absorption that simulates:

- Long and short crested random waves.
- JONSWAP, Pierson-Moskowitz or user-defined wave spectrum.
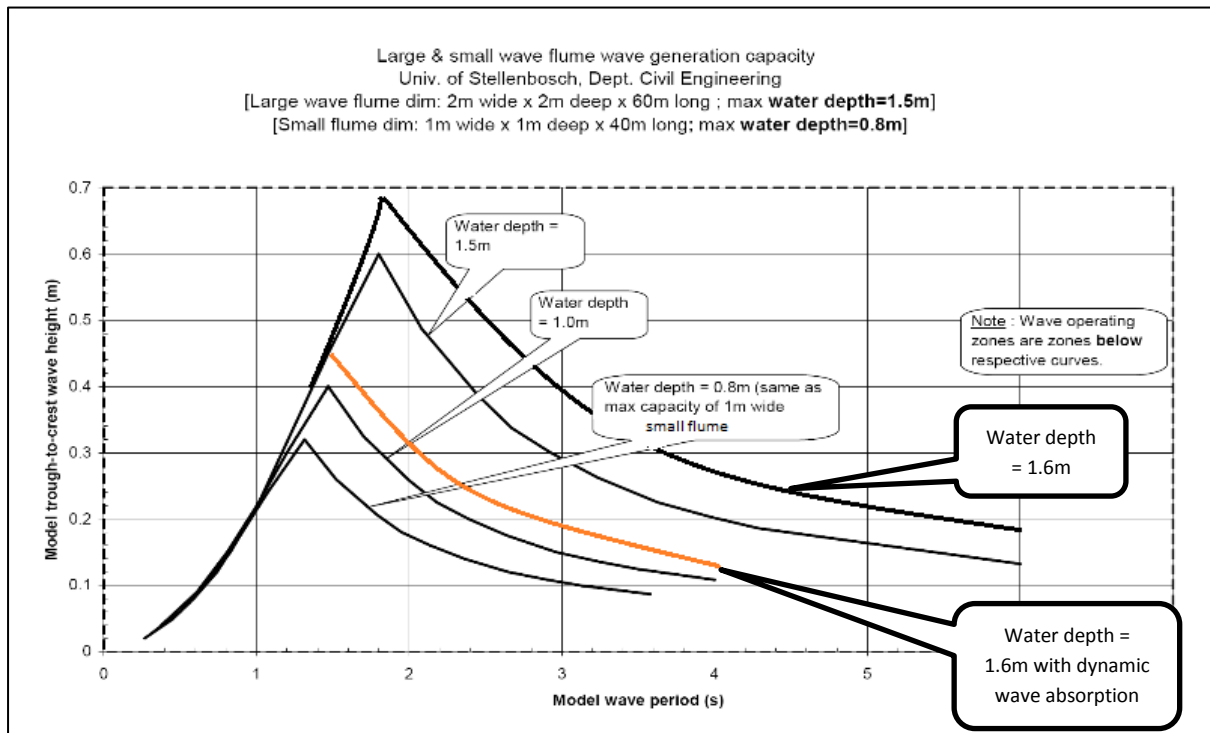- Time series of surface elevations imported from ASCII files.

Data Acquisition:

4-channel wave gauge system, 4x600mm resistive wave probes and HR DAQ software is used to acquire and analyse the data from model tests:

- Spectral analysis.
- Statistical analysis based on wave up-crossing technique.
- Reflection analysis based on four wave probes.

Wave Generation Curve:

The wave generation curve is shown in the figure below. The dynamic wave absorption was installed after these generation curves were generated. The wave absorption system significantly reduces the wave making abilities of the flume as is evident on the figure below.

Large & small wave flume wave generation capacity
Univ. of Stellenbosch, Dept. Civil Engineering
[Large wave flume dim: 2m wide x 2m deep x 60m long ; max **water depth=1.5m**]
[Small flume dim: 1m wide x 1m deep x 40m long; max **water depth=0.8m**]

Facilities Brochure:

University of Stellenbosch
Faculty of Engineering
Department of Civil Engineering
Institute for Water and Environmental Engineering
South Africa

RENEWABLE & SUSTAINABLE
ENERGY STUDIES

Large Wave/Current Flume

DESCRIPTION

The 2m wide US large flume is used for large scale wave/current structure interaction tests, design optimization and hydrodynamic studies of coastal and offshore structures and wave energy conversion devices. The concrete flume is 50m long of which 6.5m has glass walls on both sides. If required a 1t overhead gantry crane may be used to build the models.

In April 2010 the hinged type wave maker was upgraded with Dynamic Absorption System, now receives HR Wave Maker input signals, enabling fully irregular waves and design spectra on demand.

FLUME SPECIFICATIONS

Concrete flume

> Length: 50m (6.5m with glass walls)
> > 30m available for flow studies
> Width: 2m
> Max. water depth: 1.5m
> Max wave height: 0.6 m

WAVE MAKER

The flume is equipped with a hinged type wave maker with Dynamic Wave Absorption that simulates:

- Long and short crested random waves.
- JONSWAP, Pierson-Moskowitz or user-defined wave spectrum.
- Time series of surface elevations imported from ASCII files.

DATA ADQUISITION

4-channel wave gauge system, 4x600mm resistive wave probes and HR DAQ software is used to acquire and analyze the data from model tests:

- Spectral analysis.
- Statistical analysis based on wave up-crossing technique.
- Reflection analysis based on four wave probes.

Contact: Geoff Toms
e-mail: gtoms@sun.ac.za
Tel: +27 21 808 4362
Fax: +27 21 808 4351
www.civeng.sun.ac.za

University of Stellenbosch
Department of Civil Engineering
Private Bag X1
7602 MATIELAND
South Africa

Appendix C: 'Phillipi' Sand Grading Curve

The grading of the sand used in the physical model is shown below. This 'Phillipi' sand was used to fill the GSCs as served as core sand material on which to construct the GSC revetment permutations.

Particle Size Distribution

D90	0.95mm
D50	0.45mm
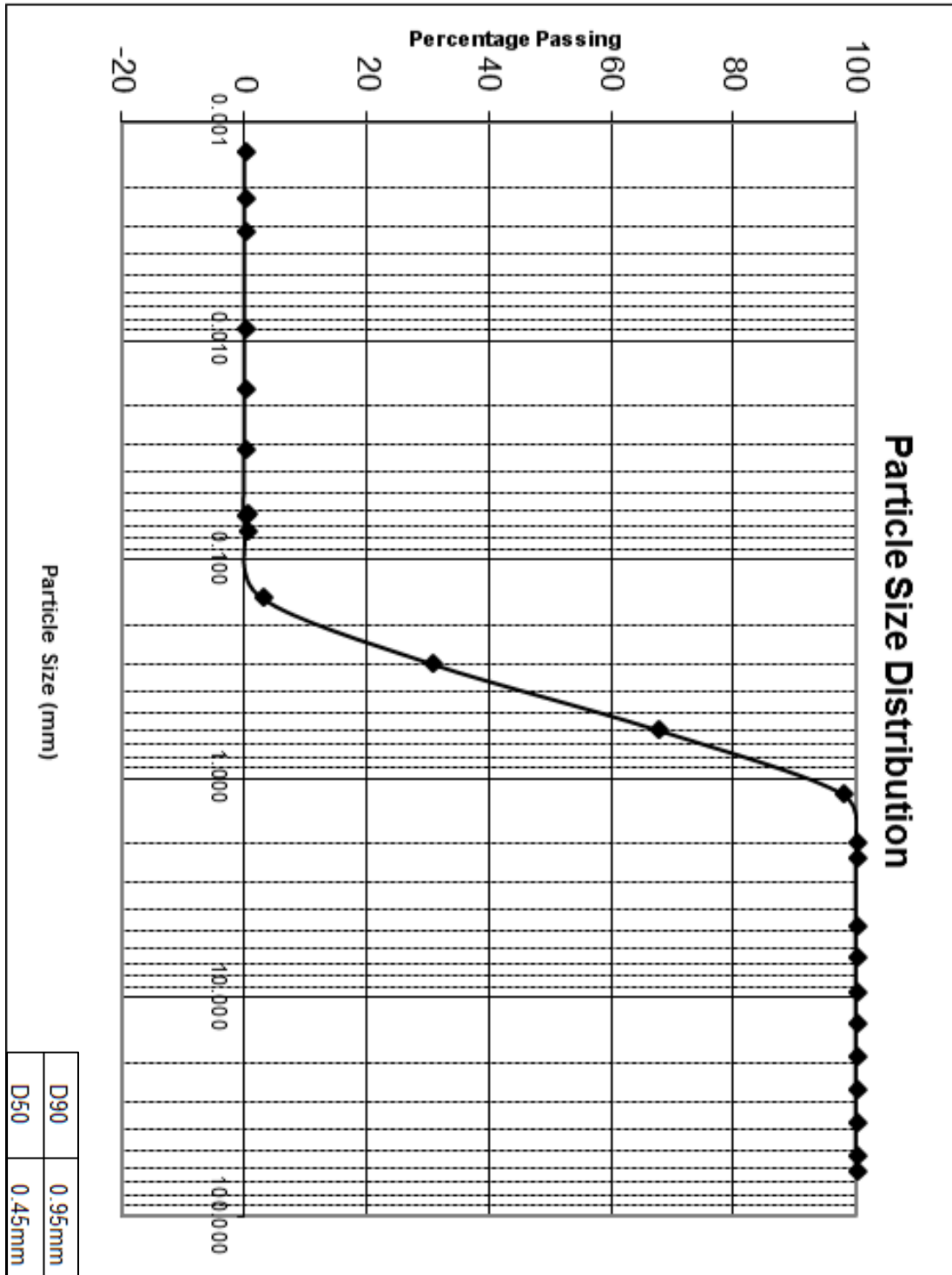
Appendix D: Linear Wave Theory Summary

Linear Wave theory is easy to apply and gives a reasonable approximation for a wide range of wave parameters (CEM, 2006). The calculation of these wave parameters are defined in Figures D-1 and D-2 that follows.
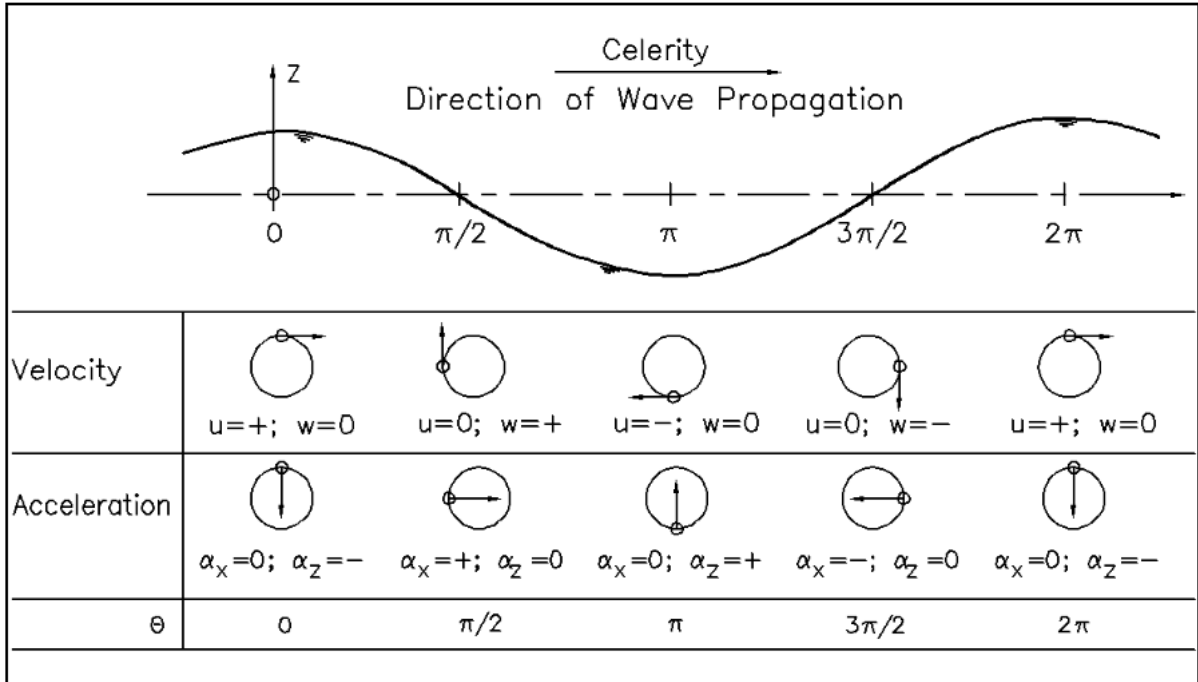

Figure D-1: Local Fluid Velocities and Acceleration (CEM, 2006)

Relative Depth	Shallow Water $\frac{d}{L} < \frac{1}{20}$ $kd < \frac{\pi}{10}$	Transitional Water $\frac{1}{20} < \frac{d}{L} < \frac{1}{2}$ $\frac{\pi}{10} < kd < \frac{\pi}{2}$	Deep Water $\frac{d}{L} > \frac{1}{2}$ $kd > \frac{\pi}{2}$
1. Wave profile	Same As >	$\eta = \frac{H}{2}\cos\left[\frac{2\pi x}{L} - \frac{2\pi t}{T}\right] = \frac{H}{2}\cos\theta$	< Same As
2. Wave celerity	$C = \frac{L}{T} = \sqrt{gd}$	$C = \frac{L}{T} = \frac{gT}{2\pi}\tanh\left(\frac{2\pi d}{L}\right)$	$C = C_0 = \frac{L}{T} = \frac{gT}{2\pi}$
3. Wavelength	$L = T\sqrt{gd} = CT$	$L = \frac{gT^2}{2\pi}\tanh\left(\frac{2\pi d}{L}\right)$	$L = L_0 = \frac{gT^2}{2\pi} = C_0 T$
4. Group velocity	$C_g = C = \sqrt{gd}$	$C_g = nC = \frac{1}{2}\left[1 + \frac{4\pi d/L}{\sinh(4\pi d/L)}\right]C$	$C_g = \frac{1}{2}C = \frac{gT}{4\pi}$
5. Water particle velocity (a) Horizontal	$u = \frac{H}{2}\sqrt{\frac{g}{d}}\cos\theta$	$u = \frac{H}{2}\frac{gT}{L}\frac{\cosh[2\pi(z+d)/L]}{\cosh(2\pi d/L)}\cos\theta$	$u = \frac{\pi H}{T}e^{\left(\frac{2\pi z}{L}\right)}\cos\theta$
(b) Vertical	$w = \frac{H\pi}{T}\left(1+\frac{z}{d}\right)\sin\theta$	$w = \frac{H}{2}\frac{gT}{L}\frac{\sinh[2\pi(z+d)/L]}{\cosh(2\pi d/L)}\sin\theta$	$w = \frac{\pi H}{T}e^{\left(\frac{2\pi z}{L}\right)}\sin\theta$
6. Water particle accelerations (a) Horizontal	$a_x = \frac{H\pi}{T}\sqrt{\frac{g}{d}}\sin\theta$	$a_x = \frac{g\pi H}{L}\frac{\cosh[2\pi(z+d)/L]}{\cosh(2\pi d/L)}\sin\theta$	$a_x = 2H\left(\frac{\pi}{T}\right)^2 e^{\left(\frac{2\pi z}{L}\right)}\sin\theta$
(b) Vertical	$a_z = -2H\left(\frac{\pi}{T}\right)^2\left(1+\frac{z}{d}\right)\cos\theta$	$a_z = -\frac{g\pi H}{L}\frac{\sinh[2\pi(z+d)/L]}{\cosh(2\pi d/L)}\cos\theta$	$a_z = -2H\left(\frac{\pi}{T}\right)^2 e^{\left(\frac{2\pi z}{L}\right)}\cos\theta$
7. Water particle displacements (a) Horizontal	$\xi = -\frac{HT}{4\pi}\sqrt{\frac{g}{d}}\sin\theta$	$\xi = -\frac{H}{2}\frac{\cosh[2\pi(z+d)/L]}{\sinh(2\pi d/L)}\sin\theta$	$\xi = -\frac{H}{2}e^{\left(\frac{2\pi z}{L}\right)}\sin\theta$
(b) Vertical	$\zeta = \frac{H}{2}\left(1+\frac{z}{d}\right)\cos\theta$	$\zeta = \frac{H}{2}\frac{\sinh[2\pi(z+d)/L]}{\sinh(2\pi d/L)}\cos\theta$	$\zeta = \frac{H}{2}e^{\left(\frac{2\pi z}{L}\right)}\cos\theta$
8. Subsurface pressure	$p = \rho g(\eta - z)$	$p = \rho g\eta\frac{\cosh[2\pi(z+d)/L]}{\cosh(2\pi d/L)} - \rho g z$	$p = \rho g\eta\, e^{\left(\frac{2\pi z}{L}\right)} - \rho g z$

Figure D-2: Summary of linear wave theory-wave characteristics (CEM, 2006)